CODIGEM

CORPORACIÓN DE DESARROLLO E INVESTIGACIÓN GEOLÓGICO-MINERO-METALÚRGICA

MINISTERIO DE ENERGÍA Y MINAS

DFID

DEPARTMENT FOR INTERNATIONAL DEVELOPMENT

BGS 1835

BRITISH GEOLOGICAL SURVEY

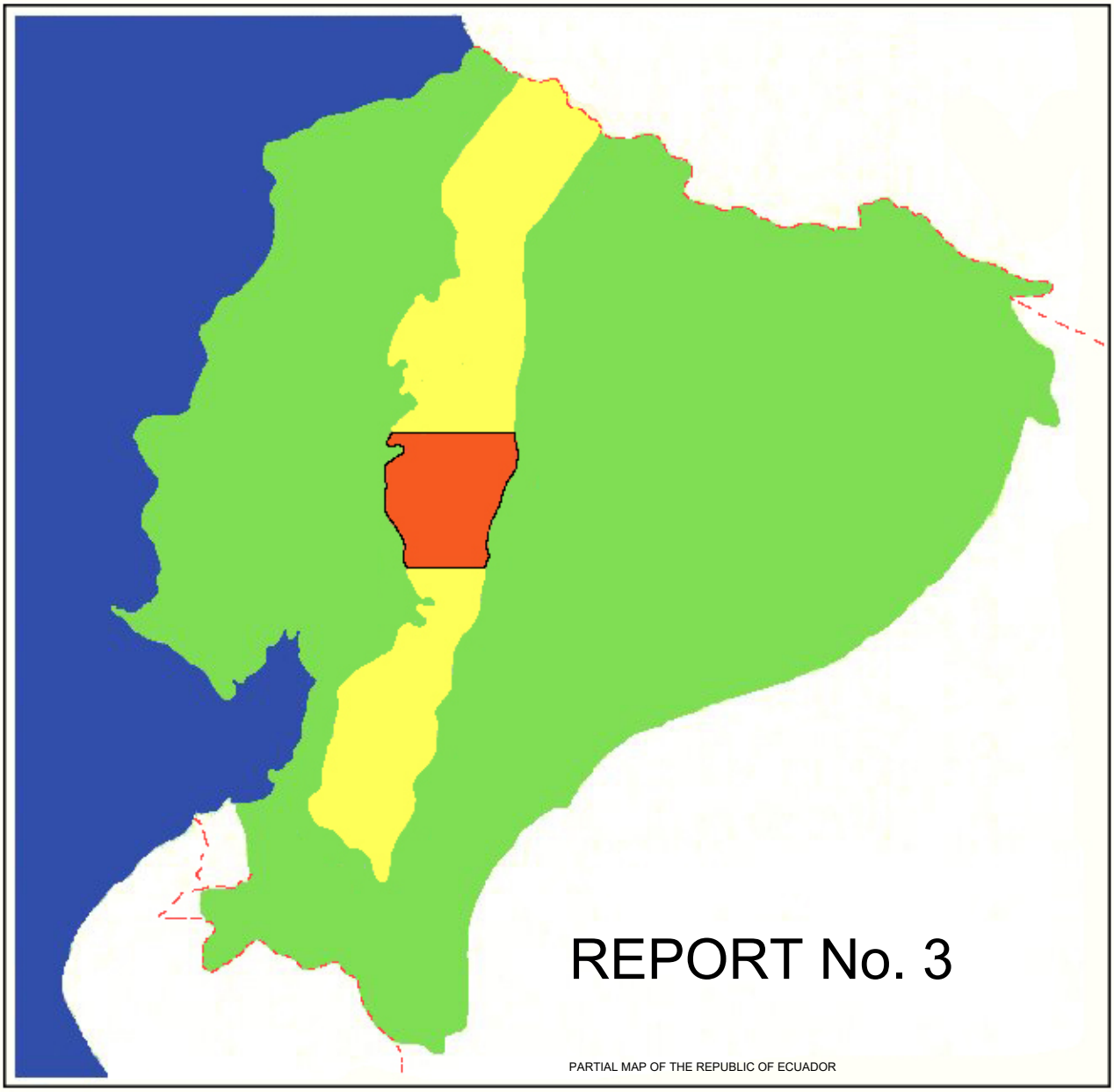

REPORT No. 3

PARTIAL MAP OF THE REPUBLIC OF ECUADOR

WORLD BANK MINING DEVELOPMENT AND ENVIRONMENTAL CONTROL PROJECT

GEOLOGICAL INFORMATION MAPPING PROGRAMME (WESTERN CORDILLERA)

PATRI MATRIQUE

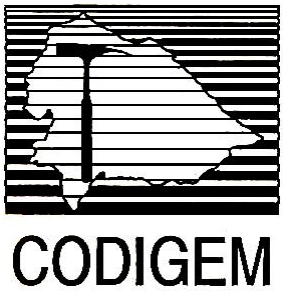

MINING DEVELOPMENT AND ENVIRONMENTAL CONTROL PROJECT

GEOLOGICAL INFORMATION MAPPING PROGRAMME

Report Number 3

GEOLOGY OF THE WESTERN CORDILLERA OF ECUADOR BETWEEN 1°00' AND 2°00'S

William McCourt

Pablo Duque

Luis Pilatasig

CODIGEM-BRITISH GEOLOGICAL SURVEY

Quito-Ecuador

1997

Stalyn Paucar

2024 edition

Reference

McCourt, W., Duque, P. & Pilatasig, L. (1997). *Geology of the Western Cordillera of Ecuador between 1°00' and 2°00'S* (Stalyn Paucar, Ed., 2024). Report Number 3. Geological Information Mapping Programme. BGS-CODIGEM/MEM.

CONTENTS

FIGURES

PLATES

APPENDICES

1. INTRODUCTION

1.1 Background

Mapping of this quadrangle, at 1:50000 scale, was carried out as part of the Geological Information Mapping Programme (GIMP) Western Cordillera of Ecuador, subcomponent 3.3, of the Mining Development and Environmental Control Technical Assistance Project (PRODEMINCA). This multi-national project is co-funded by the World Bank and the Governments of Ecuador, Sweden and the United Kingdom (through the Overseas Development Administration, ODA, now Department for International Development, DFID). One of its primary aims is to attract private investment into the Ecuadorian mining sector, through the production of an accurate and internally consistent geological and geochemical database for the Western Cordillera. Investigations were undertaken jointly by geologists of the British Geological Survey (BGS) the Corporación de Desarrollo e Investigación Geológico-Minero-Metalúrgica (CODIGEM) and national consultants of PRODEMINCA. Fieldwork was carried out between September 1995 and January 1996, and from May-November 1996, a total of 180 days covering an area of approximately 7000 km^2, with altitudes ranging from less than 200 m to over 4600 m ASL. The information presented in this report is the product of field, laboratory and office-based investigations carried out by W. J. McCourt, P. Duque, L. Pilatasig (w.e.f. 05/1996) and R. Villagómez (09/1995-02/1996) and the location of the area studied is shown in Fig. 1. Terrain and climate are extremely varied within the area, reflecting the variation in altitude from the western coastal plain to the eastern and southeastern high páramo. The western slopes of the cordillera are covered by primary tropical forest with few settlements and poor access, while the páramo area above 3500-4000 m is cold and inhospitable, populated by isolated indigenous communities.

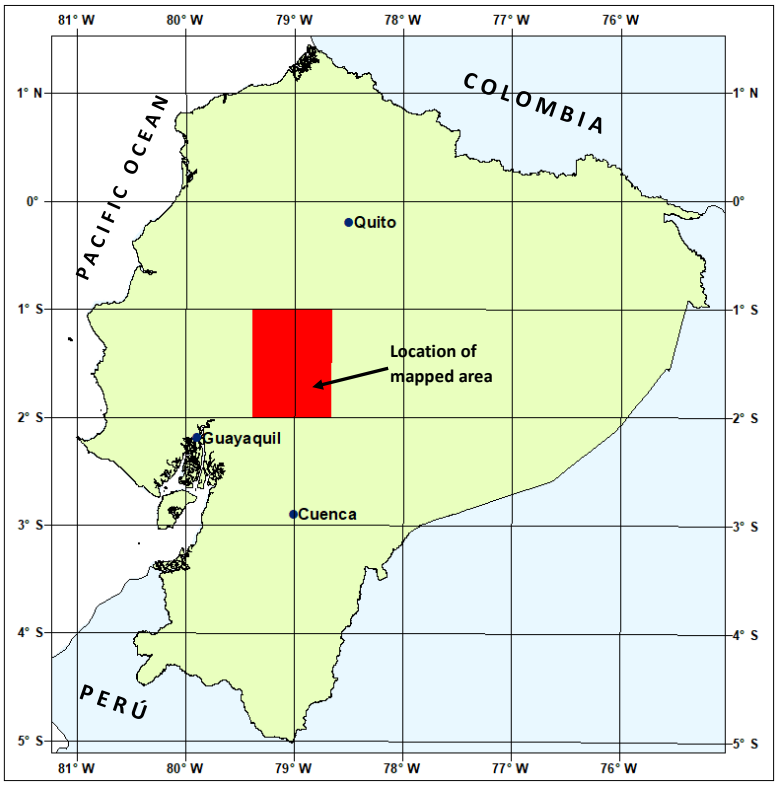

Figure 1. Location of study area

1.2 Geological framework of Ecuador

Geographically and geomorphologically Ecuador is divided into three main units, a central Andean region, the "Sierra", separating the Amazon Basin or "Oriente" in the east, from the Coastal Plain or "Costa" in the west, that reflect fundamentally different geological provinces. The Oriente is a Mesozoic to Cenozoic sedimentary basin that includes a carbonate platform sequence, overlying older cratonic basement. Both basement and cover sequences have been intruded by large granitoid batholiths mainly along the complex sub-Andean zone of folding and thrusting that separates the Oriente from the Sierra to the west. The Sierra comprises two sub-parallel mountain chains separated by a graben. The Cordillera Real to the east is dominated by linear belts of metamorphic rocks, intruded by Early Mesozoic granitoids of both S- and I-type, and capped along much of its length by Cenozoic volcanics. The Cordillera Occidental to the west of the graben is dominated by Late Mesozoic to Early Cenozoic basaltic volcanic and volcaniclastic rocks, representing at least in part accreted oceanic terranes, and clastic turbidites, intruded by Mid-Late Tertiary granitoids and overlain by post-Eocene sequences of continental margin, mainly acid to intermediate, calc-alkaline volcanics. The Interandean Depression or central graben is an important extensional structure bounded by active faults. It contains extensive Tertiary to Recent sedimentary and volcanic sequences that probably date back to Oligocene-Miocene time. The Costa comprises the low-lying region west of the Andes and represents a series of Late Cretaceous to Cenozoic fore-arc basins underlain by basic oceanic crust.

1.3 Previous geological studies

Wolf (1892) produced the first map and comprehensive geological and geographical synthesis of Ecuador. This remained the standard reference work until those of Sauer (1957, 1965), that included and complemented the earlier work by Tschopp (1948, 1953) based mainly on extensive studies of the sedimentary basins of Ecuador for the oil industry. Further systematic studies of these basins were carried out by the French Petroleum Institute (IFP, e.g. Faucher et al., 1968) that led to the publication of a 1:1000000 scale national geological map in 1969 (Servicio Nacional de Geología y Minería) and the first geodynamic synthesis by Faucher and Savoyat (1973). Between 1969-1980 systematic mapping by geologists of the Dirección General de Geología y Minas (DGGM) and the Institute of Geological Sciences (IGS), now BGS, under a bilateral Technical Cooperation Project between the Governments of Ecuador and the United Kingdom resulted in the publication of various 1:100000 regional geological maps and a new 1:1000000 national map and explanatory bulletin (DGGM and IGS, 1982; Baldock, 1982). Related publications on the geology and stratigraphy of Ecuador were those of Kennerley (1980), Bristow and Hoffstetter (1977), Bristow (1981) and Henderson (1977, 1979). Further more specialised regional studies include among others, Sigal (1968), Goossens (1972), Goossens and Rose (1973), Feininger (1977, 1978) and DGGM (1980).

A BGS-(DGGM/INEMIN)-CODIGEM technical cooperation project from 1986-1993 produced detailed reports and maps on the geology and mineral potential of the metamorphic basement of the Cordillera Real (Litherland et al., 1994; Aspden et al., 1995; BGS-CODIGEM, 1994a, b) in addition to a new 1:1000000 scale national geological and tectono-metallogenic maps (BGS-CODIGEM, 1993a, b).

1.4 Access

Access to the mapped area is good with eight major roads crossing the cordillera: Apagua-El Corazón-Moraspungo, El Corazón-Facundo Vela-Guaranda, Echeandía-Chazo Juan-Guaranda, Caluma-Guaranda, Ambato-Simiátug-Guaranda, Guaranda-Balzapamba-Babahoyo, Babahoyo-Chillanes-Pallatanga and Pallatanga-Riobamba as well as numerous local tracks many of which are passable in a four-wheeled drive vehicle. Exposure is generally abundant along many of these roads, but typically strongly weathered. In contrast the majority of the accessible rivers contain little outcrop being dominated by boulder size float material. Topographic maps at 1:50000 are available for the entire area and 1:100000 maps for 66% (Quevedo, Ambato, Chimborazo, and Riobamba). Due to climatic considerations, it is only possible to work in the summer months from (late) May to December, particularly in the páramo.

1.5 Acknowledgements

Administrative assistance to the project has been good in particular with the Ecuadorian counterpart organisation CODIGEM and the World Bank Coordinating Unit (UCP). Scientific support for the project has been provided by BGS, in particular the petrography and palaeontology divisions, while the administrative and personal support given to BGS staff by the International Division and in particular the Regional Geologist for Latin America Mr. R. B. (Rob) Evans is very much appreciated. Funding for the GIMP staff was provided by ODA and administered through Miar Townsend and Harshad Sarvia. Monitoring and advisory visits to the project on behalf of ODA, were undertaken by Geoff Walduck, and the ODA representatives in Quito Mike Dunn and Julie Ashdown, under HMA Richard Lavers, have provided invaluable assistance. The Ecuadorian project staff have worked with enthusiasm and dedication throughout the two years of Phase I of the GIMP project and without their contributions the aims of the project, in particular the successful completion of the fieldwork to schedule, could not have been completed. The GIMP secretary Fabiola Alcocer has undertaken all the numerous administrative tasks of the project admirably and particular thanks are due to the project cartographer Victor Acitimbay for producing the missing topographic base maps at 1:100000 and 1:250000 scales by hand.

Finally, we are all extremely grateful to our respective wives and families for accepting long absences from home for what to them was for no apparent logical reason!!

2. GEOLOGY OF THE WESTERN CORDILLERA OF ECUADOR

2.1 Tectonic setting

The Andes form a continuous mountain range over 7000 km along the active Pacific margin of South America, bounded to the west by a deep oceanic trench that extends from Patagonia to Colombia. The Ecuadorian part of this margin is today characterised by the essentially orthogonal subduction of the Nazca Plate beneath continental South America. In detail young oceanic crust (<20 Ma) produced at the Galápagos Rift Zone is being subducted in the Ecuadorian trench at an angle of 25-35° (Rea and Malfait, 1974; Lonsdale, 1978). The Andean Range can be conveniently divided into three segments: the Southern, Central and Northern Andes (Gansser, 1973; Sillitoe, 1974). The Western Cordillera of Ecuador forms part of the Northern Andes that are characterised by the presence of allochthonous terranes, including ophiolitic fragments (Feininger and Bristow, 1980; McCourt et al., 1984; Megard and Lebrat, 1987) that have been accreted to the margin of South America since the Middle Cretaceous (Egüez, 1986; Van Thournout, 1991).

2.2 Stratigraphic summary

The Western Cordillera of Ecuador comprises basalts to basaltic andesites, Cretaceous to Eocene, oceanic volcanic rocks and volcaniclastic turbidites of the Piñón, Cayo and Macuchi units, are overlain by clastic marine turbidites of Maastrichtian and Eocene age the Yunguilla and Apagua “units” respectively. The Cretaceous-Eocene sequences are intruded by Oligocene to Miocene, I-type, granitoid plutons and in part overlain by Oligo-Miocene to Pliocene sequences of acid to intermediate calc-alkaline volcanics capped by Quaternary strato-volcanoes. In southern Ecuador, the principal volcanic rocks of the Western Cordillera, the Celica (?), Sacapalca, and Saraguro sequences are calc-alkaline continental arc volcanics deposited directly onto the basement, that is, they are autochthonous and are thus distinguished from the allochthonous oceanic sequences to the north.

Since the studies of Wolf (1892) it has been recognised that the Western and Coastal Cordilleras are characterised by “rocas verdes y porfídicas”. Tschopp (1948) was the first to introduce a formal stratigraphy with the introduction of the term “Piñón Formation” for the basic volcanic sequences of the Costa, while retaining Wolf’s descriptive term for the basic volcanics of the Sierra. Sauer (1965) followed Tschopp in using the name Piñón Formation for the basic rocks of the Costa, and resurrected the term Cayo Formation (cf. Olsson, 1942), for the overlying Late Cretaceous, marine, volcano-sedimentary sequence, while for the basic rocks of the Cordillera he used the term “Formación Diabásica-Porfirítica”. Sauer (op. cit.) also re-introduced the term Yunguilla Formation, originally used by Thalmann (1946), for a sequence of Maastrichtian turbidites from the Quito-Nono-Nanegal area of the Western Cordillera.

Systematic mapping by geologists of the Institut Français du Pétrole in the mid-sixties resulted in the first attempts at correlating the stratigraphy of the Costa and the Western Cordillera and the name Piñón Formation was used in both areas for the Cretaceous oceanic basement comprising diabases and "rocas verdes". The name Cayo Formation was retained for the overlying volcano-sedimentary sequence on the coast and the term "Cayo de la Sierra" was introduced for its supposed equivalent in the Western Cordillera. In addition, two more Formations were described, the previously mentioned Yunguilla Formation of Maastrichtian to Paleocene age as suggested by micropalaeontological studies in the Nono area (Sigal, 1968) and a conformably overlying sequence of volcanic conglomerates, sandstones, greywackes and green-purple shales the "Cayo Rumi Formation" of assigned Paleocene age. Goossens and Rose (1973) meanwhile proposed that both the Piñón and "Formación Diabásica-Porfirítica" be renamed the Basic Igneous Complex and suggested a correlation with similar rocks from Costa Rica, Panamá and Western Colombia.

Subsequent evolution of the stratigraphy was influenced by the mapping of the IGS/DGGM project, and the tectono-stratigraphic interpretation of Henderson (1979) who proposed that the basic volcanic rocks of the Cordillera and the Costa were different in age and origin. In the early maps, both Formación Piñón and/or Complejo Básico Ígneo were used for the Costa rocks and Formación Piñón in the Sierra. From 1976 onwards, however, new names were introduced, the name Piñón was retained but restricted to the basaltic ocean floor volcanics of the Costa, while the name Macuchi Formation was created for the "rocas verdes" of the Western Cordillera interpreted as an island arc sequence and consisting mainly of basaltic to andesitic rocks, a high percentage of which had been reworked. Thus, the Macuchi as defined by Henderson, was predominantly sedimentary comprising turbiditic volcanic sandstones and siltstones, with lesser amounts of breccia, tuff and lava. The (?)overlying Late Cretaceous sedimentary rocks, formerly the "Cayo de la Sierra", were also considered to be part of the Macuchi Formation and renamed the "Chontal Member". In addition, the conglomeratic Cayo Rumi Formation on the Alóag-Santo Domingo road, was renamed the Silante Formation and interpreted to overlie the Macuchi, yet was itself overlain by the Yunguilla Formation of assigned Maastrichtian to Paleocene age. On this evidence therefore the Macuchi Formation is Late Cretaceous or older. Farther south however, to the east of La Maná, Early Eocene fossils were reported from the Macuchi Formation and andesitic sills within the sequence yielded Middle Eocene K-Ar ages. In addition, Eocene fossils were recorded from the overlying "Yunguilla-type" flysch sequence. The Macuchi Formation and by inference the overlying flysch unit were therefore interpreted to be strongly diachronous and attributed a (Late) Cretaceous to Eocene age along the length of the Cordillera.

Simultaneously with Henderson's re-interpretation of the Western Cordillera geology, Kehrer and Van der Kaaden (1979) subdivided the "Piñón de la Sierra" (Macuchi) rocks of the Alóag-Santo Domingo road section into three units. The Toachi Unit considered equivalent to the coastal Piñón Formation; the Pilatón Unit equated with the "Formación Cayo de la Sierra" (the Chontal Member of Henderson) and the distinctive, probably younger, Tandapi Beds.

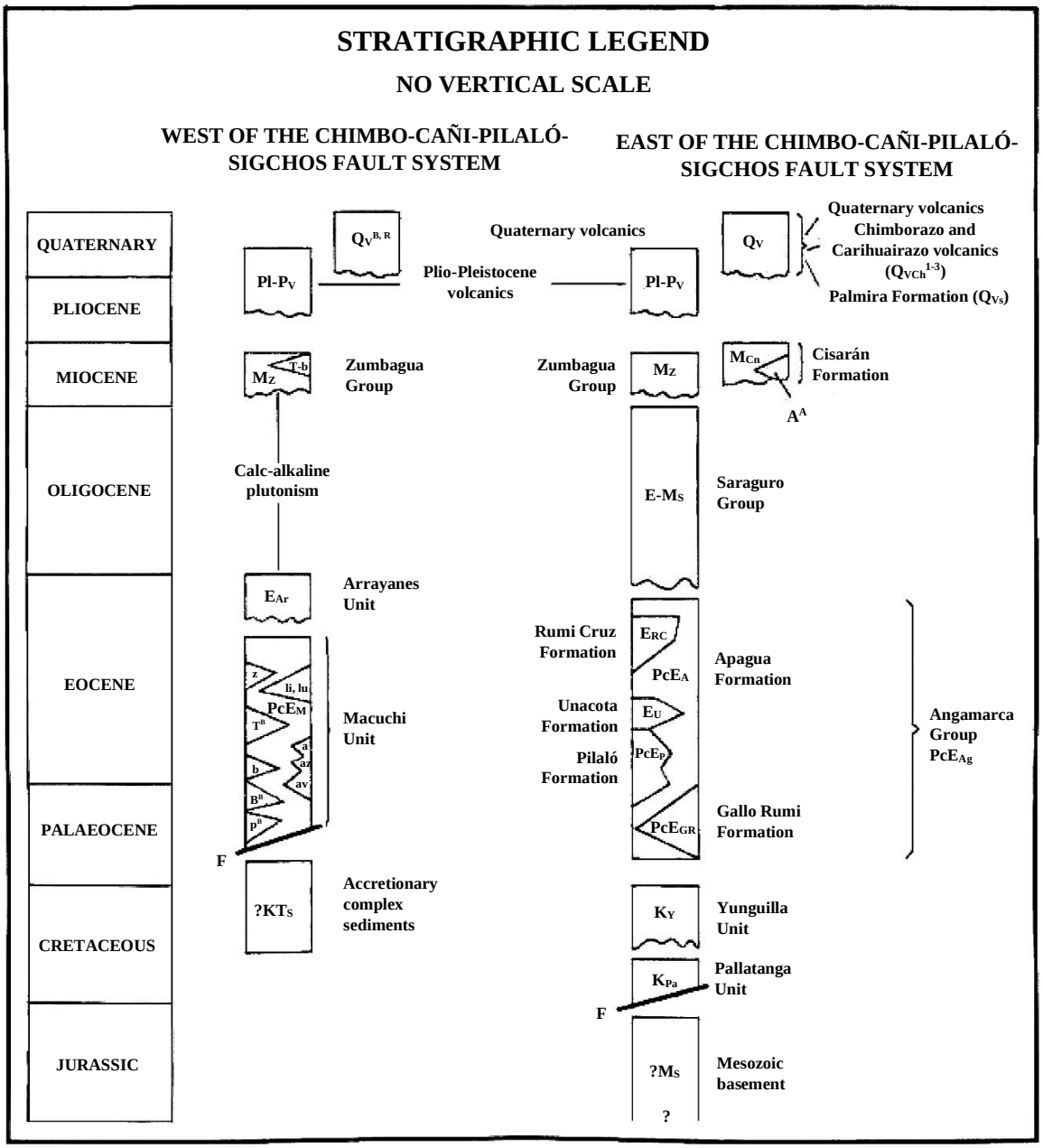

Figure 2. Stratigraphic relationships of major units

Kehrer and Van der Kaaden's nomenclature was resurrected by Egüez (1986) whose work in the central part of the Western Cordillera was fundamental to understanding and partly resolving the Macuchi-Yunguilla dilemma introduced by Henderson (1979, 1981). Egüez demonstrated the presence of two similar flysch sequences of different ages that had been mapped previously as a single unit, namely the Yunguilla Formation. East of La Maná the sandy turbidite sequence above the Macuchi, the Apagua Formation (Egüez, 1986), is of Middle to Late Eocene age; while the muddy turbidites and limestones of the Quito-Nono area, the type Yunguilla Formation, are of Late Cretaceous age. The recognition of two discrete turbidite sequences resolved much of the earlier confusion and removed the need for diachronous Formations. Egüez also re-interpreted the Silante-Yunguilla contact and reversed the relative age relations, postulating that the Silante overlies, in apparent conformable contact, the Yunguilla Formation. The age of the Silante remains problematic and poorly understood. It is clearly post-Maastrichtian in that it overlies and contains reworked fossils from the Yunguilla Formation (Savoyat et al., 1970), but the contact may represent a major non-sequence based on a Middle Miocene fission-track age of 16.8 ± 0.8 Ma from the Silante reported by Hughes and Bermúdez (1997). Egüez (1986) proposed that the Silante overlies the Macuchi, suggesting an Eocene or younger (?) Oligocene age. Van Thournout (1991), however, prefers a Paleocene age due to its conformable position above the Yunguilla and its unproven contact relationships with the Macuchi.

Egüez (1986) used the term Macuchi (s.s.) for a "volcanic-volcanosedimentary unit of Early to Middle Eocene age" and also recognised the presence of oceanic floor basalts in the Western Cordillera. He suggested the name Toachi Unit for these and equated them with the Piñón Formation of the Costa. For the associated siliceous sediments, the former Cayo de la Sierra, he proposed the name Pilatón Unit. In contrast, Santos and Ramírez (1986), although similarly recognising the presence of an Eocene turbidite sequence, which they also named the Apagua Formation, proposed to re-introduce the old stratigraphic nomenclature "Piñón de la Sierra" and "Cayo de la Sierra" for the Cretaceous basement sequences.

At about the same time, Lebrat (1985), on purely geochemical grounds, showed that the Macuchi Formation of Henderson was made up of three distinct types of "basalts", tholeiitic island-arc basalts, oceanic MORB and calc-alkaline arc basalts. The MORB material was correlated with the coastal Piñón Formation and the calc-alkaline volcanics were mistakenly correlated with the Cretaceous Celica Formation of southern Ecuador, when in fact they are part of the Oligocene Saraguro Group. The island-arc volcanics define the type Macuchi of the Western Cordillera. Similarly, Van Thournout et al. (1992) recognised the presence of three major volcanic sequences in the (North) Western Cordillera, an Early Cretaceous sequence of MORB basalts and overlying arc tholeiites, a mainly Eocene sequence of island-arc, tholeiitic to calc-alkaline, basalts and a Middle to Late Oligocene sequence of calc-alkaline volcanics of dominantly andesitic-dacitic composition. The first and second sequences correlate with the "Piñón/Toachi" and Macuchi Formations respectively of Egüez (1986) and Lebrat (1985).

Finally at least five calc-alkaline, continental-margin volcanic arc sequences are present in the Cordillera, the Late Cretaceous Celica Formation, the Paleocene-Eocene composite arc of the Sacapalca Group, an Oligocene to earliest Miocene arc typified by the Saraguro Group andesitic to rhyolitic pyroclastic deposits, Miocene volcanics and volcaniclastics of the "Pisayambo Volcanics" and the Plio-Pleistocene to Recent sequences that locally extend into the intermontane graben, for example, the Turi Formation. Many of these volcanic sequences are in general poorly defined and dated, and accordingly may contain the volcanic products of more than one phase of activity as presently mapped (cf. Pratt et al., 1997; Dunkley and Gaibor, 1997).

2.3 Geological summary of the study area

Mapped sequences in the area range in age from Cretaceous to Quaternary (Fig. 2), and are dominated by volcanic and sedimentary rocks. The oldest rocks are the oceanic basalts of the Pallatanga Unit, found in tectonic contact with two different sequences of turbidites, one of Late Cretaceous age and a second of Eocene age, the Yunguilla and Apagua sequences respectively. The latter is also in tectonic contact to the west with the volcaniclastic Macuchi Unit of Paleocene to Early-Middle Eocene age, that is intruded by numerous Oligocene to Miocene I-type granitoid plutons. Unconformably overlying these older units along the eastern edge of the area are extensive sequences of intermediate to acid continental margin calc-alkaline volcanic rocks of Mid-to Late Miocene age. The youngest rocks of the area are the products of Plio-Quaternary volcanism, andesitic lavas and dacitic-rhyolitic pyroclastics, and Holocene sedimentation.

Faulting is ubiquitous throughout the area and the dominant trend is Andean parallel, slicing up the Western Cordillera sequences into a series of NNE-SSW trending blocks linked by a complex anastomosing fault system bounded to the east and west by major, deep-seated, crustal structures (sutures): the Pallatanga Fault system and the Chimbo-Cañi Fault zone. Younger N-S trending faults with a significant vertical component are also present in the area such as the Río Chimbo Lineament. Folding although most probably present in all the pre-Pliocene units is most evident in the Yunguilla and Apagua sequences, which are folded about N-S to NE-SW axes.

3. LITHOSTRATIGRAPHY

3.1 Pallatanga Unit, K_{Pa} (McCourt et al., 1997)

3.1.1 Definition

The Pallatanga Unit is defined in this report. It corresponds to a Middle Cretaceous sequence of basic to ultrabasic rocks of oceanic affinity. Lithologies include basalt, basaltic volcanoclastics, microgabbro-diabase, peridotite and rare pillow lavas although these are much more common further south (Dunkley and Gaibor, 1997). The unit is exposed in the southeast of the area, north and northeast of Pallatanga (7265-97797) and northeast from the Malpote-Tambillo area (7240-97920) to the Quebrada Pungul section on the Guaranda-Riobamba road (7345-98230), as a series of tectonic slices within the Yunguilla Unit and Apagua Formation (sections 3.2 and 3.4).

The unit is characteristically highly tectonised. Serpentine and related minerals are common on joints and fractures and locally the degree of tectonism is sufficient to produce zones of fault gouge or crush, for example along the Río Pangor section (734-9795). Slickensides are relatively common and typically horizontal but unfortunately no convincing kinematic indicators were observed, it is likely however that many of the slickensides are related to recent movements. The most common rock types in the Pallatanga-Río Pangor section are gabbro, medium grained with a hypidiomorphic to granular texture, basalt and dolerite-diabase or microgabbro, dominated by a plagioclase-pyroxene mineralogy and a variably developed ophitic texture. Olivine is present both in basalts and ultramafic rocks. The latter range in composition from websterites to pyroxenites and are characteristically serpentinised to varying degrees. The basalts are porphyritic with phenocrysts of plagioclase, pyroxene and some olivine in a microlitic matrix or groundmass containing devitrified glass, and some are picritic in composition. The detailed petrography of this unit is included in Appendix 1, most of the rocks are moderately to strongly altered and crossed by veinlets containing calcite, prehnite, serpentine and quartz. Volcaniclastic lithologies are also present comprising basaltic tuffs and volcanic sandstones, often highly altered and variably recrystallised but with a recognisable mafic mineralogy dominated by plagioclase and pyroxene and containing sparse olivine.

In the section north of Malpote-Tambillo (724-9793) exposure is extremely poor and the area is marked by landslips within which are blocks of the above basic to ultramafic rocks, with subordinate red-purple mudstone and hyaloclastite. Almost identical rocks are recorded at outcrop along the road section to the east of Santa Rosa de Totoras (7275-98095) and as blocks and local exposure in the Ríos Cañi (728-9806), Pallo (727-98028) and Colorado (724-9802). On the Santa Rosa road section these red-purple lithologies are highly tectonised with narrow mylonitic zones, and in clear tectonic contact with sheared mafic-ultramafic lithologies.

3.1.2 Age

The age of the unit is unproven, but by tectono-stratigraphic correlation with similar lithologies of the Western Cordillera of Colombia and the Piñón Formation of the Costa it is interpreted to be of Cretaceous age, most likely Middle Cretaceous. In the coastal region of Ecuador, the Piñón is overlain conformably by Senonian to Maastrichtian sediments of the Cayo Formation, and is therefore pre-Senonian. Available radiometric ages from the basalts are not conclusive, but suggest an age of at least 113-107 Ma, Aptian-Albian (Baldock, 1982). A regional correlation with lithologically and geochemically similar sequences in the Western Cordillera of Colombia, the Grupo Diabásico or Formación Volcánica would suggest a post-Barremian but pre-Turonian age (McCourt et al., 1984). Thus, a Middle Cretaceous age is likely, ranging from Aptian to Turonian (125-90 Ma). Evidence from elsewhere in the Western Cordillera of Ecuador is in broad agreement with this age. Correlating the Pallatanga Unit with the Piñón de la Sierra or Toachi Unit of various authors, would suggest a pre-Cenomanian to Turonian age based on the reported presence of an ammonite *Inoceramus peruanus* (Faucher and Savoyat, 1973) and foraminifera *Globotruncana* sp., *Guembelina* sp., and *Globigerina* sp. (Sigal, 1968) in the overlying sediments of the (Cayo de la Sierra) Pilatón Unit. Pratt et al. (1997) report an ammonite that has affinities with the *Perispinctaceae* superfamily (Woods, 1997), from sandstones associated with basaltic pillow lavas regionally correlated with the Pallatanga Unit, along the Jubones Fault. Although too poorly preserved for specific identification, the above affinity would suggest an age range of (?)Mid-Jurassic to Early Cretaceous.

3.1.3 Interpretation

Geochemical investigations of the Pallatanga Unit rocks, show that they are tholeiitic oceanic basalts of MORB affinity (Appendix 2). In detail their LILE and HFS ratios and REE, chondrite-normalized, patterns show characteristics of T-type MORB (Sun et al., 1979) and are very similar to the Cretaceous tholeiitic volcanics of the Western Cordillera of Colombia (Lebrat et al., 1987; Marrinner and Millward, 1984). Thus, the Pallatanga Unit rocks represent either oceanic crust that belonged to a subducting plate, or the floor of a marginal basin, that presumably developed "east" of the subduction zone and its corresponding volcanic ensimatic arc. A third alternative is that the Pallatanga basalts belong to the younger Macuchi Unit, representing part of the oceanic basement on which the Macuchi arc was developed, and tectonically emplaced in their present position during the Late Eocene accretion of the arc (section 3.4.7). This interpretation, however, would suggest that the Pallatanga sequence was Early Tertiary in age. The model followed here is that the Pallatanga Unit represents fragments of an incomplete and dismembered ophiolite sequence, part of the Middle Cretaceous oceanic floor of the proto-Farallon Plate, accreted to the South American Plate in the Late Cretaceous and presently exhumed along the regional NE-SW boundary faults that mark the eastern limit of the Western Cordillera. Geochemical affinity with Colombia suggests either an oceanic ridge or oceanic plateau setting.

The volcaniclastic material associated with the Pallatanga Unit is more problematic. The tuffs and tuffaceous sandstones could be either contemporaneous or younger turbiditic sediments overlying the Pallatanga basalts. Comparable to the Piñón-Cayo relationship of the Costa. The highly tectonised nature of the Pallatanga Unit outcrop makes it impossible to elucidate its internal stratigraphy, nevertheless these volcaniclastics are considered here to be an integral part of the sequence. The red-purple mudstones and related hyaloclastites, however, are interpreted at this stage to be discrete and probably younger units, possibly part of the Macuchi Unit, tectonically emplaced to their present structural level, by subsequent faulting.

3.2 Yunguilla Unit, K_Y (cf. Yunguilla Formation Thalmann, 1946)

3.2.1 Definition

Corresponds to a sequence of fine-grained marine (T_{bde}) turbidites of Late Cretaceous age, characterised by thinly and irregularly bedded sediments. It crops out in the southeast of the area as a NNE striking belt that varies in width from 0.65 to 11.0 km, occupying a structural position along the eastern margin of the Western Cordillera immediately adjacent to the Pallatanga-Pujilí Fault zone.

Bedding is often highly contorted, typically wavy and discontinuous with evidence of soft-sediment deformation (slumping). The main lithologies are black-grey mudstones, locally calcareous, siliceous black siltstones, fine-grained well-sorted sandstones, and grey limestones. Very rare thin basaltic lavas and volcanic siltstones have been recorded within the outcrop sequence of mudstones in Qd. Cóndor Puñuna (736-9792) but not in proven intercalated contact, as a result their affinity is uncertain. Fissile black mudstones are the most characteristic unit, comprising thin 3-5 cm beds intercalated with fine-grained sandstones and more massive up to 12-15 cm thick grey siltstones. The limestones are best developed in the extreme north of the Yunguilla section interbedded with calcareous black mudstones in quarries worked by Cementos Chimborazo in the San Juan-Shobol area (744-9823). They rarely exceed 1 m thick and are separated by 10-20 cm thick black shaley mudstone bands. Their origin is probably bioclastic and are probably best interpreted as calcareous turbidites in that identified fauna, bivalves, ostracods and foraminifera are entirely marine but a mixture of shallow- and deep-water species.

Bedding consistently strikes NNE-NE and dips, to the SE and NW, varying from 30-70°. The folded and locally highly tectonised nature of the exposure makes it impossible to give an accurate estimate of thickness. In the type section to the north of Quito, however, the unit is at least 2000 m thick (Hughes and Bermúdez, 1997) which must be considered a minimum for the present area based on the outcrop width. The folding style is complex due to the thinly bedded nature of the sediments. In general terms, however, tectonic folds, as opposed to slump folds, are upright or slightly asymmetric, with widely spaced subvertical axial planes. To the east the Yunguilla Unit is unconformably overlain by the Miocene Zumbagua Group (section 3.7) and to the west is in contact with the Paleocene to Eocene Apagua Formation. The latter contact is well defined and apparently normal, although likely to be disconformable, with no obvious signs of faulting.

Plate 1a. Thinly-bedded muddy turbidite sequence of the Yunguilla Unit.
Trigoloma area (7275-97845)

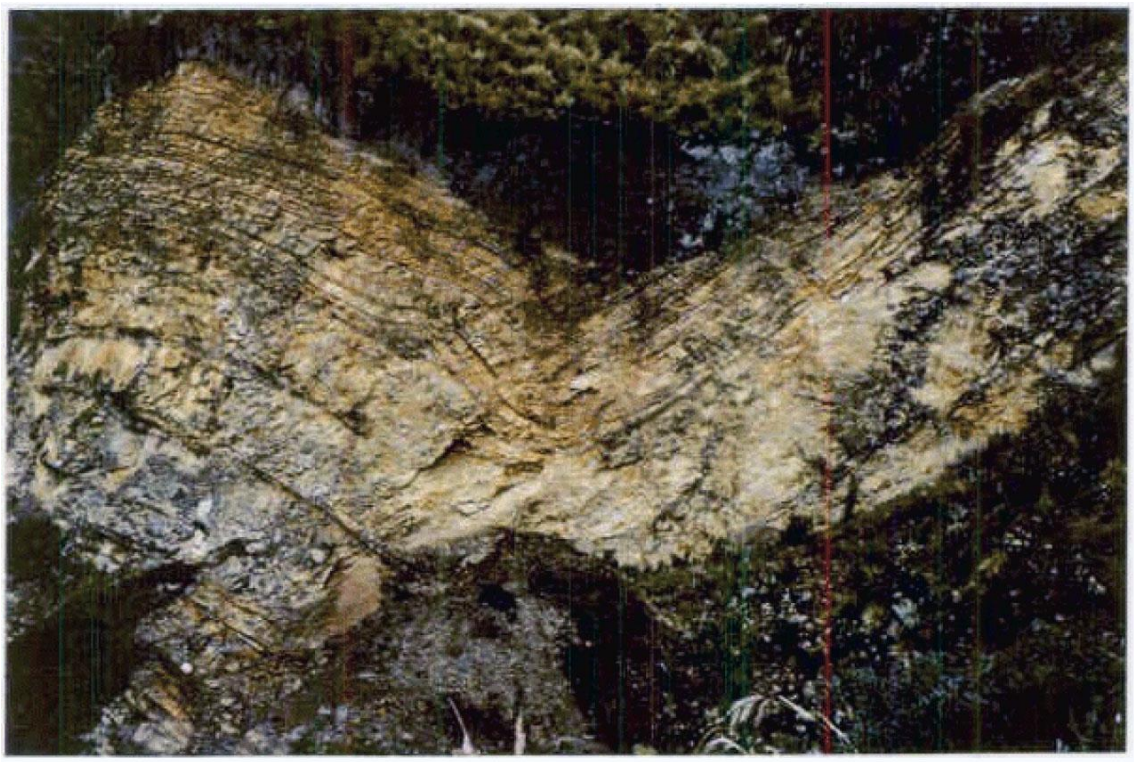

Plate 1b. Thin- to medium-bedded turbiditic sandstones and mudstones of the Yunguilla Unit with intercalated calc-arenites and limestones, San Juan area (7415-98195)

The petrography of the Yunguilla sandstones (Appendix 1) is characterised by a "mafic mineralogy" of pyroxene, amphibole, epidote-chlorite and opaques in addition to minor quartz and plagioclase, suggestive of a volcanic source that is supported by the presence of rare volcanic lithic clasts. The mudstone-siltstones, although dominated by clay minerals, also carry quartz, plagioclase and opaques, and, in common with the sandstones, aggregates of strained quartz, possibly indicative of a metamorphic input although characteristic "regional metamorphic" minerals, have not been recorded. Indeed, the overall quartz content of the Yunguilla sediments is very low.

3.2.2 Age

The age of the unit is well established in the mapped area from fossiliferous localities at San Juan-Shobol (7443-98229) on the Guaranda-Riobamba road and from the Qda. Cóndor Puñuna (7360-97920) some 20 km northeast of Pallatanga. Fossils from limestones and calcareous mudstones indicate an Early to Middle Maastrichtian age based on identifications by Thalmann (1946) and Savoyat et al. (1970) listed in Bristow and Hoffstetter (1977), and more recently by Wilkinson (1996), based mainly on foraminifera: *Heterohelix* sp., ?*Guembelina globulosa*, *Rugoglobigerina* aff. *rotundata*, *Rugoglobigerina* aff. *rugosa* and *Globigerinelloides* aff. *prairiehillensis.* A similar age has been assigned to the "Yunguilla Formation" from the type section to the north of Quito. The extensive faunal lists of Savoyat et al. (1970) quoted in Bristow and Hoffstetter (1977) as indicating a Danian age, have recently been reinterpreted by Wilkinson (pers. comm., 1977) as confirming a Late Cretaceous age, no younger than Maastrichtian.

3.2.3 Interpretation

The Yunguilla Unit represents marine turbidite fan deposition. The generally fine grain size and the characteristic presence of carbonate-rich beds indicate distal deposition away from a regular supply of coarse-grained clastic input. The petrography of the unit indicates an important mafic (volcanic) input. The Yunguilla Unit over much of its outcrop, occupies a position along the eastern margin of the Western Cordillera where it is intimately associated with ophiolitic rocks of the Pallatanga Unit. Regional evidence suggests that these oceanic rocks, and the emerging Cordillera Real, probably sourced much of the sediment for the Yunguilla Unit (section 7). Thus, is interpreted that the Yunguilla sequence was, at least in part, deposited onto the newly accreted "Pallatanga terrane" by turbidity currents possibly in a trench or fore-arc paleogeographic position.

3.3 Macuchi Unit, PcE_M (cf. Henderson, 1979; Egüez, 1986)

3.3.1 Definition

The Macuchi Unit is redefined in this report, following on from previous definitions by Henderson and Egüez (op. cit.) for reasons summarised in section 2.2. It corresponds to an Early Tertiary, sedimentary, volcaniclastic submarine arc sequence of basaltic to basaltic-andesite composition and dominantly tholeiitic affinity with intercalated pillow lavas, diabase minor "intrusions" and minor limestone horizons.

The unit is exposed throughout the western half of the study area and accounts for approximately 35% of the map, with a minimum thickness of 2000-2500 m. Its western contact with the Quaternary deposits is disconformable, often corresponding to a marked break of slope, and to the east its main contact is with the turbidites of the Apagua Formation. Although locally difficult to prove in the field, this latter contact is interpreted as a major fault juxtaposing two broadly contemporaneous, but lithologically distinct sequences. It is a high-angle, westerly dipping, reverse fault in the south of the area exposed immediately east of the Río Chimbo at (7240-97850) and along the Río Colorado-Pallo (7236-98000) and is interpreted as a normal fault in the area to the southwest of Angamarca. Elsewhere, this same contact where exposed is sharp but not recognizably faulted.

The Macuchi Unit although comprising a variety of lithologies is difficult to subdivide, since most internal contacts are either transitional or not exposed. The main rock types recognised are volcanic sandstones, breccias, tuffs, volcanic siltstones, cherts, pillow breccias, hyaloclastites, diabase-microgabbro, sub-porphyritic basalts and calcarenites in approximate order of abundance, although the first three or four lithologies predominate. The volcanic sandstones and breccias are intimately related and are massive, hard, green, poorly sorted, medium- to coarse-grained and lithic-rich. The lithic fragments comprise fine-grained purple-green clasts of altered (?) lava and vesicular basaltic andesite in a chloritised matrix containing volcanic glass often as recognisable shards. Some of the sandstones are turbidites, thin- to thick-bedded with rare grading and loading structures that indicate eastward younging, as seen for example in the Estero Sapanal (6967-98882). Breccias are unsorted and matrix-supported, basaltic in composition and commonly associated with hyaloclastites. Sequences of pillow lavas and pillow breccias with intercalated cherts are present for example south of El Corazón at (7129-98715), but are not common and are typically deeply weathered. The lavas are fine-grained with vesicular rims and plagioclase-pyroxene phyric. Unfortunately, it proved impossible to obtain material fresh enough for geochemical analysis, but published data from the type section (Lebrat, 1985), confirmed by Hughes and Bermúdez (1997), indicate a basaltic-andesite composition. Calcareous rocks are found only in the Balzapamba area, for example, Chaupiyacu (699-9805) and comprise calcarenites and limestones dominated by calcite (>90%) ± epidote-quartz. They have been contact metamorphosed producing high grade cordierite-bearing hornfels and marbles characterised by the presence of quartz-wollastonite-biotite and rare garnet. As a result, any fossils that may have been present have been completely destroyed. The limestones reported by Henderson (1979) from his Macuchi Formation at the Chimbo hydroelectric plant are considered here to belong to the Angamarca Group, occupying a similar stratigraphic level within the group of the Unacota Formation (see below).

Plate 2a. Basaltic-andesite pillow lavas and pillow breccias. Macuchi Unit, Río Chimbo area (7202-97714)

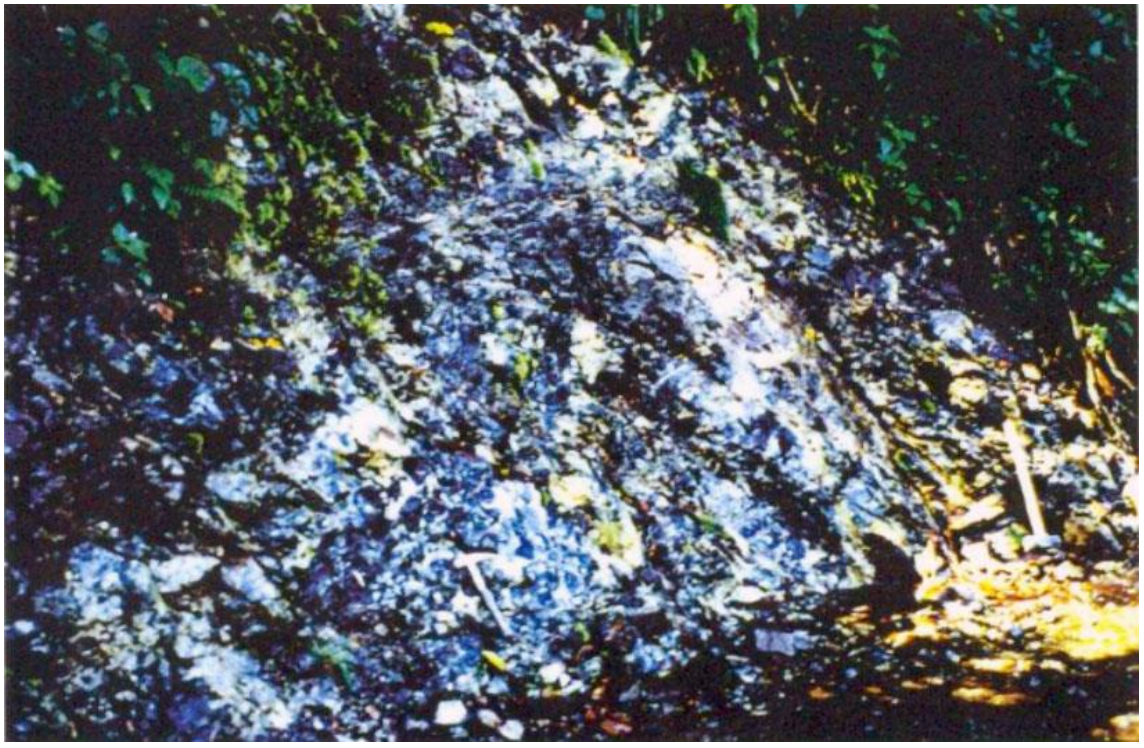

Plate 2b. Breccias and hyaloclastites, Macuchi Unit, Río Chimbo area at (7224-97848)

The detailed petrography of the main lithologies of the Macuchi Unit is given in Appendix 1. Essentially the volcanic rocks comprise microphenocrysts of plagioclase with varying but subordinate amounts of (clino)pyroxene ± amphibole ± olivine in an altered groundmass of plagioclase-opaques ± amphibole ± chlorite, various secondary minerals and some volcanic glass. The volcanoclastic rocks comprise plagioclase and pyroxene, in addition to lithic clasts, quartz, chlorite-epidote, actinolite, biotite, shards and a mixture of prehnite-pumpellyite-zeolite. The latter are interpreted to indicate that the Macuchi rocks have undergone low-grade non-deformative metamorphism similar to the hydrothermal-burial type produced during the development of a submarine volcanic arc (cf. Aguirre and Atherton, 1987).

3.3.2 Age

The age of the Macuchi is relatively well defined, although the base is nowhere exposed. Lower to Middle Eocene radiolarians are reported from siliceous sediments in the Qdas. Milagro-Tilipulo (714-9901), north of the map area (Egüez, 1986). In the same section Early Eocene foraminifera are reported from a lenticular limestone horizon and cross-cutting andesitic sills are dated at 42 ± 2 and 36 ± 2 Ma (Mid-Late Eocene). In addition, the Macuchi sequence is intruded and hornfelsed by a suite of plutons that range in age from 35-11 Ma, and thus is pre-Oligocene. In conclusion the unit is Early Eocene or older and it is possible that the older parts of the sequence are Paleocene in age.

3.3.3 Whole-rock geochemistry

Six samples were analysed for major oxides and a total of 20 trace elements (Appendix 2). In addition, selected samples were submitted for REE analysis. Fresh unaltered material is scarce in the Macuchi sequence and it is accepted that the analysed samples although relatively fresh are not ideal. Nevertheless, the more immobile elements, particularly the HFS elements, provide a valuable indication of the probable tectonic setting of the unit.

The samples are subalkaline basalts or basaltic andesites of tholeiitic (dominantly) to calc-alkaline character. All the samples have normative quartz and the Ti/V ratio is low, features typical of island arc basalts. The majority of the trace element tectonic discrimination diagrams indicate that the Macuchi rocks are volcanic-arc, that is orogenic or subduction, basalts and, in contrast to the Pallatanga Unit rocks, have no MORB affinity. Although the diagrams are not uniquely conclusive, they emphasize the island arc affinities of the Macuchi population. This conclusion is supported by the normalized spider plots, that have a subduction-related signature with negative Ta-Nb and Ti anomalies relative to adjacent elements. Data from other sections of the Macuchi Unit (Lebrat et al., 1987; Hughes and Bermúdez, 1997) confirm these broad conclusions as does the available mineralogical evidence from pyroxenes (Aguirre and Atherton, 1987), REE patterns from the Macuchi rocks (Appendix 2, Fig. 38) are relatively flat, displaying a lack of heavy-REE fractionation and only minimal enrichment of LREE's (Lebrat, 1985; Van Thournout et al., 1992) indicative of island arc tholeiites to moderately differentiated calc-alkaline basalts from a "mature" arc. In conclusion the geochemical characteristics of the unit most closely correspond to those of tholeiitic basalts with some calc-alkaline affinities and suggest an oceanic island arc setting.

3.3.4 Interpretation

All the lithologies and facies present in the Macuchi Unit, with the exception of the limestones, are considered to be the products of submarine effusive volcanism. The pillow-lavas, amygdaloidal to sub-porphyritic basalts, diabase and hyaloclastites represent the eruptive material, while the volcanic sandstones and breccias represent reworked material deposited on the slopes of the volcanic edifices, mainly by mass-flow. The sandstones and siltstones are turbidites representing deposition from low- to medium-density currents "derived from" the Macuchi volcanic centre. The limestones are interpreted as the remnants of fringing reefs to the arc. It is therefore proposed that the Macuchi Unit represents an ensimatic volcanic arc the product of an (?)eastward dipping intra-oceanic subduction zone. The coeval Apagua Formation, is interpreted to have been deposited in the marginal sea that lay between the Macuchi arc and the South American plate, or in a fore-arc/trench setting along the continental margin. The present-day juxtaposition of the two reflects the Late Eocene collision and accretion of the allochthonous oceanic Macuchi arc to the continental South American Plate (cf. Section 7).

3.4 Angamarca Group, PcE_{Ag} (Hughes and Bermúdez, 1997)

This newly defined group comprises the Pilaló Formation, the Apagua Formation, the Unacota Formation, the Rumi Cruz Formation and the Gallo Rumi Formation (Fig. 2) and the total thickness of the group is of the order of 4000 m. The clastic turbidites of the Apagua Sandstone Formation are the dominant lithology and throughout most of the area define the main faulted contact with the volcanoclastic Macuchi Unit to the west.

3.4.1 Pilaló Formation, PcE_P (Hughes and Bermúdez, 1997)

***3.4.1.1 Definition*:** The Pilaló Formation is a volcanoclastic sequence corresponding to coarse-grained sandstones and breccias characterised by igneous lithoclasts of andesitic composition present in the northwest of the map, south of the type area at the village of Pilaló (723-9895).

The sequence was originally named the Pilaló Volcanics by Egüez and Bourgois (1986) but has been reinterpreted by Hughes and Bermúdez (1997) as a discrete Formation of the Angamarca Group. Its upper contact with the Middle Eocene Unacota Formation is not exposed in the present area but Hughes and Bermúdez report an apparent conformable, possible non-sequence, contact in the Río Pilaló. In the area of Cerro Cóndor Matze (727-9885) sandstones of the Apagua Formation, that appear to conformably underlie the Pilaló Formation are of Early to Mid-Paleocene age (section 3.4.2). While the Pilaló Formation is intruded by a plagioclase-phyric basalt/andesite stock of Late Oligocene age (24.7 ± 1.2 Ma, K/Ar, WR, Egüez and Bourgois, 1986).

***3.4.1.2 Age*:** There is no age evidence from the Pilaló Formation itself. Based on the above field relationships, however, the Pilaló Formation would appear to be of Paleocene age, most probably extending into the Eocene.

3.4.2 Apagua Formation, PcE_A (Apagua Unit of Egüez, 1986)

***3.4.2.1 Definition*:** Corresponds to a coarsening-upward sequence of regularly bedded sandy turbidites, comprising alternating sandstones and mudstones in beds 10-30 cm thick often with a conspicuous orange-brown colour (?goethite) at outcrop.

The type section is exposed on the La Maná-Latacunga road close to the village of Apagua (7307-98932) where Egüez (1986), Egüez and Bourgois (1986) and, Santos and Ramírez (1986) originally defined the Apagua (Unit) Formation, distinguishing it from the Yunguilla Formation of Henderson (1979). Their Apagua "Formation" comprised two members, a lower one consisting of fine- to medium-grained clastic turbidites and an upper one of coarse to very coarse conglomerates, both of which are assigned an Eocene age. These correspond in the present classification to the Apagua and Rumi Cruz Formations of the Angamarca Group (Hughes and Bermúdez, 1997).

The Apagua Formation is exposed along the eastern margin of the map. There are two main sections. The northern one extends from the type section of Egüez and Bourgois (1986) and, Santos and Ramírez (1986) southwards to Angamarca (7304-98768), and the southern one extends southwest from the main Guaranda-Riobamba road to Pallatanga. In the northern section, the Formation is about 1500 m thick and corresponds to steeply dipping, well-bedded siltstones and fine-grained sandstones in Bouma T_{cde} sequences, with massive coarser-grained sandstones becoming more common towards the top. The sandstones are graded, locally with pebbly basses and weakly developed sole structures, and the sequence as a whole represents deposition from low- to high-density turbidity currents (Hughes and Bermúdez, 1997). In the southern section, the Formation is well exposed, but folded, along the Guaranda-Riobamba road section east from Qda. San Juan to Qda. Tililag. It comprises characteristically well-bedded, fine- to medium-grained micaceous sandstones with intercalated thinly bedded silicified black siltstones showing parallel lamination. Dewatering structures, flute casts and probable ripple structures have been recorded from the section and the sandstones are commonly graded, all interpreted to indicate deposition from low-density turbidity currents as T_{cde} sequences.

Petrographically the sandstones are characterised by a high quartz content and the presence of sericite mica, they are clean and well-sorted with very few lithics and virtually no mafic minerals apart from minor amounts of chlorite-biotite and epidote.

A sequence of black, variably calcareous, highly contorted, slumped and tectonised mudstones with intercalated limestones and siltstones is present on the main Guaranda-Riobamba road section extending NE along the Río Ganguis from Pungul (7350-98230). These are considered to be part of the Yunguilla Unit on lithological correlation with the San Juan-Shobol section, rather than the Apagua Formation as shown on the National Map (BGS and CODIGEM, 1993a). Along strike, to the SW, from this section are further exposures of muddy calcareous turbidites, along with tectonised basic rocks of the Pallatanga Unit. Our interpretation is that these Cretaceous rocks form the local basement of the Apagua Formation and are exposed as a result of folding and/or faulting.

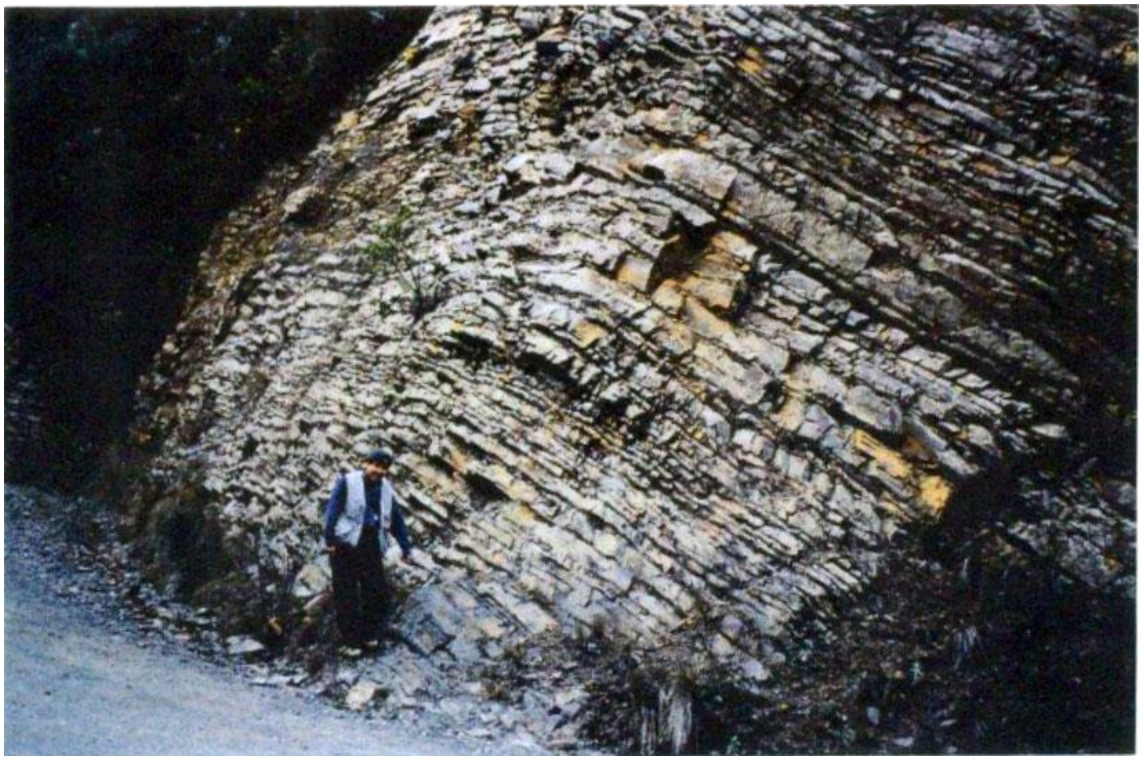

Plate 3a, b. Typical regularly bedded sandy turbidites of the Apagua Formation (Angamarca Group). Río Tauri section at (7363-98220)

***3.4.2.2 Age*:** The Eocene age for the Formation is based on abundant palaeontological evidence (e.g. Santos and Ramírez, 1986; Egüez, 1986). In the "type" section, the turbidites locally overlie limestones of the Unacota Formation with apparent conformity, and foraminifera from the limestones indicate Middle to Late Eocene ages, although a Middle Eocene age is preferred by Egüez and Bourgois (1986). Foraminiferal ages from the Apagua turbidites also indicate an Early to (?)Late Eocene age (Egüez, 1986). Evidence from the present area is sparse, however, rare fossils encountered in intercalated mudstones from the Angamarca area, at Mayhua Pucara (7275-98853), indicate a broad Paleocene-Eocene age based on *Nuttallides crassaformis*, *Gyroidinoides plantus*, *Trochammina* sp., *Turrilina* sp. cf. *robertsi* (Wilkinson, 1997). The presence of the diagnostic planktonic foraminifera *Morozovella pseudobulloides* however confirms an Early to Mid-Paleocene age (foraminiferal zones P1-P3) for the lower part of the sequence. A possible Late Cretaceous (Coniacian-Maastrichtian) age suggested by the reported presence of three species of *Heterohelix* from the same stratigraphic level in the sequence (Petroproducción Report 045-PPG-96, 1996) could not be confirmed by BGS biostratigraphers, who were unable to establish the presence of this genus in the same sample. In addition, the presence of *Turrilina brevis*, which is confined to the Palaeogene (zones P6-P15) would strongly suggest that the identified Cretaceous fauna is the result of reworking possibly (?)from the Yunguilla Unit. In conclusion therefore the age of the Apagua Formation as defined in this report is taken to be Early Paleocene to Middle to Late Eocene.

3.4.3 Unacota Formation (E_U) (cf. Unacota Limestone, Egüez, 1986)

***3.4.3.1 Definition*:** Corresponds to a horizon of thick-bedded, parallel-laminated, sparites and massive micrites intercalated with the Apagua Formation.

The Formation is poorly exposed on the map, but north of 1°S it is well exposed on the La Maná-Latacunga road, 3 km SW of Apagua, and in the Río Chilcas (7291-98947). Here it is unconformably overlain by thin-bedded mudstones and siltstones of the Apagua Formation (Hughes and Bermúdez, 1997). The nature of the limestones and the presence of stromatolite-type algal mats on the above road section support an interpretation as algal mounds or reefs.

***3.4.3.2 Age*:** Abundant algal and foraminiferal evidence indicates a Mid- to Late Eocene age.

3.4.4 Rumi Cruz Conglomerate Formation, E_{RC} (Hughes and Bermúdez, 1997)

***3.4.4.1 Definition*:** Corresponds to massive, thickly-bedded and laterally extensive sheets of conglomerates, intercalated breccias and coarse-grained sandstones, at the top of the Angamarca Group.

The Formation is best exposed to the south of the village of Apagua, where it forms a 20 km north-south trending ridge of very coarse conglomerates, breccias and coarse-grained sandstones that conformably overlie the Apagua Formation. The conglomerates are polymictic but of a uniform composition typified by well-rounded clasts, 2-15 cm in diameter, of quartz, chert, black silicified mudstone and rare muscovitic granite and are both clast- and matrix-supported. The medium-bedded sandstones present locally within the sequence are characterised by coarsening-upward cycles. Fossil wood fragments have been reported by Hughes and Bermúdez (1997) from the conglomerate sequence along with thin red siltstone horizons, the latter are also found in the present area.

***3.4.4.2 Age*:** The age is unproven, however, in that the conglomerates are in conformable contact with the Apagua turbidites which in turn overlie the Unacota Formation, they are assigned a post-Middle Eocene age.

3.4.5 Gallo Rumi Conglomerate Formation, PcE_{GR} (McCourt et al., 1997)

***3.4.5.1 Definition*:** Corresponds to a local sequence of conglomerates, micro-conglomerates and pebbly quartz arenites intercalated with massive sandstones within the main outcrop of the Apagua Formation around the village of San José de Gallo Rumi (7369-98218) on the Guaranda-Riobamba road section.

The conglomerates are characterised by their high quartz content. Milky quartz clasts comprise up to 70% of the population, along with silicified black mudstone or chert, and rare volcanic rocks. The clasts are rounded to sub-rounded, but rarely exceed 1-3 cm, contrasting these conglomerates with those of the Rumi Cruz Formation, and some imbrication and grading are present locally. The conglomerates are of the order of 600 m thick, although complicated by folding, and form a series of well- defined NNE-trending ridges. In addition, small conglomeratic lenses are found within the massive sandstones of the Apagua Formation.

***3.4.5.2 Age*:** Although there is no palaeontological evidence for the age of this Formation, it is interpreted to be the same general age as the Apagua Formation and accordingly is assigned a Paleocene to Eocene age. Due to its structural position close to the normal contact of the Apagua Formation and the Yunguilla Unit at the east end of the Guaranda-Riobamba road section, however, it may belong to the lower part of the Angamarca Group.

Plate 4a. Massive to thickly-bedded conglomerates and sandstones of the Gallo Rumi Formation (Angamarca Group) N of San José de Gallo Rumi (7370-98218)

Plate 4b. Conglomerates of the Gallo Rumi Formation at San José de Gallo Rumi

***3.4.5.3 Interpretation*:** The Angamarca Group is a coarsening-upward basin-fill sequence, that shows a progradation from a submarine fan to fan-delta environment (Hughes and Bermúdez, 1997). Individual lithologies represent either turbidites from a volcanic source (Pilaló Formation) or reefal limestone intervals (Unacota Formation). The clastic sediments of the Apagua Formation are interpreted to be the lower to middle parts of deep-sea fans, representing deposition from low- to high-density turbidity currents. The coarse conglomerates and breccias of the Rumi Cruz Formation are considered to be fan-delta deposits. The very high degree of rounding of the clasts implies recycling, possibly from older fluvial deposits. Conglomerates are relatively common within submarine fan sequences, being interpreted as feeder channel deposits (Reading, 1986), but normally have a very limited lateral extend and a channel geometry, in marked contrast to the Rumi Cruz conglomerate-breccias. The presence of fossil wood and "red-beds" towards the top of the sequence, plus the sheet-like nature and great lateral extent of the conglomerates, suggests a terrestrial influence. Accordingly, a fan-delta environment seems a likely scenario with the mature clast material derived from reworking of a fluvial hinterland source being redeposited by mass flow into shallowing water. If this model is accepted then changing from a submarine fan environment to a fluvial one implies uplift, and may indicate a major tectonic event in the Late Eocene. Although the source area for the sediments is unproven, the high percentage of quartz supports a continental sialic hinterland possibly the present Cordillera Real. The lack of true metamorphic debris, however, is not fully consistent with this explanation and it may be that much of the unit is (semi-) allochthonous to the cordillera (?)representing trench deposits outboard of the continental landmass rather than continental margin sedimentation in a back-arc environment as proposed by Egüez (1986).

3.5 Arrayanes Unit, E_{Ar} (McCourt et al., 1997)

3.5.1 Definition

This volcanosedimentary unit is defined in this report. It corresponds to a well-stratified, subhorizontal, sequence of fine-grained sediments and basaltic andesite to andesitic "lavas" of probable latest Eocene age, that is present only within the area of the Macuchi outcrop. The type section is located west and northwest of the village of Los Arrayanes (7135-98513).

The Arrayanes Unit comprises regular bedded siliceous mudstones and fine-grained quartz-arenites, mafic-rich green fine-grained volcanic sandstones with subordinate tuffs, and intercalated aphyric basalts or plagioclase-phyric sub-porphyritic basaltic-andesites. Outcrops of the Arrayanes Unit are characteristically a yellow-brown "ochre" colour with prominent manganese staining on fracture and joint surfaces. Although dips are variable the unit is characterised by sub-horizontal to low-dipping strata. Contacts with the underlying Macuchi are poorly exposed but appear to be discordant, they are however definitely not tectonic, while the unconformably overlying sequences are calc-alkaline volcanics of the Zumbagua and younger units.

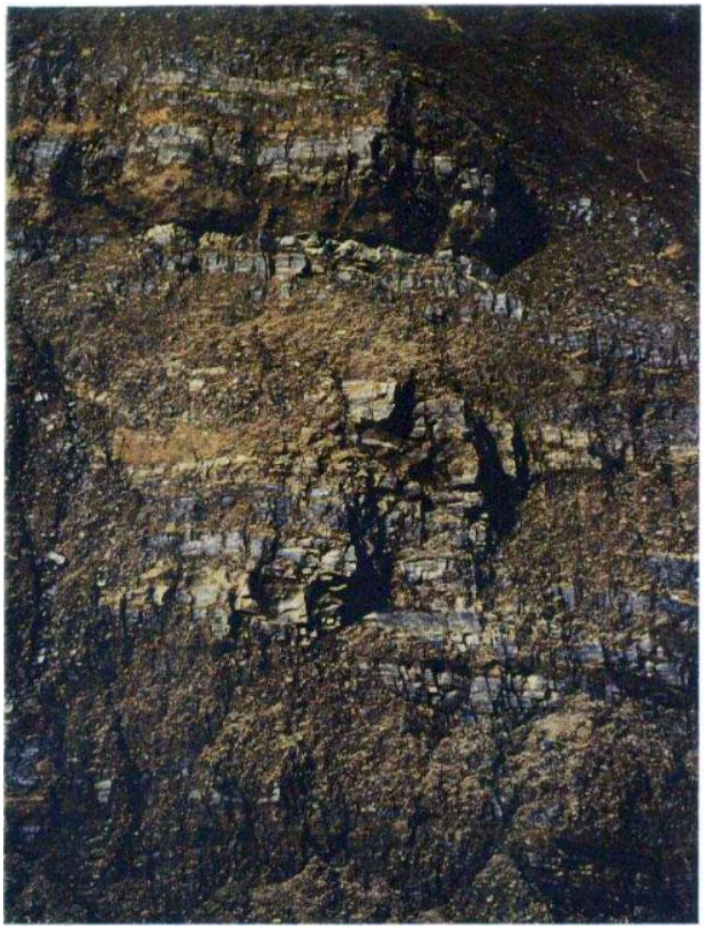

Plate 5a. Flay-lying fine-grained sandstones and siltstones of the Arrayanes Unit, Palma Loma area (7045-98330)

Plate 5b. Basaltic “lava” within sediments of the Arrayanes Unit at Santa Ana (7022-98306)

Petrographically the sediments are fine-grained, well-sorted, sandstones and mudstones, interpreted as distal turbidites, in T_{abce} cycles with a high volcanic input. Grading although present is not common, but convolute laminations and flame structures both indicate correct way-up, younging to the southeast. In thin section they are dominated by a quartz-plagioclase-epidote, ± pyroxene, ± chlorite, ± mica, ± amphibole mineralogy in a clay-rich matrix with opaques. The intercalated volcanics, probably lavas or (?) sills, are porphyritic basaltic andesites with phenocrysts of plagioclase (An_{54-60}), hornblende and subordinate clinopyroxene of diopsidic-augite composition and aphyric basalts. The latter have microphenocrysts of plagioclase (An_{62-65}), pyroxene and amphibole in an aphanitic groundmass containing devitrified glass. The four samples analysed from this unit have compositions that confirm their petrology and are classified as low-k tholeiitic to moderately differentiated calc-alkaline basaltic andesites.

3.5.2 Age

Over 20 samples submitted for palaeontological analysis have proven to be barren. A sample from exposures to the west of Chillanes (7115-97882) collected in 1992 (M. Litherland, pers. comm.) yielded rare calcareous microfauna, specifically planktonic foraminifera. These were tentatively identified as *Globorotalia* cf. *wilcoxensis* (Wilkinson, 1992) suggestive of a (?)Late Paleocene to Eocene age and as a result the sediments were assigned to the Apagua Unit (Formation) on the 1:1000000 National Map (BGS-CODIGEM, 1993). Regional considerations, however, strongly suggest that the Arrayanes Unit is of Late Eocene age. It is lithologically and petrographically distinct from the Apagua Formation, but is also distinguished from it by a lack of folding. This is interpreted as indicating that the Arrayanes Unit post-dated the tectonic activity that deformed the Paleo-Eocene Apagua and Macuchi sequences. This deformation is interpreted to be the result of the collision and accretion of the Macuchi Arc in the Late Eocene. In that the sediments of the Arrayanes Unit are hornfelsed by plutons of the Oligo-Miocene plutonic arc of the Western Cordillera (section 4), it must be older than 35 Ma, and effectively limits the deposition of the unit to the latest Eocene (38-35 Ma).

3.5.3 Interpretation

The Arrayanes Unit is tentatively interpreted as a sequence of distal turbidites deposited onto the Macuchi “allochthonous block” either following or during its accretion to the South American Plate. The sediments may be derived, in part, from erosion of the emergent arc and the volcanics represent the final stages of activity of the arc, accounting for their calc-alkaline character, reflecting continued subduction during and after its initial collision and docking with the continent. It is possible that this volcanism is the “northern continuation” of the Saraguro Arc of southern Ecuador (Dunkley and Gaibor, 1997).

3.6 Saraguro Group (undifferentiated), E-M_S (Dunkley and Gaibor, 1997)

3.6.1 Definition

Corresponds to a sequence of intermediate to acid, calc-alkaline, subaerial volcanic rocks with important (ignimbritic) welded tuff horizons at the top and andesitic lavas towards the base. It correlates, in part, with the Saraguro Formation of Kennerley (1973), the Saraguro Group of Baldock (1982) and the Saraguro Volcanics of the National Map (BGS-CODIGEM, 1993a). The majority of the group is Oligocene in age although actual dates range from the Late Eocene to Early Miocene (38.6-22.8 Ma).

On the present map it is limited to an approximately north-south strip, some 20 km long and 2-4 km wide, exposed "along" the Macuchi-Apagua contact to the east of Guaranda (7230-98240), and lithologically similar rocks close to Columbe (7539-97910). These Saraguro Group rocks comprise a mixture of grey-green porphyritic, plagioclase ± hornblende-phyric, andesitic lavas, breccias and tuffs, the latter with shards. They disconformably overlie the Apagua Formation and are unconformably overlain by younger volcanic rocks of the Zumbagua Group. The lavas are fresh and comprise andesine plagioclase (An_{50}), augite and hornblende phenocrysts in a matrix of plagioclase microlites and volcanic glass. A sample (M3-970) submitted for geochemical analysis corresponds to a calc-alkaline basaltic andesite.

3.6.2 Age

In that it overlies the Apagua Formation and is unconformably overlain by the Middle Miocene Zumbagua Group, the age of this sequence is relatively well controlled. Samples from the Guaranda section submitted for age dating proved unsuccessful, but a sample from lithologically similar volcanics in the extreme southeast of the area at Columbe (7539-97910), yielded a fission track (FT) age on zircon of 24.4 ± 1 Ma (Late Oligocene). In regional terms, however, the sequence of volcanic rocks east of Guaranda probably correlates with the Unidad Huigra of Egüez et al. (1992) with a K/Ar age of 36 ± 0.9 Ma. This unit corresponds to the Ocaña Formation of Dunkley and Gaibor (1997) with FT dates of 37 ± 1.5 Ma and 39 ± 1.3 Ma (Late Eocene). Compositionally, however, the Guaranda Saraguro rocks correlate better with lithologies of the (?)Oligocene Puñay Unit of Dunkley and Gaibor (1997) exposed to the west of Huigra.

3.6.3 Interpretation

The Saraguro Group is considered to be the result of continental margin volcanism. It reflects eastward directed subduction that was initiated at, or close, to the Oligocene-Eocene boundary, following the accretion of the Macuchi arc terrane. In very broad terms, the products of this volcanic episode were andesitic lavas and tuffs followed by dacitic to rhyolitic tuffs as the arc matured.

3.7 Zumbagua Group, M_Z (Hughes and Bermúdez, 1997)

These rocks are depicted on the 1982 and 1993 1:1000000 National Maps as part of the "Formación Pisayambo" and "Volcánicos Pisayambo" respectively, a very extensive volcanic and volcano-sedimentary Miocene to Pliocene sequence that occurs throughout central Ecuador. The local name Zumbagua (Group) is herein considered more appropriate for the sequences exposed on the eastern margin of the Western Cordillera, that form much of the high rugged terrain to the west and southwest of Ambato extending north to the young volcanic centres of the Illinizas and Quilotoa and south to the Chimborazo volcano. The sequence is well-exposed along the Apagua-Pujilí road especially around Zumbagua (734-9894) from where it takes its name.

3.7.1 Definition

Corresponds to a sequence of volcanosedimentary rocks as defined by Hughes and Bermúdez (op. cit.), comprising coarse-grained sandstones and debrite breccias of Miocene age. In addition, plagioclase-phyric andesitic to dacitic tuffs and lahars are included in the present map.

The Zumbagua Group covers much of the northeast part of the map, forming the high ground, in excess of 3500 m to the northeast of Salinas (7207-98450) and east of Simiátug (7272-98576) and Angamarca (7303-98768). It unconformably overlies Paleogene sequences of the Apagua, Arrayanes and Macuchi units, as well as the Saraguro Group, and is locally overlain unconformably by Plio-Quaternary volcanics. The lithologies of the Zumbagua Group are predominantly coarse-grained, comprising very poorly sorted (?reworked) sandstones and unsorted, matrix-supported, debrite breccias, in beds up to several metres thick. In addition, plagioclase-phyric, greyish, andesitic to dacitic, tuffs are present in the western part of the sequence, and are overlain by spectacular, horizontal, composite laharic units over 40 m thick around Salinas. The sandstones are tuffaceous, lithic- and crystal-rich (quartz-plagioclase-K feldspar-amphibole-biotite), and lithic clasts within the sandstones, breccias and lahars are almost exclusively of intermediate composition volcanic material. The debrite-breccias are massive and chaotic, and are clearly the products of mass-flow processes, probably locally derived "laharic flows" triggered by volcanic activity.

3.7.2 Age

The age of the Zumbagua Group is Middle to Late Miocene, based on ages from the Latacunga-Riobamba area (Lavenu et al., 1992), the type section (Hughes and Bermúdez, 1997) and the present area, ranging from 17 to 8 Ma (Appendix 3). In addition, it is intruded by a number of micro-tonalite/granodiorite plutons, the largest of which immediately south of Zumbagua was dated at 6.27 ± 0.17 Ma by the K/Ar method on hornblende (Hughes and Bermúdez, 1997).

3.7.3 Interpretation

The Zumbagua Group was deposited in a terrestrial environment with mass-flow being the main depositional process. A substantial part of the sequence comprises volcanically triggered debrites and lahars of andesitic-dacitic(-rhyolitic) composition. Hughes and Bermúdez (1997) suggest a depositional environment of an intermontane basin fed by subaerial, acid to intermediate composition, volcanic source. The tuffs of the Salinas-Simiátug area, represent the primary volcanic products of this effusive source.

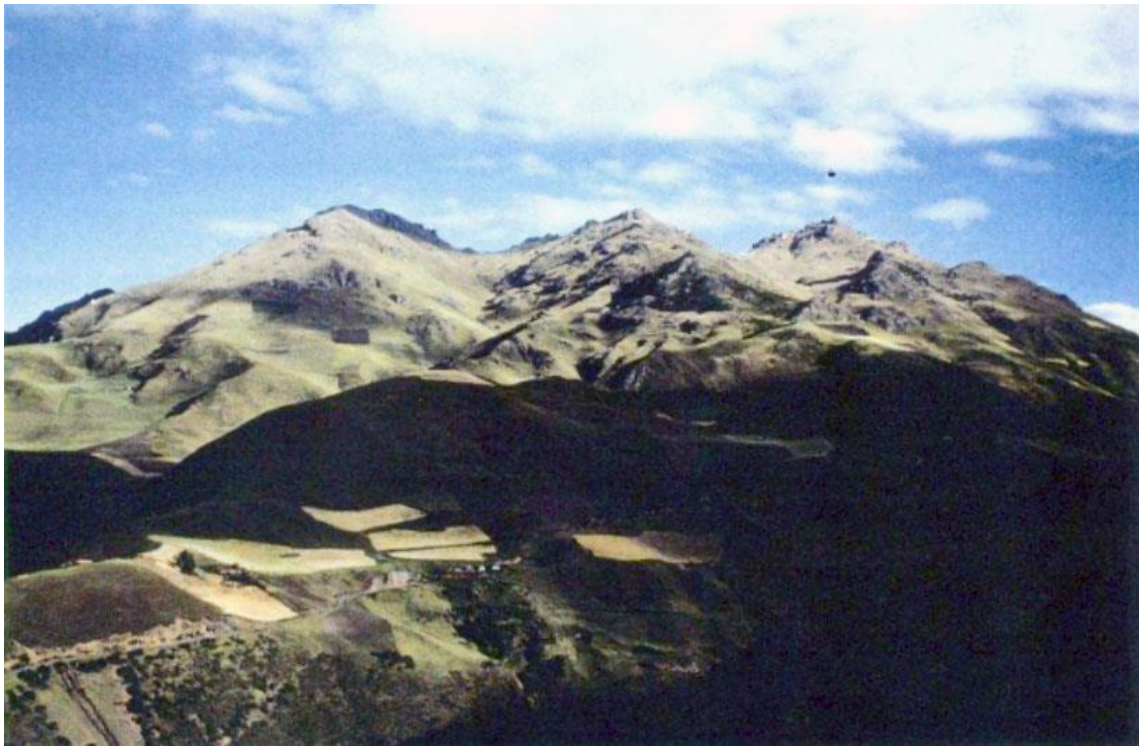

Plate 6. Craggy topography of the volcanosedimentary “mass-flow” deposits of the Zumbagua Group looking NW from Pillopamba (7330-98230). Smoother topography in the foreground corresponds to the Apagua Formation

Plate 7. Laharic units of the Zumbagua Group at Salinas (7210-98450)

3.8 Cisarán Formation, M_{Cn} (Dunkley and Gaibor, 1997)

3.8.1 Definition

Corresponds to a thick sequence of andesitic and dacitic lavas with intercalated sediments, overlain by coarse andesitic breccias, volcanic sandstones and pumiceous pyroclastic deposits, locally capped by andesite-dacite lavas of Late Miocene age.

The Formation is defined from the high ground between Zhud and Alausí to the south of 2°S and takes its name from Cerro Cisarán at (7439-97432). On the map it extends south from Chimborazo to the edge of the area. It is best exposed along the track from Pallatanga to El Olivo (7341-97802), where plagioclase-phyric andesitic lavas and tuffs, formerly included in the Alausí Formation, are overlain by tuffaceous sandstones and fine-grained green to purple volcanic sandstones and siltstones. The (?) upper part of the section, exposed along the track up to Calpa (7447-97985) and extending north to the Sicalpa area (747-9811), consists of poorly exposed chaotic mass-flow deposits comprising tuffaceous sandstones and breccias with ubiquitous igneous lithic clasts, and pyroclastics. The stratigraphy of the Formation is poorly defined in the present area due to limited exposure and difficulties of access, often the result of conflicts with the local indigenous population. It almost certainly overlies and blankets a pre-existing topography of the Saraguro Group volcanic rocks and is overlain by Quaternary ash and pumice deposits. Accordingly, is extremely variable in thickness. Dunkley and Gaibor (1997), however, report a thickness of up to 2200 m from the type section at Cerro Cisarán.

3.8.2 Age

The Formation rests upon the Late Miocene Turi Formation to the south of 2°S. Fission track ages of 6.8 ± 0.8 and 7.15 ± 0.4 Ma have been obtained from within the sequence near Zhud (7253-9693) and on Cerro Cisarán (Dunkley and Gaibor, 1997) and 6.9 ± 0.7 Ma from lavas southeast of Pallatanga. Thus, a latest Miocene age is proven.

3.8.3 Interpretation

The Formation represents a combination of sub-aerial volcanism and broadly contemporaneous sedimentation, with younger mass-flow deposits. Ages from the sequence overlap with those from the younger part of the Saraguro Group and further more detailed work may result in it being included in this broad division representing Middle to Late Miocene continental arc volcanism.

3.9 Undifferentiated Plio-Pleistocene Volcanics, Pl-P_V

3.9.1 Definition

Corresponds to local sequences of younger, post-Zumbagua, volcanics that have not been studied in any detail. They correspond mainly to the "Volcánicos Lourdes" and "Volcánicos de Sagoatoa" of the San Miguel, Guaranda and Ambato 1:100000 geological sheets (DGGM, 1978-1979) that form part of the dominantly Pliocene Sicalpa Group of Baldock (1982).

The Volcánicos Lourdes crop out to the W and SSW of San Miguel de Bolívar on the road-track northwest from Pisco Urcu (7160-98085) to Cochabamba (7122-98144). The type area is at La Gruta de Lourdes, comprising a poorly exposed sequence of deeply weathered acid (?dacitic) volcanic rocks characterised by the presence of large quartz ± feldspar phenocrysts and extensive hydrothermal argillic alteration (silica-kaolin), silicification and sulphide (chalcopyrite-pyrite, ± bornite) mineralisation. Similar lithologies are present southwest of Sicoto exposed in the Río Sicoto and along the road to Cerritos (7099-97917), although they lack extensive hydrothermal alteration. The Volcánicos Sagoatoa are exposed to the northwest of Ambato corresponding to an (older) eroded, stratovolcanic cone with radial drainage and comprising lavas and subordinate tuffs of two-pyroxene andesite. Petrographically the andesites comprise phenocrysts of hypersthene, augite and zoned plagioclase in a matrix of (?)oligoclase, magnetite and volcanic glass.

3.10 Undifferentiated Quaternary volcanic deposits, Q_V

Correspond to the "Volcánicos Cotopaxi" of BGS-CODIGEM (1993a) National Map and the combined Cangahua Formation, Altar and Cotopaxi Groups of Baldock (1982) and on the present map incorporates the rocks of the Chimborazo Volcano. The sequence comprises Pleistocene, air-fall tuffs, breccias and agglomerates, and andesitic lavas from the older centres (Chimborazo, Carihuairazo and the Illinizas) covered by younger volcanic ash, pumice deposits, debris flows and minor lavas of the younger volcanoes and volcanic centres (Cotopaxi, Tungurahua, Pululahua and Quilotoa). The products of the older centres are mainly andesitic whereas the younger ones are more variable, with early phases of dacitic activity followed by a major andesitic phase then basaltic or dacitic activity. Included in this broad unit are the Guaranda depression volcanic rocks, a series of andesitic tuffs and interstratified porphyritic andesite lavas of Pleistocene age. The tuffs are most probably from the Chimborazo Volcano and the lavas local fissure eruptions; at 7229-98231 the andesites are pyroxene-phyric and display spectacular columnar jointing.

The youngest Q_V unit of probable Late Pleistocene to Holocene age (Bristow and Hoffstetter, 1997) is a largely unstratified, partially consolidated andesitic tephra deposit composed of characteristically brown-yellow fine-grained tuff or volcanic-ash commonly 50-80 m thick, with pumice deposits at or towards the base: "Cangahua". According to Baldock (1982) and Bristow and Hoffstetter (1977) the Cangahua is an aeolian deposit of volcanic origin.

3.10.1 Chimborazo and Carihuairazo volcanics, Q_{VCh}^{1-3}

The spectacular Chimborazo Volcano (7431-98381) is an E-W elongated stratovolcano located some 30 km NW of Riobamba, and some 25 km NE of Guaranda, and occupies the eastern central part of the mapped area. It is the highest volcano in Ecuador rising to a height of 6310 m and having a local relief of over 2500 m with a basal diameter of some 20 km (Hall and Mothes, 1994). It is historically inactive and has most probably been so for the last 11000 years (Clapperton, 1990). According to Hall and Mothes (op. cit.) the eruptive style of Chimborazo distributed pyroclastic material over a wide area. The products are exposed along the Ambato-Guaranda road section, and include lavas, pyroclastic flows, debris avalanches, lahars and ash-fall deposits. They vary in composition from basaltic andesites to hornblende-bearing dacites ranging in SiO_2 from 56-65% (Hall and Mothes, 1994).

Activity of the Chimborazo and Carihuairazo volcanoes was most probably initiated in the Early Pleistocene, although a single date of 1.8 Ma is latest Pliocene. These products (Q_{VCh}^{1}) the Carihuairazo and older Chimborazo lavas, comprise porphyritic pyroxene-andesites containing augite, hypersthene and minor olivine phenocrysts in a fine-grained matrix of plagioclase microlites and volcanic glass. The younger Chimborazo lavas (Q_{VCh}^{2}) are confined to the southeastern flanks, and comprise vesicular pyroxene-phyric andesites and rare dacites of "Middle Pleistocene" age dated at 0.035 Ma (C14, Kilian, 1987). The youngest products of the Chimborazo activity (Q_{VCh}^{3}) are located along its western flanks comprising scoriaceous and pumiceous, coarse-grained tuffs containing feldspar, pyroxene, magnetite and andesitic lithics, andesitic-dacitic lavas and debris flows/lahars. This final phase of activity coincided with the final stages of glaciation in the latest Pleistocene (0.018 Ma).

3.11 Quaternary alluvial and colluvial deposits Q_A, Q_C, Q_{Ca}

Holocene alluvium occurs along the course of major river valleys and is the product of fluvial deposition in modern river systems. Occasional older river terraces are present locally, for example along the Río Chimbo, and extensive colluvium deposits including alluvial cones occur along the western margin of the cordillera. Colluvium is particularly extensive in the northwest quadrant where it is difficult to distinguish from the underlying deeply weathered and often landslipped Macuchi Unit.

4. INTRUSIVE ROCKS

Plutons and minor intrusions are present throughout the mapped area, but are particularly common within the western half. In general terms they can be divided into two groups, major plutons of calc-alkaline I-type granitoids intruding the Macuchi volcanoclastic sequence and porphyritic and microtonalitic dykes, sheets and stocks intruding the flysch and younger volcanic sequences, often along fault structures.

The plutons are elongate north-south, characteristically deeply weathered but with sharp, obvious contacts and locally produce extensive contact aureoles. They comprise medium- to coarse-grained, hypidiomorphic, primary textured biotite-hornblende tonalites and granodiorites, that are characteristically xenolith free and unfoliated. A common feature is the presence of sporadic mafic clots or restites of microdioritic composition. All the plutons lack pegmatitic fringes and are dyke-free, aplogranitic sheets although present are not common. Mineralisation in the form of disseminated sulphides at the contacts, both within the granitoid and its hornfelsed country rock is typical. There are four major intrusions in the area, from north to south the El Corazón pluton, the Echeandía (La Industria) pluton, the Chazo Juan-Telimbela pluton and the Balzapamba-Las Guardias pluton (Fig. 3). In addition, there are several minor plutons most probably representing apophyses of the major ones, that suggest that the Macuchi block may be underlain by a composite batholith at depth. The presence of minor plutons in the northwest, however, is inferred from river float and thus their size is likely to be exaggerated.

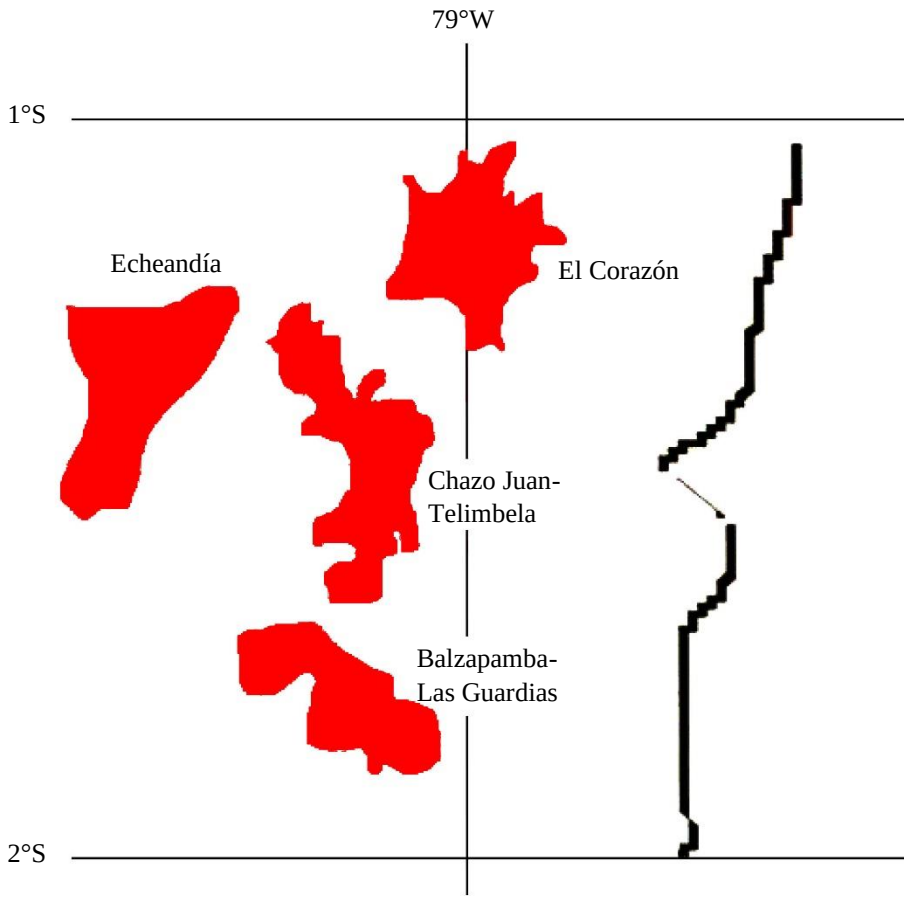

Figure 3. Location of major plutons

A major gabbroid body is present in the extreme southwest of the area to the east of San José del Tambo (6965-97840) comprising a mixture of rock types including gabbro, quartz-gabbro, hornblende diorite, microgabbro and hornblende-pegmatites, all of the lithologies are mafic-rich and, excluding the pegmatites, hypidiomorphic to porphyritic in the finer-grained phases. Mineralogically, they comprise plagioclase (An_{70-58}) diopsidic augite, opaques and variable amounts of orthopyroxene, hornblende and remnant (?)olivine. Alteration products include chlorite, serpentine, fibrous amphibole, epidote and quartz. In some phases there appears to be an incipient metamorphism characterised by the presence of pumpellyite-prehnite ± epidote. Gabbroic rocks particularly microgabbro-diabase are relatively common throughout the Macuchi Unit outcrop, and provisionally the San José gabbro is interpreted to be at a deeper level in the Macuchi volcanic pile.

4.1 Whole-rock geochemistry

The granitoids range in composition from quartz diorite-tonalite to granodiorite on all common classification-nomenclature plots with a concentration of samples in the tonalite field (Appendix 2 Figs. 1-4) and are typical subduction-related, I-type granitoids (Chappell and White, 1974; Pitcher, 1983). Thus, they are calc-alkaline and meta-aluminous to weakly peraluminous (Appendix 2 Figs. 5-6 and 9). On the tectonic classification plots of Whalen et al. (1987) and Pearce et al. (1984) they are orogenic volcanic arc granitoids (Appendix 2 Figs. 7, 8, 10 and 11), and on normalized spider diagrams they show LIL enrichment with depletion of Nb, Ti and Y-Yb (Appendix 2 Figs. 12, 13). The latter is a typical geochemical signature of calc-alkaline magmas formed in a subduction setting and characteristic of volcanic arc granitoids, most probably reflecting amphibole and garnet retention at the site of partial melting in the mantle wedge (Briqueu et al., 1984; Foley and Wheller, 1990). In addition, low values of Rb/Zr (<1) suggest a primitive continental arc (Appendix 2 Fig. 11, Brown et al., 1984) compatible with their tectonic setting within young accreted oceanic sequences, and comparable with the transitional (M-) I-type calcic granitoids of Pitcher (1983, 1993).

4.2 Age

A major K/Ar age dating programme was undertaken on the plutons of the Western Cordillera and 32 mineral ages on either hornblende and/or biotite were obtained to supplement previous ages (Baldock, 1982; BGS-CODIGEM, 1993a). The ages from the present study, ranging from 34.27 ± 0.8 to 10.08 ± 0.2 Ma, are given in Appendix 3. In detail concordant hornblende-biotite ages from the Balzapamba-Las Guardias pluton indicate an Early Oligocene age 34.27 ± 0.8, 33.08 ± 0.4 and 33.37 ± 0.3 Ma, supporting previously published ages of 31.7 ± 1, 30.8 ± 1 and 30.1 ± 1 Ma (Kennerley, 1980; JICA, 1991). Younger ages of 25.7 ± 0.9 and 19.8 ± 3 Ma are also available from this same pluton (JICA, 1991). Parts of the Balzapamba pluton are, however, hydrothermally altered and mineralised and this may be the reason for the younger ages.

Ages from the Chazo Juan-Telimbela tonalitic pluton are more consistent at 21.4 ± 0.19, 20.66 ± 0.18, 19.52 ± 0.26 and 19.11 ± 0.79 Ma, agreeing with published ages of 20.9 ± 0.7 and 19.4 ± 0.6 (JICA, 1991). Suggesting an Early Miocene (21-18 Ma) intrusive age for this pluton. The most westerly intrusion (Echeandía-La Industria) is dated at 26.49 ± 0.73, 25.58 ± 0.5 and 23.14 ± 0.79 Ma, again agreeing with Late Oligocene published ages (JICA, 1991). The El Corazón pluton yielded consistently younger, Middle Miocene, ages of 16.06 ± 0.32, 15.82 ± 0.13, 14.84 ± 0.18, 14.80 ± 0.41 and 14.13 ± 0.35 Ma. While the most southerly intrusion, the Undushig pluton has concordant Late Oligocene, hornblende-biotite, ages of 24.08 ± 0.48 and 25.42 ± 0.51 Ma.

Thus, major and widespread plutonic activity apparently ranged from the Early Oligocene to the Middle Miocene (34-14 Ma) with possible pulses at 34-30 Ma, 26-19 Ma and 16-14 Ma. Two minor intrusive phases were also dated. Microtonalite sheets intruding the Apagua Formation southwest of its type area produced an age of 23.65 ± 0.48 Ma, and one of a series of high-level microgranodioritic stocks intruding the Yunguilla Unit at Juan de Velasco (736-9800) NE of Pallatanga was dated at 10.08 ± 0.2 Ma.

4.3 Interpretation

The geochemical data confirm the volcanic arc character of the Western Cordillera granitoids and provide definite evidence for the existence of an active margin of this part of the South American Plate from the Oligocene to Middle Miocene. This period of activity broadly corresponds to that of the Saraguro Group volcanism and it is interpreted that the two are different manifestations of the same subduction regime.

5. STRUCTURE

5.1 Introduction

The Western Cordillera of Ecuador has an overall NNE trend although it varies in orientation from NE-SW to approximately N-S along its length. Its western limit is the base of the Andean foothills where the Macuchi sequences disappear beneath the Quaternary deposits of the Coastal Plain approximating to the NNE-SSW trending Guayaquil-Babahoyo-Santo Domingo-Fault zone (Baldock, 1982) that extends into Colombia as the El Tambor-Río Mira Fault and its extension the Atrato-San Juan Fault zone. The eastern limit of the Western Cordillera is probably the complex NNE-SSW trending Calacalí-Pallatanga Fault zone (Aspden et al., 1987) and its extension north into Colombia the Cali-Cauca-Patía Fault (McCourt et al., 1984). Thus, the Western Cordillera is limited to the east and west by deep-seated faults interpreted as sutures, and has been sliced up into a series of elongate NNE-SSW trending fault bounded blocks of varying complexity by a series of steep, subparallel anastomosing faults.

5.2 Faulting

Regional fault trends in the mapped area are NE-SW and N-S. Faults are rarely exposed, however, being inferred from regional considerations and neotectonic evidence, mainly geomorphological expression (cf. Lavenu, 1994). The main NE-SW faults occur in the southeast of the mapped area and form part of **Pallatanga Fault system** (this report). The Pallatanga Fault (*s. s.*, Baldock, 1982) corresponds to a NNE-SSW striking fault along the Río Pangor Valley that "south of Pallatanga swings SW through the Bucay depression to join up with the Naranjal-Jambelí Fault". It is here renamed the Pangor Fault, a sub-vertical, easterly dipping local reverse fault along which rocks of the ophiolitic Pallatanga Unit (section 3.1) have been thrust westwards over the Yunguilla Unit (7345-97958). Further north this same fault trends almost N-S, and shows morphological evidence of Holocene right-lateral movement with a small reverse component (Winter and Lavenu, 1989).

As used in this report, the Pangor Fault is a major strand of the Pallatanga Fault system, the latter corresponding to the eastern limit of Cretaceous oceanic rocks of MORB affinity and correlating with the Calacalí-Pujilí Fault (Litherland and Aspden, 1992) to the north. The main fault of this system to the south is the Bulubulu Fault (Dunkley and Gaibor, 1997) that defines the eastern contact of the MORB rocks with local metamorphic basement. Along much of its length the Pallatanga Fault System coincides with the eastern boundary fault of the Western Cordillera (Van Thournout, 1991; Lebrat et al., 1985) but south of 2°S it swings southwest to emerge close to Palenque, defining the western limit of the Cordillera. The trace of the main faults of the Pallatanga Fault System is marked in the present area, by slivers of highly sheared basic rock (K_{Pa}) and/or pulverized Yunguilla Unit, typically exposed in areas of landslip. In the Qda. Mocata NE of the village of the same name at (7300-97810) such a fault shows evidence, S-C structures, of dextral movements.

Plate 8. Río Chimbo lineament looking south along Río Chimbo at (7220-97910)

Plate 9. Trace of the Pangor Fault (Pallatanga Fault System) looking NE from the village of Pallatanga (7280-97800)

To the west of the main fault zone there are numerous parallel fault sets the most important of which extends northeast from the Tambillo area (724-9794) to the Chimborazo Volcano that straddles the fault line (cf. Litherland and Aspden, 1992). Along the length of this Tambillo Fault are exposed tectonised basic rocks of the Pallatanga Unit (727-9803) often intimately associated with highly tectonised black mudstones interpreted to belong to the Yunguilla Unit that possibly forms the matrix of the dismembered ophiolitic rocks of the Pallatanga Unit. This fault is interpreted as a satellite fault of the Pallatanga (-Calacalí) suture possibly reactivated during Miocene to Pliocene time, coinciding with the development of the principal intermontane basins of southern Ecuador (Lavenu and Noblet, 1989). Immediately to the west of the Tambillo Fault is another fundamental structure expressed neotectonically as the Río Chimbo Lineament, considered to be a reactivated fault line related to Neogene uplift (Baldock, 1982). The Río Chimbo Lineament is interpreted to be related to the Macuchi-Apagua faulted contact defined as the **Chimbo-Cañi Fault system** (this report). This is exposed south of Cañi (7236-98042) and in the Río Colorado-Pallo (724-9802) as a belt of tectonised, sheared, basic rocks and pulverized black and red-purple mudstones of unproven affinity. The lineament is easily traced on aerial photographs and satellite imagery as far north as Guaranda and is thought to continue northwards as far as Simiátug from where it possibly continues north to join up with the Río Toachi Lineament on the adjoining map sheet (Hughes and Bermúdez, 1997). Alternatively, it, or a related structure, swings NE along the Río Colorado to the NW of Chimborazo, where tectonised basic and ultrabasic slivers of K_{Pa} have been mapped (7385-98545) to join up with the main Pujilí boundary fault. This entire zone is considered to be an area of active faulting related to Mio-Pliocene and Quaternary reactivation of the Pallatanga-Pujilí suture. The Chimbo-Cañi Fault continues north to the Pilaló area, to join up with the Pilaló-Sigchos Fault of Hughes and Bermúdez (1997). We consider this regional fault zone to be a Late Eocene "suture" related to the accretion of the Macuchi terrane to continental South America (section 7).

Several minor faults are present, the majority of which cannot be represented at the 1:200000 scale, these are either NW-SE or ENE-WSW to E-W trending structures with small scale local offsets. In addition, there are numerous NNE and NE trending lineaments evident on the aerial photographs coinciding with prominent drainage directions that probably are faults or fractures.

5.3 Folding

Folds are present in the Apagua and Yunguilla sequences about N-S, NNE-SSW or NE-SW axes, although complicated in the latter by disharmonic folding related to soft sediment deformation (slumping) that is regionally characteristic of this unit. Folding of the Macuchi Unit almost certainly occurred, but is rarely evident in the field. Large scale N-S to NNE-SSW trending open folding or warping is evident on aerial photographs in the Zumbagua Group in the northeast quadrant of the map. The folding in the Apagua and Yunguilla turbidite sequences is considered to reflect the Late Eocene deformation during the accretion of the Macuchi terrane and it is noteworthy that the pre-Oligocene sediments of the Arrayanes Unit have not been folded by this event (cf. Section 3.5). The folding that affects the Zumbagua Group must be Late Miocene or younger in age and thus related to a different tectonic event.

6. ECONOMIC GEOLOGY

There is relatively little important mineralisation in the area, only minor amounts of porphyry related sulphides and possible epithermal gold.

The main areas of interest from the point of view of base and precious metal mineralisation were identified during the San Miguel Project (1975-1979) undertaken jointly by geologists of DGGM (presently CODIGEM) and the IGS (presently BGS). Several prospects for porphyry copper ± gold-molybdenum mineralisation were identified and recommended for further investigation (Aucott et al., 1979). Almost all the areas of interest are related to granitoid intrusions or their contacts with the host Macuchi volcanics. Limited follow-up work identified areas of priority interest, 9 of which are in the present study area: Chazo Juan (706-9846), La Industria-Yatubi (688-9826), Tres Hermanas (700-9826), Telimbela (704-9816), Balzapamba (703-9805 to 708-9808), San Miguel (716-9808), Las Guardias (708-9800), Sicoto (712-9798) and Tambillo (723-9784). All of these areas were evaluated and the most promising were followed up, as part of the Bolívar Project (Phases I-III) carried out jointly by geologists of the Japanese International Cooperation Agency (JICA) and INEMIN (presently CODIGEM) between 1988-1991. As a result of the preliminary evaluation, Balzapamba and Telimbela were identified as the targets and a programme of drilling was carried out in the zones of highest interest at El Torneado (708-9808), Osohuayco (7075-9806) and NE Telimbela at Ashuaca (7056-98172). Full details of the Bolívar Project are given in the Phase I, II, III reports (JICA, 1989, 1990, 1991) and briefly summarized below.

6.1 Balzapamba area

Mineralisation, mainly copper sulphides, occurs within the granitoid pluton and adjacent hornfelsed Macuchi rocks at El Torneado, Osohyauco, Las Juntas and El Cristal, either as disseminated "porphyry copper type" in the granitoid or associated with quartz veins in the volcanics. Ore minerals are principally pyrite and chalcopyrite. At Las Palmas and Cochapamba, a younger hot-spring mineralisation is present in the Plio-Pleistocene "Lourdes Volcanics" (Section 3.9). Extensive widespread quartz-kaolin-halloysite alteration is recorded with disseminated weak pyrite ± hematite mineralisation observed at the surface. At El Torneado both network and disseminated sulphide mineralisation are present test drilling established, however, that the mineralised zone was of low grade and concluded that any previous centre of mineralisation had been eroded away and therefore potential was low. Two discrete mineralised zones were recognised at Osohuayco (North and South) and the southern one was drilled based on an IP survey. Drilling intersected a zone of very low-grade sulphide mineralisation in hornfelsed Macuchi (0.05% Cu).

6.2 Telimbela

Granitoid-hosted "porphyry-type" mineralisation, disseminated pyrite, chalcopyrite ± bornite ± molybdenite, occurs in the Telimbela area with seven discrete mineralised zones recorded. The most promising is centred on Qdas. Ugshacocha and Ashuaca close to the school at Ashuaca. Preliminary drilling indicated grades of between 0.23-0.72% Cu and the Ashuaca area was targeted for follow-up drilling.

All other areas of low priority, mineralisation at Chazo Juan and Las Guardias is of the porphyry type but small in scale and discontinuous and some “epithermal” hot-spring type alteration with very minor gold mineralisation is recorded from the La Industria-Yatubi area.

During the present survey, several small areas of alteration and sulphide, mainly pyrite, mineralisation were observed in the contact zones of the Chazo Juan-Telimbela pluton and sporadically in other areas within the Macuchi Unit. They occur along the same general lineament often coinciding with the outcrop of the Arrayanes Unit sediments. The most extensive area is NE of the Balzapamba pluton towards Las Palmas (7080-98105). In hydrothermal alteration, quartz-pyrite mineralisation and quartz pegmatites with tourmaline occur at the southern end of the Echeandía pluton at Santa Rita-Yatubi (6875-98225) and NE of Cerro Samama (6888-98177).

6.3 Non-metallic resources

It includes the limestones and calcarenites of the Yunguilla Unit quarried for cement around San Juan-Shobol (744-9823) and at Cuiquiloma (7372-98273). Limestones of the Macuchi in the Balzapamba area specifically around Chaupiyacu (699-9805) and Cadial (700-9807) and potential sources of road aggregate in local basalts and microgabbros both in the Macuchi and Arrayanes Units particularly where they are hornfelsed as for example NE of Las Guardias at Los Pogyos (705-9799). In addition, the Quaternary to Recent volcanics along the eastern side of the area between Riobamba and Ambato are important sources of pumice, both as an abrasive and a filler in cement (Pozzolan), building materials, ornamental stone, etc. (Báez et al., 1994).

7. GEOLOGICAL HISTORY

The geological history of the area is interpreted in terms of plate-tectonic processes and in particular accretion tectonics. The oldest rocks are the oceanic basalts of the Pallatanga Unit of probable Mid- to Late Cretaceous age. It is proposed that these rocks represent fragments of an incomplete ophiolite sequence, part of the Middle Cretaceous oceanic floor of the (proto-) Farallón Plate. The Pallatanga sequence was accreted to NW South America in the Late Cretaceous, most probably the Campanian. Aspden et al. (1992) reported widespread resetting of major isotopic systematics in the pre-Cretaceous rocks of the Cordillera Real between 85-65 Ma. A similar resetting event was reported by McCourt et al. (1984) from the metamorphic rocks of the Central Cordillera of Colombia. Both authors correlated this resetting with the accretion of the Western Cordillera terrane, corresponding to the Pallatanga Unit in Ecuador, the Grupo Diabásico in Colombia and correlated oceanic rocks in Panama. In the Oriente of Ecuador, the Albian to Santonian (?-Early Campanian) Napo Formation was eroded prior to the deposition of the Maastrichtian Tena Formation (Baldock, 1982). It is proposed that the erosion of the Napo Formation was related to a period of uplift and emergence of the proto-Cordillera Real in the Campanian (83-74 Ma), resulting from the collision and accretion of the Mid-Cretaceous oceanic Western Cordillera terrane of the Northern Andes along the complex (Cali-Cauca-Patía) Calacalí-Pallatanga Fault system, a Late Cretaceous suture. As a result of the (?) Middle- to Late Campanian emergence of the Cordillera Real, the Maastrichtian Tena Formation and Yunguilla Unit were deposited in contrasting continental and marine environments on either side of the Cordillera Real (Baldock, 1982). The marine Yunguilla turbidite sequence was lain down in the west at least in part on top of the Cretaceous oceanic terrane.

Subsequent to this event a (?) new subduction regime was established and the ensimatic Macuchi island arc developed during the Early Tertiary. At the same time the clastic turbidites of the Paleocene-Eocene Apagua Formation and related units were deposited in a fore-arc or trench environment in the marginal sea between the Macuchi arc and the continental edge. Also, about this time, in southern Ecuador, the calc-alkaline Sacapalca arc was developed in a continental margin setting. In the (early) Late Eocene the Macuchi island-arc sequence was obliquely accreted from the SW onto the continental edge, possibly the result of dextral strike-slip tectonics along a regional NNE trending fault (cf. Feininger and Bristow, 1980). A similar latest Eocene scenario was proposed by McCourt et al. (1991) for the western margin of the Western Cordillera of Colombia. As a direct result of this tectonic event, the Apagua, Macuchi and older units were deformed and slices of the Cretaceous ophiolitic Pallatanga Unit were tectonically emplaced into the Yunguilla Unit. During the accretion process it is proposed that the Macuchi arc sequence was sliced up and translated northwards to its present-day position. Following or possibly during the accretion event, the turbidites and basaltic volcanics of the Arrayanes Unit were deposited on top of the Macuchi terrane. Approximating the Eocene-Oligocene boundary and continuing through to the Miocene, continued subduction resulted in a major calc-alkaline volcanic arc being developed along the Ecuadorian Andes continental margin, the Saraguro Arc. In the mapped area, volcanism appears to have been restricted to fissure eruptions along old fault lines, but a major plutonic arc was developed along the eastern edge of the Macuchi block between 35-20 Ma, for example, the Balzapamba and Telimbela plutons.

At around 22 Ma, a well-documented major reorientation of relative plate motions occurred in the Northern Andean region, the result of the breakup of the Farallón Oceanic Plate into the Nazca and Cocos Plates (Pilger, 1983). Events relating to this change are not clear in the mapped area in that plutonism appears to continue into the Early Miocene, however in the southern part of the Western Cordillera there was a break in volcanic activity, with major uplift and deformation of the Saraguro Group sequences about this time (Pratt et al., 1997). During the Miocene-Pliocene following the above re-organisation, the geological evolution of Ecuador was that of an active continental margin dominated by strike-slip faulting, with E-W extension resulting in the formation of inter-montane basins (Lavenu and Noblet, 1989; Pratt et al., 1997). The entire Western Cordillera was the site of extensive sub-aerial, acid-intermediate volcanism, the products of which are seen in the mapped area as the Zumbagua Group and undifferentiated Plio-Pleistocene units. About 2 Ma ago, there was a further reorganization of the Pacific Plate system (Rea and Malfait, 1974), the result of the Carnegie Ridge coming into contact with the active subduction zone. As a consequence of this many of the older structures of the Western Cordillera were reactivated, for example, the Río Chimbo Lineament. To the north of 2°30’S large stratiform andesitic volcanoes formed along reactivated regional faults, such as the Calacalí-Pallatanga suture, that most probably acted as conduits for the magma.

8. BIBLIOGRAPHY

AGUIRRE L. and ATHERTON M. P. (1987) Low grade metamorphism and geotectonic setting of the Macuchi Formation, Western Cordillera of Ecuador. *Journal of Metamorphic Geology*, **5**, 473-494.

ASPDEN J. A., BONILLA W. and DUQUE P. (1995) The El Oro metamorphic complex, Ecuador: geology and economic mineral deposits. *Overseas Geology and Mineral Resources*, No. 67, 63 pp.

ASPDEN J. A., HARRISON S. M. and RUNDLE C. C. (1992) New geochronological control for the tectono-magmatic evolution of the metamorphic basement. Cordillera Real and El Oro Province of Ecuador. *Journal of South American Earth Sciences,* Vol. 6, 77-96.

ASPDEN J. A., LITHERLAND M., DUQUE P., SALAZAR E., BERMÚDEZ R. y VITERI F. (1987) Un nuevo cinturón ofiolítico en la Cordillera Real, Ecuador, y su posible significación regional. *Politécnica (Quito), Monografía de Geología,* Vol. 12, 81-94.

AUCOTT J. W., PUIG C., QUEVEDO L. and BÁEZ N. (1979) Exposición geoquímica regional en el centro occidental del Ecuador (Proyecto San Miguel). Institute of Geological Sciences, Nottingham UK.

BÁEZ N., NÚÑEZ R., TIRADO R. and LOACHAMIN R. (1994) Rocas y minerales Industriales en el Ecuador, Quito-Ecuador, 202p.

BALDOCK J. W. (1982) Geología del Ecuador. Boletín de la Explicación del Mapa Geológico (1:1000000) de la República del Ecuador. Ministerio de Recursos Naturales y Energéticos. Quito, 54 pp.

BRISTOW C. R. (1981) An annotated bibliography of Ecuadorian geology. *Overseas Geology and Mineral Resources, Institute of Geological Sciences,* No. 58, 38 pp.

BRISTOW C. R. and HOFFSTETTER R. (1977) *Lexique Stratigraphique International.* (2nd Edition). Centre National de la Recherche Scientifique, Paris.

BRITISH GEOLOGICAL SURVEY and CORPORACIÓN DE DESARROLLO E INVESTIGACIÓN GEOLÓGICO MINERO Y METALÚRGICO (1993a) National geological map of Ecuador, scale 1:1000000. (Keyworth, Nottingham; BGS, and Quito; CODIGEM).

BRITISH GEOLOGICAL SURVEY and CORPORACIÓN DE DESARROLLO E INVESTIGACIÓN GEOLÓGICO MINERO Y METALÚRGICO (1993b) National tectono-metallogenic map of Ecuador, scale 1:1000000. (Keyworth, Nottingham; BGS, and Quito; CODIGEM).

BRITISH GEOLOGICAL SURVEY and CORPORACIÓN DE DESARROLLO E INVESTIGACIÓN GEOLÓGICO MINERO Y METALÚRGICO (1994a) Geological and metal occurrence map of the Northern Cordillera Real metamorphic belt Ecuador. (1:500000).

BRITISH GEOLOGICAL SURVEY and CORPORACIÓN DE DESARROLLO E INVESTIGACIÓN GEOLÓGICO MINERO Y METALÚRGICO (1994b) Geological and metal occurrence map of the Southern Cordillera Real metamorphic belt Ecuador. (1:500000).

BRIQUEU L., BOUGAULT H. and JORON J. L. (1984) Quantification of Nb, Ta, Ti and V anomalies in magmas associated with subduction zones: petrogenetic implications. *Earth and Planetary Science Letters*, **68**, 297-308.

BROWN G. C., THORPE R. S. and WEBB P. C. (1984) The geochemical characteristics of granitoids in contrasting arcs and comments on magma sources, *Journal Geological Society, London*, **141**, 413-426.

CHAPPELL B. W. and WHITE A. J. R. (1974) Two contrasting granite types. *Pacific Geology*, **8**, 173-174.

CLAPPERTON C. (1990) Glacial and volcanic geomorphology of the Chimborazo-Carihuairazo Massif Ecuadorian Andes. *Transaction of the Royal Society of Edinburgh Earth Sciences*, **81**, 91-116.

DIRECCIÓN GENERAL DE GEOLOGÍA Y MINAS (1976) Mapa geológico del Ecuador, Chimborazo, Hoja 69 (1:100000). (Quito).

DIRECCIÓN GENERAL DE GEOLOGÍA Y MINAS (1978) Mapa geológico del Ecuador, Ambato, Hoja 68 (1:100000). (Quito).

DIRECCIÓN GENERAL DE GEOLOGÍA Y MINAS (1978) Mapa geológico del Ecuador, Riobamba, Hoja 70 (1:100000). (Quito).

DIRECCIÓN GENERAL DE GEOLOGÍA Y MINAS (1979) Mapa geológico del Ecuador, Quevedo, Hoja 48 (1:100000). (Quito).

DIRECCIÓN GENERAL DE GEOLOGÍA Y MINAS (1979) Mapa geológico del Ecuador, Guaranda, Hoja 49 (1:100000). (Quito).

DIRECCIÓN GENERAL DE GEOLOGÍA Y MINAS (1979) Mapa geológico del Ecuador, San Miguel, Hoja 50 (1:100000). (Quito).

DIRECCIÓN GENERAL DE GEOLOGÍA Y MINAS (1980) Mapa metalogénico del Ecuador, escala 1:1000000. (Paladines A. and Sanmartín H.) Quito, Ecuador.

DIRECCIÓN GENERAL DE GEOLOGÍA Y MINAS and INSTITUTE OF GEOLOGICAL SCIENCES (1982) Mapa Geológico Nacional de la República del Ecuador (1:1000000). (Quito).

DUNKLEY P. N. and GAIBOR A. (1997) Geology of the area between 2 and 3 degrees south. Western Cordillera, Ecuador. Open File Report WC/97/26, British Geological Survey.

EGÜEZ A. (1986) Evolution Cénozoïque de la Cordillère Occidental Septentrionale d'Equateur (0°15'S o 1°10'S). Les mineralisation associées. Unpublished Ph. D. thésis, Université Pierre et Marie Curie, Paris, 116p.

EGÜEZ A. and BOURGOIS J. (1986) La Formación Apagua, edad y posición estructural en la Cordillera Occidental del Ecuador. Memoria Cuarto Congreso Ecuatoriano de Geología, Minas y Petróleos, **Tomo 1**, 161-178. Quito.

FAUCHER B., JOYES R., MAGNE F., GRANJA V. J., GRANJA B. J. C., CASTRO R. y GUEVARA G. (1968) Informe geológico sobre las posibilidades petroleras de las provincias costeras de la República del Ecuador. Institute Français du Pétrole. (Servicio Nacional de Geología y Minas; Quito).

FAUCHER B. and SAVOYAT E. (1973) Esquema Geológico de los Andes Ecuatorianos. *Revue de géographie et de Géologie Dynamique (2),* **XV Fase 1-2**, 115-142. Paris.

FEININGER T. (1977) Simple Bouguer gravity anomaly map of Ecuador (1:1000000). Escuela Politécnica Nacional, Quito, Ecuador.

FEININGER T. (1978) Geologic map of the western part of the El Oro Province (1:50000). Escuela Politécnica Nacional, Quito, Ecuador.

FEININGER T. and BRISTOW C. R. (1980) Cretaceous and Paleogene geologic history of coastal Ecuador. *Geologische Rundschau*, Vol. 69, 849-874.

FOLEY S. F. and WHELLER G. E. (1990) Parallels in the origin of the geochemical signatures of island arc volcanics and continental potassic igneous rocks: the role of residual titanites. *Chemical Geology*, **85**, 1-18.

GANSSER A. (1973) Facts and theories on the Andes. Journal of the Geological Society of London, Vol. 129, 93-131.

GOOSSENS P. J. (1972) Metallogeny in the Ecuadorian Andes. *Economic Geology*, **67**, 458-468.

GOOSSENS P. J. and ROSE W. I. (1973) Chemical composition and age determination of tholeiitic rocks in the Basic Igneous Complex, Ecuador. *Bulleting Geological Society of America*. **84**, 1043-1052.

HALL M. L. and MOTHES P. A. (1994) Tefroestratigrafía holocénica de los volcanes principales del valle interandino, Ecuador. P. 47-68. *In* El Contexto Geológico del Espacio Físico Ecuatoriano (ed. R. Marocco). Colegio de Geógrafos del Ecuador, Quito-Ecuador, 113 p.

HENDERSON W. G. (1977) Geology of the Cordillera Occidental of Northern Ecuador. Internal report IGS/DGGM Quito 79p.

HENDERSON W. G. (1979) Cretaceous to Eocene volcanic arc activity in the Andes of northern Ecuador. *Journal of the Geological Society of London,* Vol. 136, 367-378.

HENDERSON W. G. (1981) The Volcanic Macuchi Formation, Andes of Northern Ecuador. *Newsl. Stratigr.,* **9**, 157-168.

HUGHES R. A. and BERMÚDEZ R. A. (1997) Geology of the area between 1 degree south and the Equator, Western Cordillera, Ecuador. Open File Report WC/97/25. British Geological Survey.

IRVINE T. N. and BARAGAR W. R. A. (1971) A guide to the chemical classification of the common volcanic rocks. *American Journal of Earth Sciences,* **8**, 523-548.

JAPAN INTERNATIONAL COOPERATION AGENCY (1989) Report on the mineral exploration in the Bolívar area, Republic of Ecuador, Phase I, CODIGEM, Quito.

JAPAN INTERNATIONAL COOPERATION AGENCY (1990) Report on the mineral exploration in the Bolívar area, Republic of Ecuador, Phase II, CODIGEM, Quito.

JAPAN INTERNATIONAL COOPERATION AGENCY (1991) Report on the mineral exploration in the Bolívar area, Republic of Ecuador, Phase III, CODIGEM, Quito.

KENNERLEY J. B. (1973) Geology of Loja Province Southern Ecuador. Institute of Geological Sciences. *Overseas Geology and Mineral Resources, Photogeological Unit,* **23**, 34 pp.

KENNERLEY J. B. (1980) Outline of the geology of Ecuador. Institute of Geological Sciences. *Overseas Geology and Mineral Resources,* No. 55, 20 pp.

KEHRER W. and VAN DER KAADEN G. (1979) Notes on the geology of Ecuador, with special reference to the Western Cordillera. *Geol. Jahrbuch,* **35**, 5-57.

KILIAN R. (1987) The development of the Chimborazo (6310m), Carihuairazo (5102m) and other volcanoes in Ecuador. *Zentralbl. Geol. Palaeontol.* **1**, **H7-8**, 955-965.

LAVENU A. and NOBLET C. (1989) Synsedimentary tectonic control of Andean intermontane strike-slip basins of southern Ecuador. *International Symposium on Intermontane Basins; Geology and Resources, Chiang Main, Thailand,* 306-317.

LAVENU A., NOBLET C., BONHOMME M. G., EGÜEZ A., DUGAS F. and VIVIER G. (1992) New K/Ar age dates of Neogene and Quaternary volcanic rocks from the Ecuadorian Andes. Implications for the relationships between sedimentation, volcanism and tectonics. *Journal of South American Earth Sciences,* **5**, 309-320.

LE MAITRE R. W (1989) A classification of Igneous Rocks and glossary of terms Blackwell Publications London, 193p.

LEBRAT M. (1985) Caractérisation géochimique du volcanisme ante-orogénique de l'Occident Equatorien : implications géodynamiques. Unpubl. Ph. D. Thésis. Centre Géologique et Geophysique de Montpellier. 119p.

LEBRAT M., MEGARD F., JUTEAU T. and CALLE J. (1985) Pre-orogenic volcanic assemblage and structure in the Western Cordillera of Ecuador, between 1°40'S and 2°20'S. *Geologische Rundschau,* **74**, 343-351.

LEBRAT M., MEGARD F., DUPUY C. and DOSTAL J. (1987) Geochemistry and tectonic setting of pre-collision Cretaceous and Paleogene volcanic rocks of Ecuador. *Bulletin of the Geological Society of America,* **99**, 569-578.

LITHERLAND M. and ASPDEN J. A. (1992) Terrane-boundary reactivation: a control on the evolution of the Northern Andes. *Journal of South American Earth Sciences,* **5**, 71-76.

LONSDALE P. (1978) Ecuadorian Subduction System. *Bulletin American Association of Petroleum Geologists,* **62**, 2454-2477.

MARRINER G. F. and MILLWARD D. (1984) The petrology and geochemistry of Cretaceous to Recent volcanism in Colombia: the magmatic history of an accretionary plate margin. *Journal of the Geological Society of London,* **141**, 473-486.

McCOURT W. J., ASPDEN J. A. and BROOK M. (1984) New geological and geochronological data from the Colombian Andes: Continental growth by multiple accretion. *Journal of the Geological Society of London,* **141**, 831-845.

McCOURT W. J., MUÑOZ C. A., and VILLEGAS H. (1991) Regional geology and gold potential of the Guapi-Napi drainage basin and the upper Timbique river, Department of Cauca SW Colombia. *BGS Overseas Geology Series,* Technical Report WC/90/34, 62p.

McCOURT W. J., DUQUE P. and PILATASIG L. (1997) Proyecto de Desarrollo Minero y Control Ambiental, Programa de Información Cartográfica y Geológica. Report No. 3. Geology of the Western Cordillera of Ecuador between 1°00'S and 2°00'S.

MESCHEDE M. (1986) A Method of discriminating different types of mid-ocean ridge basalt and continental tholeiites with the Nb-Zr-Y diagram. Cem. Geol., **56**, 207-218.

MEGARD F. and LEBRAT M. (1987) Los terrenos exóticos del occidente Ecuatoriano y sus relaciones con Sudamérica. Coloquio Ecuador 86, Quito, *Casa Cultura*, **240**, 161-172.

OLSSON A. A. (1942) Tertiary deposits of north-western South America and Panamá. *Proceedings of the American Scientific Congress.* Washington, 231-287.

PEARCE J. A. (1975) Basalt geochemistry used to investigate past tectonic environments on Cyprus. *Tectonophysics*, **25**, 41-77.

PEARCE J. A. and NORRY M. J. (1979) Petrogenic implications of Ti, Zr, Y and Nb variations in volcanic rocks. *Contributions to Mineralogy and Petrology*, **69**, 33-47.

PEARCE J. A., HARRIS N. B. W. and TINDLE A. G. (1984) Trace element discrimination diagrams for the tectonic interpretation of granitic rocks. *Journal of Petrology*, **25**, 956-983.

PILGER R. H. (1983) Kinematics of the South American subduction zone from global reconstructions. Geodynamics of the Eastern Pacific Region, Caribbean and Scotia Arcs. *American Geophysical Union Geodynamics Service*, **9**, 113-126.

PITCHER W. S. (1983) Granite type and tectonic environment. *In* Mountain Building Processes (Hsü, K. Editor). Academic Press London, 19-40.

PITCHER W. S. (1993) The nature and origin of granite. Blackie Academic and Professional Press London, 321 p.

PRATT W. T., FIGUEROA J. F. y FLORES B. G. (1997) Proyecto de Desarrollo Minero y Control Ambiental, Programa de Información Cartográfica y Geológica: Report No. 1. Geology of the Western Cordillera of Ecuador between 3°00'S and 4°00'S.

REA D. K. and MALFAIT B. T. (1974) Geologic evolution of the Northern Nazca Plate. *Geology*, **2**, 317-320.

READING H. G. (1986) Sedimentary Environments and facies. (2nd Edition). Blackwell Scientific Publication, London, 615 p.

SANTOS M. and RAMÍREZ F. (1986) La Formación Apagua, una nueva unidad eocénica en la Cordillera Occidental ecuatoriana. *Memorias Cuarto Congreso Ecuatoriano de Geología, Minas y Petróleos*, **Tomo 1**, 179-189.

SAUER W. (1957) *El mapa geológico del Ecuador. Memoria explicativa.* (Universidad Central; Quito).

SAUER W. (1965) *Geología del Ecuador.* Edit. Ministerio de Educación Pública. Quito, 383 p. (Quito).

SAVOYAT E., VERNET R., SIGAL J., MOSQUERA C., GRANJA J. and GUEVARA G. (1970) Formaciones sedimentarias de la Sierra tectónica andina en el Ecuador. Informe Instituto Francés del Petróleo y Servicio Nacional de Geología y Minería, Quito.

SERVICIO NACIONAL DE GEOLOGÍA Y MINERÍA (1969) Mapa geológico de la República del Ecuador. (1:1000000). (Quito).

SHERVAIS J. W. (1982) Ti vs. V plots and the petrogenesis of modern and ophiolitic lavas. *Earth and Planetary Science Letters,* **59**, 101-118.

SIGAL J. (1968) Estratigrafía micropaleontológica del Ecuador, datos anteriores y nuevos. Informe Instituto Francés del Petróleo y Servicio Nacional de Geología y Minería, Quito.

SILLITOE R. H. (1974) Tectonic segmentation of the Andes: implication for magmatism and metallogeny. Nature, London, Vol. 250.

STEINMANN M. (1977) Fission-track age determinations on Zircons. Consultants Report, GIMP mapping project Ecuador, Geological Institute **ETH,** Zürich, Switzerland, 59p.

SUN S. S., NESBITT R. W. And SHARASKIN A. Ya. (1979) Geochemical characteristics of mid-ocean ridge basalts. *Earth and Planetary Science Letters,* **44**, 119-138.

THALMANN H. E. (1946) Micropalaeontology of Upper Cretaceous and Paleocene in Western Ecuador. *Bulletin of the American Association of Petroleum Geologists*, **30**, 337-347.

TSCHOPP H. J. (1948) Geologische Skizze von Ekuador. *Bull. Assoc. Suisse Géol. Ing. Pét.,* Vol. 15, 14-45.

TSCHOPP H. J. (1953) Oil explorations in the Oriente of Ecuador. 1938-1950. *Bulletin of the American Association of Petroleum Geologists,* Vol. 37, 2303-2347.

VAN THOURNOUT F. (1991) Stratigraphy, magmatism and tectonism in the Ecuadorian Northwestern Cordillera: metallogenic and geodynamic implications. Unpublished PhD. Thesis Katholieke Universiteit Leuven.

VAN THOURNOUT F., HERTOGEN J. and QUEVEDO L. (1992) Allochthonous terranes in northern Ecuador. *In:* Andean Geodynamics, Special Volume, *Tectonophysics*, **205**, 205-222.

WALLRABE-ADAMS H. J. (1991) Petrology and Geotectonic development of the Western Ecuadorian Andes: The Basic Igneous Complex. *Tectonophysics,* **185**, 163-182.

WHALEN J. B., CURRIE K. L. and CHAPPELL B. W. (1987) A-type granites: geochemical characteristics, discrimination and petrogenesis. *Contributions Mineralogy and Petrology*, **95**, 407-419.

WILKINSON I. P. (1992) Calcareous microfauna from a suite of samples from Ecuador. Cordillera Occidental. Technical Report WH/92/121R, Biostratigraphy and Sedimentology Research Group BGS Nottingham UK.

WILKINSON I. P. (1996) Foraminifera from a suite of slides from the Western Cordillera of the Ecuadorian Andes. Technical Report WH/96/99R, Biostratigraphy and Sedimentology Research Group BGS Nottingham UK.

WILKINSON I. P. (1997a) Foraminifera from a suite of six samples from Ecuador. Technical Report WH/96/85R, Biostratigraphy and Sedimentology Research Group BGS Nottingham UK.

WILKINSON I. P. (1997b) Foraminifera from Angamarca-Ecuador. Technical Report WH/97/117R, Biostratigraphy and Sedimentology Research Group BGS Nottingham UK.

WINTER T. and LAVENU A. (1989) Morphological and microtectonic evidence for a major active right-lateral strike-slip fault across central Ecuador (South America). *Annales Tectonicae*, **3**, 123-139.

WOOD D. A. (1980) The application of a Th-Hf-Ta diagram to problems of tectonomagmatic classification and to establishing the nature of crustal contamination of basaltic lavas of the British Tertiary volcanic province. *Earth and Planetary Scientific Letters*, **50**, 11-30.

WOODS M. A. (1997) Biostratigraphic interpretation of macrofaunas from Ecuador. Technical Report WH/97/13R, Biostratigraphy and Sedimentology Research Group BGS Nottingham UK.

WOLF T. (1892) Geografía y Geología del Ecuador. Brockhaus, Leipzig.

APPENDIX 1 OF REPORT:

GEOLOGY OF THE WESTERN CORDILLERA
OF ECUADOR
BETWEEN 1°00' AND 2°00' S

PETROGRAPHY

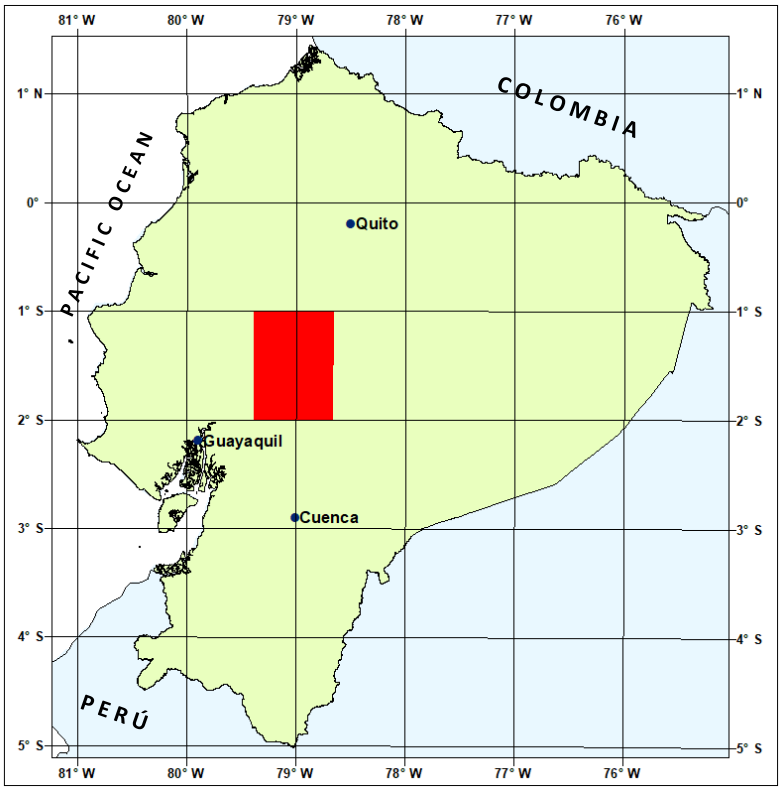

GEOLOGICAL INFORMATION MAPPING PROGRAMME
(LOCATION OF MAP 3 AREA)

W. MCCOURT
P. DUQUE
L. PILATASIG

QUITO, 1997

CONTENTS

PETROGRAPHY – MAP 3

A total of 728 rock samples were collected, out of which 335 thin sections were prepared. The following petrographic descriptions are based on the study of these sections. The names of 39 samples were confirmed using the nomenclature defined by chemical composition for extrusive rocks, and by norms, meso-norms, and factors for intrusive rocks.

Different types of rocks outcrop in the region, which for descriptive purposes are grouped into six categories: turbidites, green rocks, mafic and ultramafic rocks, intrusive rocks, metamorphic rocks, and others. Each category is further subdivided as needed.

I. TURBIDITES

A. Angamarca Group

This corresponds to a siliciclastic basin-fill sequence, thickening upwards. It comprises four mappable Formations in the area: Apagua Formation, Gallo Rumi Formation, Rumi Cruz Formation, and Pilaló Formation.

1. Apagua Formation

This Formation consists of sandstones and shales. It is located in the central belt of the study area and is cut by thin inliers of green rocks, ultramafic rocks, and other turbidites along fault systems that have undergone reactivation. A characteristic feature is the presence of strata with uniform thickness in individual outcrops. In general, a north-south strike dominates with a slight dip to the east. The sediments are folded at all scales, but no evidence of metamorphism is observed.

a. Sandstone: Dominates the Apagua Formation. It is clean, generally interbedded with shale, gray to black, fine-grained, well-sorted, with varying amounts of quartzose or clayey cement, fine clasts of quartz-muscovite-opaques ± plagioclase ± biotite ± chlorite ± epidote ± calcite.

b. Shale: Fine-grained, gray in color, composed of clay-opaques-quartz-micaceous material ± calcite ± epidote. The contribution of micaceous material is significant.

2. Gallo Rumi Formation

Exposed in the vicinity of Gallo Rumi, along the Guaranda-Riobamba road, this Formation comprises a sequence of conglomerates, microconglomerates, and pebbly quartzose sandstones interbedded with massive sandstones. The most important component is the conglomerate.

The **conglomerate** is coarse-grained, rounded to sub-rounded, with sparse quartzose matrix, and clasts predominantly of quartz (1 to 3 cm in diameter), with subordinate amounts of reddish to black lithics. The Formation exhibits intense folding.

3. Rumi Cruz Formation

In the mapped area, it outcrops around the Villa de Apagua. It is composed of very coarse conglomerates and sandstones with local development of red siltstone horizons.

The **conglomerate** is polymictic, of uniform composition, with rounded quartz clasts up to 15 cm in diameter, and subordinate amounts of black chert and silicified black shale.

4. Pilaló Formation

In the study area, it consists of basic volcanic and volcanoclastic rocks, some of which have undergone incipient contact metamorphism.

a. Volcanic rocks: They are composed of black **andesites**, medium- to coarse-grained, with phenocrysts of plagioclase-pyroxene-opaques, within a matrix of plagioclase-pyroxene-devitrified glass-opaques. The plagioclase is andesine and is altered; the pyroxene is chloritized. At least one occurrence, based on grain size, could be classified as microdiorite.

b. Volcanoclastic rocks: These are green **breccias**, with medium-grained clasts in a fine-grained matrix. The clasts are volcanic and volcanoclastic lithics ± quartz ± plagioclase ± pyroxene. The matrix is composed of devitrified glass ± plagioclase ± epidote. Occasionally, there are amygdules filled with chlorite-calcite.

B. Yunguilla Unit

The Yunguilla Unit consists of shales and fine sandstones with minor limestone horizons. Shales predominate. In several outcrops, incipient metamorphism is observed, manifested by the development of lineation perpendicular to the bedding. It is characterized by fine bedding.

1. Shale

The shale is black, generally calcareous, mineralogically dominated by clay, with minor contributions of quartz, chlorite, calcite, and opaques. In a few outcrops, fossils were found that are not specific to a particular age.

2. Sandstone

It is a clastic rock, with clasts ranging from coarse- to fine-grained, with a fine-grained matrix, slightly oriented; containing a significant mafic contribution. The clasts are composed of quartz-plagioclase-opaques ± calcite ± pyroxene ± amphibole ± epidote ± chlorite ± lithics; the matrix is clayey. The lithics are of varied composition; the clasts are generally altered.

3. Limestone

Fine-grained rock, whitish, ranging from stratified to massive, usually having a dirty appearance, and in some areas, intensely tectonised. Composed almost exclusively of calcite (>95% by volume) with very subordinate amounts of quartz ± plagioclase ± opaques ± clay ± fossils.

II. GREEN ROCKS

These rocks occupy the entire western part of the area. They are characterized mainly by being volcanoclastic and volcanic rocks of green color, fragmented to varying degrees. The volcanoclastic rocks have a volcanic appearance, are generally fine-grained, with small, angular clasts, green and red in color. Some exhibit filled amygdules, while others have sparsely or non-fragmented crystals; the matrix is modally variable and composed essentially of chloritized devitrified glass, and glass shards are common. They range from tuffs and hyaloclastites to volcanic sandstones. The volcanic rocks are essentially rather fine-grained basalts that are only slightly porphyritic. In some places, pillow lavas are observed.

This classification aims to be descriptive rather than genetic. The green rocks have been grouped into three units: the Macuchi Unit, Arrayanes Unit, and the Zumbagua Group. The volcanic rocks have been classified by their mode and, when whole rock geochemistry analyses have been available, by their chemical composition. Due to the lack of a unique classification scheme for volcanoclastic rocks, an effort has been made to follow the BGS Rock Classification Scheme.

The adopted classification scheme is as follows: In the field, the rocks have been globally identified as **volcanoclastic**. Microscopic examination reveals that if the rock contains glass clasts, it has been designated as **hyaloclastite** (considering that this, according to the BGS recommendation, is a genetic term that defines a rock with angular glass fragments formed by the rapid cooling of lavas during subaqueous intrusion). If the rock lacks glass clasts, especially if it has amygdules, it has been named **tuff** with the qualifier of **lithic, crystalline, or vitreous**, depending on whether lithic fragments, crystals, or chloritic matrix predominate. The terms **sandstone and breccia** have been restricted to rocks that exhibit sedimentary characteristics, either in outcrop, hand sample, or thin section.

The main petrographic characteristics of the green rocks are as follows:

A. Macuchi Unit

This unit is made up of volcanic and volcanoclastic rocks, locally interbedded with sediments. In a few areas, microgabbros have been observed, though their relationship with the Macuchi Unit is not obvious. The volcanic rocks are essentially slightly porphyritic fine-grained basalts; the volcanoclastic rocks are tuffs, volcanic sandstones, hyaloclastites, and breccias, all characterized by a green color generally due to the chloritization of volcanic glass. The sediments include cherts, limestones, siltstones, and calcarenites. The Unit is intruded by numerous bodies of intermediate composition. Contact aureoles with variable degrees of metamorphism have formed around the intrusions. Some samples also show signs of incipient submarine metamorphism.

1. Volcanic rocks

The volcanic rocks consist of basaltic andesites, basalts, and tuffaceous basalts.

The **basaltic andesites** are porphyritic, with medium- to fine-grained phenocrysts and a fine-grained matrix, sometimes showing an intergranular texture, and generally highly altered. Mineralogically, they are composed of a matrix of plagioclase-opaques ± amphibole ± chlorite ± alteration material, with phenocrysts of plagioclase-amphibole ± opaques, with secondary epidote and chlorite. The plagioclase is partially zoned and twinned, ranging in composition from An_{51} to An_{55}, while the amphibole is pleochroic hornblende, varying from green to pale brown (2Vx-80°). A few samples show scarce amygdules filled with secondary material (quartz-chlorite).

The **basalts** are black to greenish, porphyritic, with medium- to fine-grained phenocrysts in an aphanitic matrix, sometimes showing a pilotaxitic texture and rarely hyalophitic; they are altered. They are composed of phenocrysts of plagioclase-pyroxene-opaques ± amphibole ± olivine, with one or more of the following secondary phases: chlorite, epidote, chlorophaeite, serpentine, calcite. The matrix consists of plagioclase ± amphibole ± devitrified glass. The plagioclase is partially zoned and twinned, ranging in composition from An_{58} to An_{66}. The pyroxene is colorless, varying from augite to diopsidic augite, while the amphibole is pleochroic hornblende, ranging from yellow-green to dark green, and may represent altered pyroxene.

The **tuffaceous basalts** are characterized by a predominance of matrix over phenocrysts, a slightly porphyritic texture, abundant devitrified glass, and the presence of amygdules. They are quite altered. The phenocrysts consist of plagioclase-pyroxene-opaques ± chlorite ± epidote ± pumpellyite ± quartz; the matrix is composed of devitrified glass-plagioclase, and the amygdules are filled with quartz ± epidote ± pumpellyite. The plagioclase is highly altered, and the pyroxene is augite.

2. Volcanoclastic rocks

The volcaniclastic rocks consist of tuffs, hyaloclastites, volcanic sandstones, and breccias. Glass shards are relatively common, indicating that the rocks have a pyroclastic origin, although the deposition may not necessarily have occurred through pyroclastic processes. In fact, in older volcaniclastic rocks, it is difficult to define the mode of deposition. In the area, some of the rocks exhibit slightly broken crystals and have a homogeneous composition, suggesting they may have been deposited by pyroclastic processes. However, others show sedimentary features such as sub-rounded grains, bedding, evidence of reworked clasts, etc., indicating an epiclastic deposition (mass flow?).

The **tuffs** are classified as crystalline, lithic, or vitreous, depending on whether crystals, lithic fragments, or glass predominate. They are porphyroclastic, with a chloritic matrix resulting from very fine-grained devitrified glass.

Crystalline tuffs are fine-granular, containing crystalline clasts, whole or fractured, of plagioclase ± clinopyroxene ± olivine ± amphibole ± opaques ± quartz ± epidote ± chlorite ± calcite ± prehnite; lithic clasts of volcanic or volcaniclastic material, with a matrix of devitrified glass-plagioclase, amygdales filled with ± quartz ± plagioclase ± pyroxene ± lithics ± chlorite ± calcite ± epidote ± prehnite ± zeolite; occasionally with chloritized shards. Plagioclase typically forms microlites and appears to be of intermediate composition. The pyroxene is augitic.

Lithic tuffs have a fragmental texture, scarce matrix, and few amygdales; they are fine-grained with lithic and crystalline clasts. The lithics are from volcanoclastic rocks and, to a lesser extent, basic volcanic rocks. The crystals consist of plagioclase ± quartz ± pyroxene ± amphibole ± epidote ± chlorite ± calcite ± opaques. The matrix is composed of devitrified glass ± plagioclase. The amygdales are filled with ± quartz ± chlorite ± calcite ± epidote. The plagioclase has an intermediate composition (andesine-labradorite). There are few chloritized shards.

Vitreous tuffs are fragmental, characterized by a fine-grained matrix dominated by devitrified glass, with or without lithic clasts, and partially fragmented crystals of plagioclase (andesine-labradorite) ± pyroxene ± quartz ± opaques ± calcite ± chlorite ± epidote ± pumpellyite; amygdales filled totally or partially with ± quartz ± pyroxene ± chlorite ± zeolite ± epidote ± calcite ± pumpellyite ± prehnite; the presence of a few chloritized shards is recorded.

Hyaloclastites contain clasts of devitrified glass, and their other characteristics are similar to those of the tuffs: amygdales filled with chlorite ± calcite ± quartz ± epidote ± prehnite; crystals mainly consist of altered plagioclase, with a matrix of devitrified glass.

Volcanic sandstones are green, with sub-rounded to sub-angular grains, uniform, with an average size < 2 mm, and fine cement; they are occasionally crudely bedded, containing plagioclase (mostly andesine) ± quartz ± pyroxene ± chlorite ± epidote ± calcite ± opaques ± muscovite ± biotite ± olivine ± amphibole ± pumpellyite. The cement is composed of quartz ± clay ± calcite ± micaceous material ± chlorite.

Breccias range from medium to coarse-grained, with an average grain size > 2 mm; they contain reddish to black lithics and crystalline fragments of plagioclase ± pyroxene ± amphibole ± opaques ± chlorite ± epidote ± calcite. The matrix consists of chlorite ± plagioclase ± epidote. In a few samples, there are amygdales filled with quartz and/or other secondary material.

3. Sedimentary Rocks

Sedimentary rocks include cherts, quartzose siltstones, limestones, calcarenites, and sandstones. Limestones, calcarenites, and sandstones occur, with rare exceptions, exclusively in the Balzapamba sector, where they have undergone intense contact metamorphism. These rocks are described in detail in the section on metamorphic rocks. The few **limestones** that outcrop in other areas are white, fine-grained, finely stratified, and composed almost exclusively of calcite (>90%), with subordinate amounts of quartz and clay.

Quartzose siltstones are also scarce, green in color, fine-grained, with small, sub-angular clasts composed of quartz-chlorite-opaques ± clays ± plagioclase in a clayey matrix.

Cherts are massive, fine-grained, and slightly porphyritic, composed of chalcedony, micro-quartz, and mega-quartz with subordinate amounts of chlorite, plagioclase, Fe-oxides, epidote, and opaques.

Sandstones are clastic, medium to coarse-grained, and sub-rounded. They are composed almost exclusively of quartz covered by a thin reddish patina, likely from Fe-oxides.

4. Other Rocks

This group includes **gabbroic rocks** that occur sporadically, and their relationship with the Macuchi Unit is not well established, although they seem to constitute its basal part. Generally, they are green, altered, porphyritic microdiorites and microgabbros.

Microdiorites are fine to medium-grained, slightly porphyritic, containing plagioclase-amphibole-epidote-opaques ± prehnite ± chlorite. The plagioclase has an An_{46} composition, and the amphibole is a pleochroic hornblende, brownish to bluish-green.

Microgabbros have medium-grained phenocrysts and a fine-grained matrix with intersertal to subophitic texture oriented in domains. They are composed of plagioclase-pyroxene-amphibole-opaques ± chlorite ± epidote ± quartz ± calcite. The matrix consists of plagioclase-pyroxene. The composition of the plagioclase ranges from An_{54} to An_{63}. The pyroxene is diopsidic augite. The primary amphibole is a hornblende similar to that found in the microdiorites.

B. Arrayanes Unit

It forms a thin belt within the Macuchi Unit in the western part of the study area; in the north and center, it is continuous, and towards the south, it branches into thinner belts. It is cut by relatively large granodioritic/tonalitic intrusions around which it forms contact aureoles. Petrographically, it is composed of volcanic and sedimentary rocks with a minor component of volcanoclastic rocks.

1. Volcanic rocks

Andesites, basaltic andesites, and basalts occur, with the latter being predominant.

The **andesites** are dark, porphyritic, medium-grained within a fine-grained matrix of plagioclase. The phenocrysts are plagioclase-amphibole-opaques. The plagioclase is intermediate (An_{52}), and the amphibole is a slightly pleochroic hornblende, ranging from green to colorless.

The **basaltic andesites** are greenish-black, clearly porphyritic with phenocrysts of plagioclase ± amphibole ± pyroxene ± serpentine ± opaques in a fine to medium-grained matrix, sometimes intersertal, composed of plagioclase-amphibole-chlorite ± pyroxene ± opaques. The plagioclase has an intermediate composition (An_{54} to An_{60}), the pyroxene is diopsidic augite, and the amphibole is pale hornblende.

The **basalts** are black to greenish, only slightly porphyritic, with an aphanitic matrix (plagioclase microlites–devitrified glass) and phenocrysts of plagioclase ± clinopyroxene ± orthopyroxene ± amphibole ± epidote ± serpentine. The plagioclase is generally saussuritized, has a fairly uniform composition (An_{62} to An_{65}), the clinopyroxene is diopsidic augite, the orthopyroxene is optically negative and slightly pleochroic, and the amphibole is pale hornblende.

Spatially, the basalts tend to be located towards the western part of the area. Their texture seems to suggest submarine eruptions, in contrast to the porphyritic phases, which could be products of subaerial eruptions.

2. Volcanoclastic rocks

These are **crystalline to glassy tuffs**, fine-grained, porphyroclastic, with or without amygdales and scarce volcanic lithics. The matrix has abundant devitrified glass and plagioclase. The clasts consist of plagioclase ± pyroxene ± opaques ± epidote ± chlorite ± quartz ± lithics. The plagioclase is of intermediate composition.

3. Sedimentary rocks

These include sandstones, volcanic sandstones, siltstones, and green to brown shales, which are sub-horizontal and distinctly different from the turbidites of Apagua or Yunguilla.

The **sandstones** are fine-grained, with clasts of quartz-opaques ± chlorite ± pyroxene ± epidote ± muscovite ± biotite and clay cement.

The **volcanic sandstones** are green, fine-grained, somewhat porphyroclastic, some with crude bedding. The clasts consist of quartz-epidote-plagioclase ± calcite ± chlorite ± opaques. The matrix contains ± clay ± chlorite ± plagioclase ± epidote ± pyribol.

The **siltstones** are black, fine-grained, non-oriented, with sub-rounded to sub-angular grains; composed of quartz-plagioclase-opaques-clay.

The **shales** are very fine-grained, silicified, well-sorted, with an oriented texture; composed of clay-micaceous material-opaques-chlorite.

C. Zumbagua Group

This is a sequence of extrusive rocks (lavas and pyroclasts) and sedimentary rocks (sandstones) that occupy part of the central-eastern section of the study area. The lavas are andesites and basalts; the pyroclasts are tuffs and ignimbrites. In some locations, subordinate conglomerates are present. Columnar structure is common. The sandstones are coarse-grained and contain clasts of volcanic material.

1. Volcanic rocks

These are gray, porphyritic rocks with a fine-grained matrix, ranging from **andesites to basalts**. The phenocrysts consist of plagioclase (An_{43} to An_{66})-opaques ± clinopyroxene ± orthopyroxene ± amphibole ± quartz. The clinopyroxene is diopsidic augite; the orthopyroxene is a slightly rosy pleochroic enstatite (2Vx-75°); the amphibole is pale green hornblende. The plagioclase is twinned and partially zoned. The matrix consists of plagioclase ± amphibole ± opaques.

2. Volcanoclastic rocks

The **tuffs** are black, massive, with clasts of plagioclase-lithics-opaques ± clinopyroxene ± chlorite ± calcite ± epidote. The matrix is devitrified glass. The ignimbrites are basaltic, fragmental, with partially broken and altered crystals of plagioclase-clinopyroxene-orthopyroxene-opaques in a non-oriented glassy matrix.

3. Sedimentary rocks

The **sandstones** are coarse-grained, poorly sorted, rich in lithics (volcanics) and/or crystals (quartz-feldspar-amphibole). Some horizons are tuffaceous.

III. MAFIC AND ULTRAMAFIC ROCKS

They occur in several elongated inliers, approximately aligned in a N-NE to S-SW direction, cutting through various types of rocks apparently along ancient faults. In general, there is a mixture of green rocks, gabbros, ultramafic rocks, and occasionally even ancient turbidites.

This section also considers gabbroic rocks that occur within the Macuchi Unit, whose relationship with it is unknown.

A. Pallatanga Unit

This Unit comprises the rocks found in the mentioned inliers. It consists of a set of rocks that vary in composition from mafic to ultramafic and in character from intrusive to extrusive, also encompassing some sedimentary rocks likely transported during the emplacement of the main bodies.

1. Mafic rocks

These include green rocks of varied composition and origin, basalts, picritic basalts, and gabbros.

The **green rocks** are highly altered; they encompass tuffs, volcanic sandstones, and other rocks that are difficult to classify due to alteration. The volcanic sandstones are clastic, of medium grain, somewhat recrystallized, with scarce matrix and the presence of plagioclase-pyroxene ± olivine ± serpentine ± calcite ± opaques ± quartz ± lithics, with veinlets of prehnite and/or quartz. The tuffs have clasts of similar composition and some additionally contain perovskite or chlorophaeite, a matrix with devitrified glass and amygdales filled with one or more of the following phases: chlorite, quartz, chalcedony, zeolites, epidote, prehnite. Among the rocks that are difficult to classify are intensely tectonised rocks with calcite-quartz-clays-plagioclase-opaques; others are red, with quartz-Fe oxides-vermiculite, which could suggest hydrothermal alteration of ultramafic rocks followed by subsequent quartz recrystallization.

The **basalts** are also altered porphyritic, with a fine-grained matrix rich in devitrified glass and phenocrysts of plagioclase-clinopyroxene-orthopyroxene-olivine-opaques ± calcite. The plagioclase has a composition of An_{56} to An_{65}, the clinopyroxene is a colorless diopside augite, and the orthopyroxene is hypersthenic.

Picritic basalts are porphyritic with a fine-grained matrix of pyroxene-olivine with subordinate plagioclase. The phenocrysts are also pyroxene-olivine and very scarce plagioclase. The pyroxene is diopsidic augite; pyroxene and olivine are serpentinized, and the plagioclase is sericitized. Some samples exhibit vesicles filled with quartz and prehnite.

The **gabbros** are hypidiomorphic, of medium to fine grain; some have an ophitic texture and others slightly porphyritic, which causes them to grade into microgabbros. All are strongly altered. Their composition is plagioclase-pyroxene ± olivine ± amphibole ± chlorite ± epidote ± serpentine ± quartz ± opaques ± calcite ± sphene. Several are cut by veinlets of calcite, prehnite, talc, or serpentine. The plagioclase has a composition of An_{50} to An_{60}; it is highly altered. The pyroxene is a greenish or brownish augite, not pleochroic. In a microgabbro, augite and pigeonite coexist. (Inverted pigeonite is a common cumulative phase in basic plutonic rocks of tholeiitic affinity. The change from enstatite to pigeonite occurs in non-early differentiated rocks.)

2. Ultramafic rocks

Ultramafic rocks have varied compositions; they range from websterites to pyroxenites and are serpentinised to varying degrees. For the most serpentinised rocks, it is not possible to recognize the protolith.

Websterite contains clinopyroxene-orthopyroxene ± spinel ± opaques; the clinopyroxene is diopsidic, the orthopyroxene is hypersthenic, and the spinel is greenish with a tabular appearance.

There are **pyroxenites with olivine** (clinopyroxene with smaller amounts of olivine) and **orthopyroxenites with amphibole** (orthopyroxene-amphibole-talc-sapphirine-opaques). Orthopyroxene and clinopyroxene are similar to those in websterite. The presence of sapphirine indicates contamination with crustal material. Epidote, chlorite, and calcite veins occur as secondary minerals and suggest low-grade metamorphism. In at least one sample, vermiculite appears as a result of hydrothermal alteration.

The presence of websterite instead of harzburgite could suggest a mid-ocean ridge affinity, contrasting with a seafloor setting.

B. Undifferentiated gabbroids

To the south of the study area, near San José del Tambo, there is a moderately sized body of gabbroic rocks. Smaller bodies are also found in the south embedded within Macuchi rocks.

These gabbroids include gabbros, quartz-gabbros, microgabbros, and microdiorites that are quite similar to one another. The **gabbros** have variable grain sizes and an hypidiomorphic to slightly porphyritic texture. Mineralogically, they are composed of plagioclase-clinopyroxene-opaques ± orthopyroxene ± opaques with chlorite ± serpentine ± amphibole ± epidote ± quartz as alteration or incipient metamorphism phases. The **quartz-gabbros** contain quartz in their paragenesis. Plagioclase varies in composition from An_{58} to An_{70}; the pyroxene is diopsidic augite; orthopyroxene, when present, is scarce and occurs as inclusions within clinopyroxene.

Microdiorites and microgabbros are porphyritic to slightly porphyritic, generally altered, with mineralogy similar to that of gabbros, featuring phenocrysts of plagioclase and pyroxene. The plagioclase is usually twinned and zoned but saussuritized.

IV. INTRUSIVE ROCKS

Several bodies of granodiorites/tonalites of varying extent and calc-alkaline affinity occur in the study area, intruding into green rocks and sediments of the Macuchi and Arrayanes Units, forming contact aureoles. The intrusives are notably homogeneous both mineralogically and chemically. Their ages range from 10.8 to 34.3 Ma.

In this report, the intrusives are divided into five main bodies: El Corazón, Echeandía, Chazo Juan-Telimbela, Balzapamba, and Undushig. Additionally, there are several minor intrusives.

A. Tonalites/granodiorites

All major intrusives are classified as tonalites and granodiorites. Their mineralogy is very uniform, and the main difference lies in the estimated percentage of K-feldspar, which for various samples is close to the boundary between the two categories. The rocks are medium to coarse-grained, with an essentially hypidiomorphic, non-oriented to allotriomorphic texture, consisting of plagioclase-quartz-biotite-amphibole-opaques ± K-feldspar ± clinopyroxene ± zircon ± sphene. The plagioclase is generally zoned and twinned, somewhat altered; the quartz is anhedral and clear; the biotite is reddish; the pale amphibole, pleochroic from greenish to brownish, is a magnesian hornblende; the opaques are black; K-feldspar is usually less altered than plagioclase. Some characteristics of the main bodies are mentioned below.

1. El Corazón

All analyzed rocks are granodiorites. The K-feldspar varies from microcline to orthoclase. The plagioclase composition is concentrated in the range of An_{40} to An_{46}, with two extreme values of An_{36} and An_{54}.

Along the Río Cinde - El Corazón road, there is a massive white aplite phase, kaolinized, composed of plagioclase-quartz-K feldspar-opaques, with secondary calcite.

2. Echeandía

The plagioclase has a composition of An_{44} to An_{47}, with few values as low as An_{40} and as high as An_{54}. In some tonalites, clinopyroxene ± orthopyroxene occur. The clinopyroxene is aegirinic augite; the orthopyroxene is hypersthene. The K-feldspar varies from microcline to orthoclase.

In the Caluma sector near La Magdalena, a pegmatitic phase occurs, coarse-grained, allotriomorphic, composed of partly poikiloblastic quartz and interstitial tourmaline needles. The tourmaline belongs to the schorl-elbaite series, which is typical of pegmatite core areas.

3. Chazo Juan - Telimbela

All analyzed rocks are tonalites, with little to no K-feldspar. The plagioclase has an average composition of An_{44}, with an anomalous value of An_{64}.

4. Balzapamba

The rock ranges from tonalite to granodiorite. The K-feldspar is orthoclase, and the composition of the plagioclase varies from An_{43} to An_{46}.

5. Undushig

The rock varies from tonalite to monzodiorite. The plagioclase has an average composition of An_{50}.

B. Minor intrusives

There are several intrusions of granodioritic to tonalitic character that intrude the Arrayanes, Pallatanga, Macuchi, Yunguilla Units, Zumbagua, Group and Apagua Formation. Generally, they are porphyritic, medium-grained, with plagioclase-quartz-amphibole-opaque ± pyroxene ± K feldspar, and as secondary phases ± chlorite ± epidote ± muscovite.

V. METAMORPHIC ROCKS

Metamorphic rocks in the study area are scarce. However, contact aureoles surrounding the intrusions are notable, some with peculiar mineralogy. Additionally, in several mafic and ultramafic rocks, an incipient regional metamorphism is observable, probably of submarine origin, and in the Yunguilla sediments near Pallatanga, an incipient dynamic metamorphism is present. In very localized sectors along the fault system of the Chimbo River, mylonites and ultramylonites have developed.

A. Contact metamorphism

1. Hornfels

Around the intrusions, contact metamorphism aureoles are usually observed; the protoliths are rocks from the Yunguilla, Macuchi, and Arrayanes Units. No contact aureoles are observed in the Apagua Formation.

The **hornfels** from Yunguilla are silicified sediments, fine-grained meta-sandstones or meta-shales in which recrystallized quartz is observed. The meta-sandstones have a paragenesis of quartz-plagioclase ± epidote ± pumpellyite ± chlorite ± calcite.

The hornfels whose protoliths are from the Arrayanes Unit are generally of low metamorphic grade; in the sedimentary origin rocks, there is recrystallization of quartz and formation of chlorite ± epidote ± muscovite. In the igneous origin rocks, there is ± epidote ± pumpellyite ± chlorite ± calcite. A rock between Telimbela and Caluma has developed epidote-quartz-garnet.

The hornfels in Macuchi are more varied; most have developed the same minerals as in Arrayanes, although in the meta-sandstones, incipient growth of biotite is observed. However, in the surroundings of Balzapamba, the metamorphosed calcarenites and limestones form fine to medium-grained marbles, granofelsic in texture, with a mineralogy dominated by calcite (calcite ± epidote ± quartz ± wollastonite), fine-grained hornfels composed of quartz-wollastonite-biotite-muscovite; black hornfels, fine-grained and fibrous, composed of cordierite-anthophyllite-biotite-talc-opaque plagioclase. This association is characteristic of the metasomatism of basalts followed by metamorphism. The changes in the overall chemistry of a basalt to transform into a cordierite-anthophyllite rock are precisely those characteristic of submarine metamorphism; that is, the protolith would be marine greenschist that has undergone subsequent thermal metamorphism.

B. Regional metamorphism

1. Submarine metamorphism

In volcanoclastic rocks of the Macuchi Unit, it is possible to observe one or more minerals (prehnite, pumpellyite, zeolite) characteristic of submarine metamorphism filling vesicles and thin veins. In several undifferentiated gabbroids, the presence of chlorite, amphibole, epidote, and quartz seems to indicate metamorphism in the lower part of the greenschist facies. In the rocks of the Pallatanga Unit, the secondary minerals (epidote, chlorite, calcite veins) suggest low-grade metamorphism (prehnite-pumpellyite facies or the lower part of greenschist facies) compatible with submarine metamorphism. The absence of the characteristic prehnite-pumpellyite association may be due to the presence of CO_2 in the fluid.

C. Dynamic metamorphism

Mylonites outcrop in regions of more intense tectonism, especially in areas adjacent to the Chimbo River, whose course is associated with a significant fault system. Where they can be recognized, the protoliths of the mylonites are turbidites or green rocks. In other sectors, mainly between Trigoloma and Panza Redonda, dynamic metamorphism is manifested by a double lineation in shales and sandstones.

VI. OTHER ROCKS

In the area of Map 3, rocks of more or less restricted extent or younger age than those already described occur. These are:

A. Saraguro Group

In the studied area, this group is represented by andesites and basaltic andesites, gray, porphyritic with phenocrysts of plagioclase (An_{51})-opaque ± augite ± oxyhornblende ± olivine, in a matrix of microlites of plagioclase and slightly devitrified glass, which outcrop in a N-S belt east of Guaranda.

B. Cisarán Formation

Andesites and glassy tuffs that are assigned to this Formation further south are observed. The **andesites** are porphyritic, fine-grained, with a trachytic texture (microlites of plagioclase oriented in subdomains); mineralogically, they are composed of phenocrysts of plagioclase (An_{38})-amphibole-opaques, in a matrix of glass and plagioclase. The **tuffs** are fragmental, with clasts of volcanic lithics-augite-plagioclase-opaques ± olivine, in a glassy matrix with microlites of plagioclase.

C. Plio-Pleistocene rocks

These are mainly undifferentiated andesitic and dacitic volcanic rocks, outcropping near San Miguel de Bolívar and northwest of Ambato. The former constitutes a poorly exposed weathered sequence that has been hydrothermally altered, with large phenocrysts of quartz and feldspar. The latter consists of tuffs and andesitic lavas of two pyroxenes.

D. Quaternary rocks

These are black to gray basalts, porphyritic, with phenocrysts of plagioclase (An_{60})-opaques ± augite ± amphibole, in a fine-grained matrix composed of plagioclase and devitrified glass. There are also tuffs, breccias, lavas, and ashes from Pleistocene and younger volcanic centers.

APPENDIX 2 OF REPORT:

GEOLOGY OF THE WESTERN CORDILLERA
OF ECUADOR
BETWEEN 1°00' AND 2°00' S

ROCK GEOCHEMISTRY

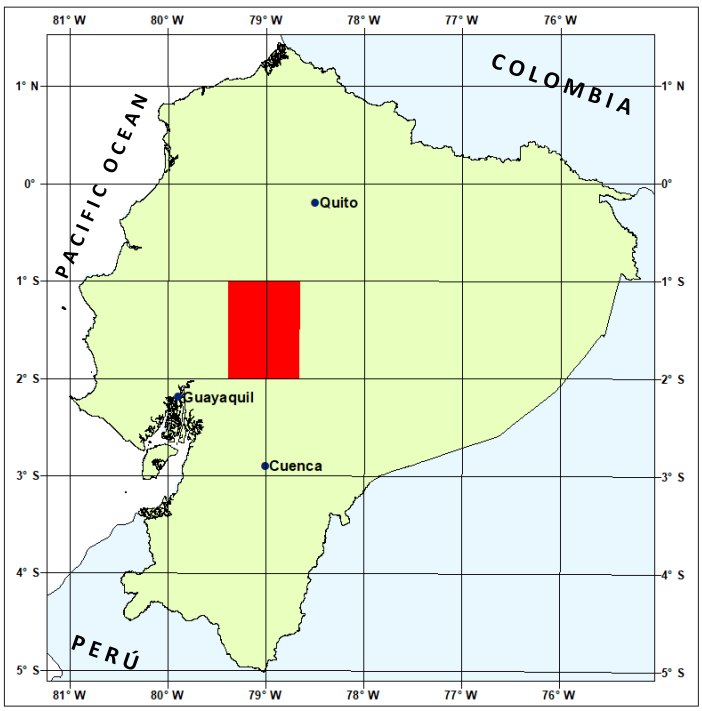

GEOLOGICAL INFORMATION MAPPING PROGRAMME
(LOCATION OF MAP 3 AREA)

W. MCCOURT
P. DUQUE
L. PILATASIG

QUITO, 1997

CONTENTS

I. INTRODUCTION

Petrological research in the Western Cordillera is scarce. The most well-known rocks are probably those from certain sectors of the Macuchi Unit. Lebrat (1985) conducted a geochemical study based on global analyses of major and trace elements. Aguirre and Atherton (1987) investigated the metamorphism of the same rocks at a section of the Latacunga-Quevedo road. This study is based on the interpretation of 41 total whole rock geochemical analyses (major elements, trace elements, and Rare Earth Elements) from samples of the various units exposed in the region covered by Map 3. The outcropping igneous rocks are mainly subdivided into two groups: granitoids and mafic rocks.

The interpretation was carried out using the computational packages NewPet (Clarke, 1994), Triplot (Baedke and Thompson, 1993), and Microsoft Excel.

II. GRANITOIDS

A. Classification

They are classified into five major intrusions: El Corazón, Chazo Juan-Telimbela, Echeandía, Balzapamba, and Undushig. Additionally, there are several minor intrusions likely apophyses of the aforementioned ones.

Geochemically, the intrusions are notably uniform. For their classification, diagrams based on multi-cations (Debon and Le Fort, 1983), weight percent of alkalies (Middlemost, 1985), molecular norms (Barker, 1979), and mesonorms (Le Maitre, 1989) were utilized. According to all schemes and petrographic classification, the rocks vary from tonalites to granodiorites. Several of them plot toward the boundary of the fields. The intrusive of El Corazón is essentially granodioritic, Echeandía consists of granodiorites and tonalites, similarly Balzapamba; whereas Chazo Juan-Telimbela and Undushig are predominantly tonalitic.

Figures 1 to 4 present the various classification schemes used for the granitoids. The legend of Figure 1 is applicable to all classification graphs.

B. Origin

Regarding their geochemical characteristics, the granitoids are essentially meta-aluminous (biotite + hornblende) with some peraluminous characteristics (biotite), which is confirmed by the petrography. As shown in Figures 5 and 6, all granitoids plot toward the boundary between the fields. Those from El Corazón and Balzapamba are always meta-aluminous, while those from Chazo Juan-Telimbela and Echeandía fall into both fields.

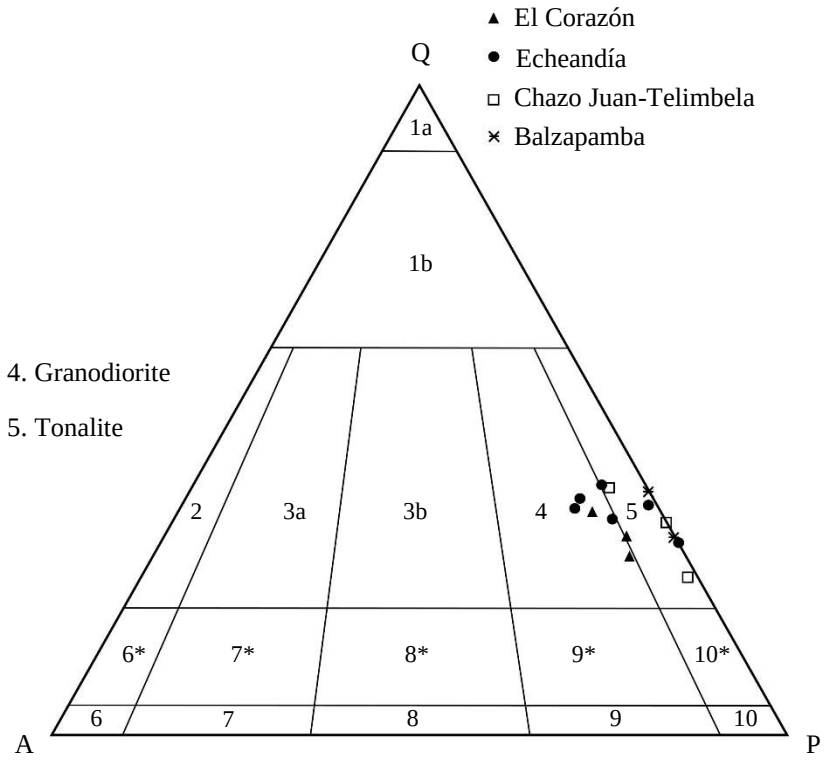

Figure 1. Mesonormative QAP classification for granitoids (Le Maitre, 1989)

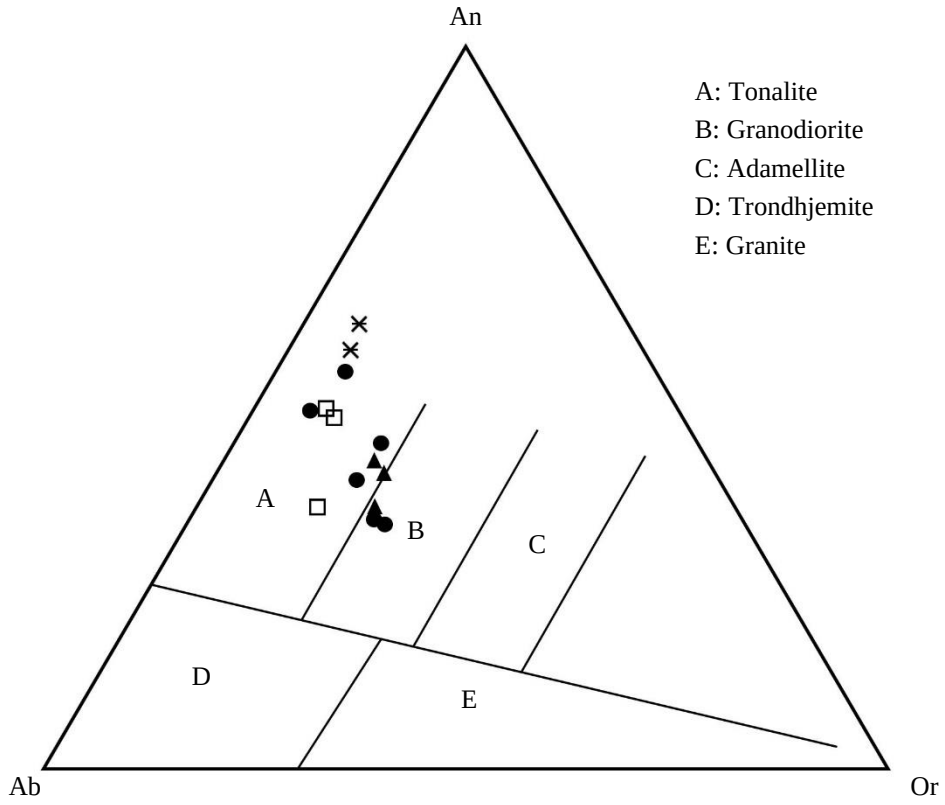

Figure 2. Normative Ab-An-Or classification for granitoids (Barker, 1979)

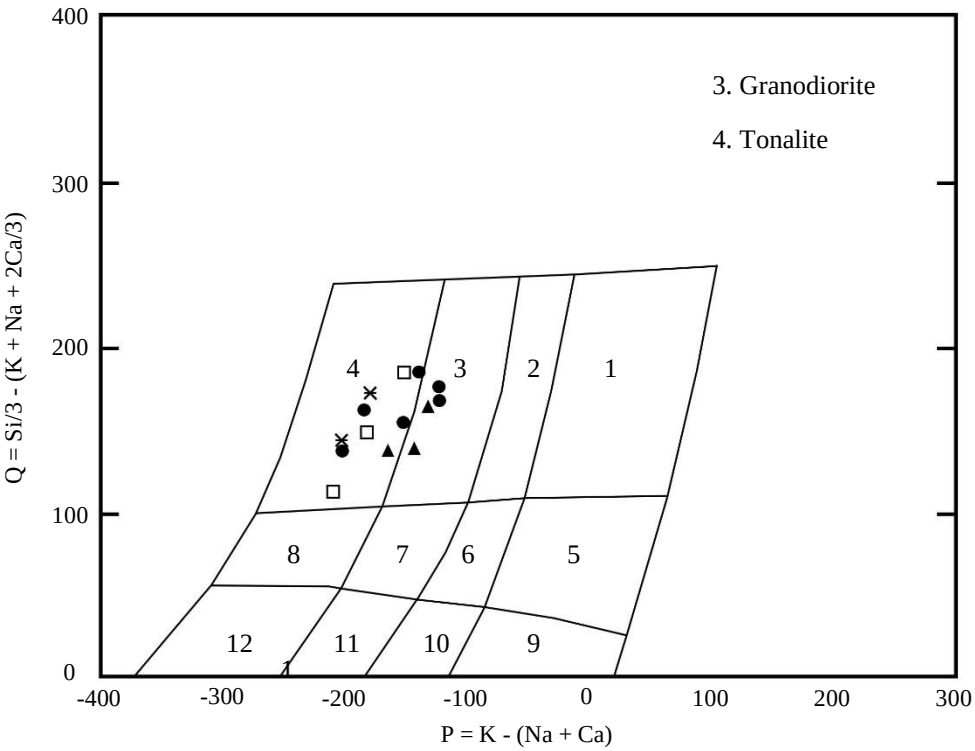

Figure 3. Multi-cationic Q-P classification for granitoids (Debon & Le Fort, 1983)

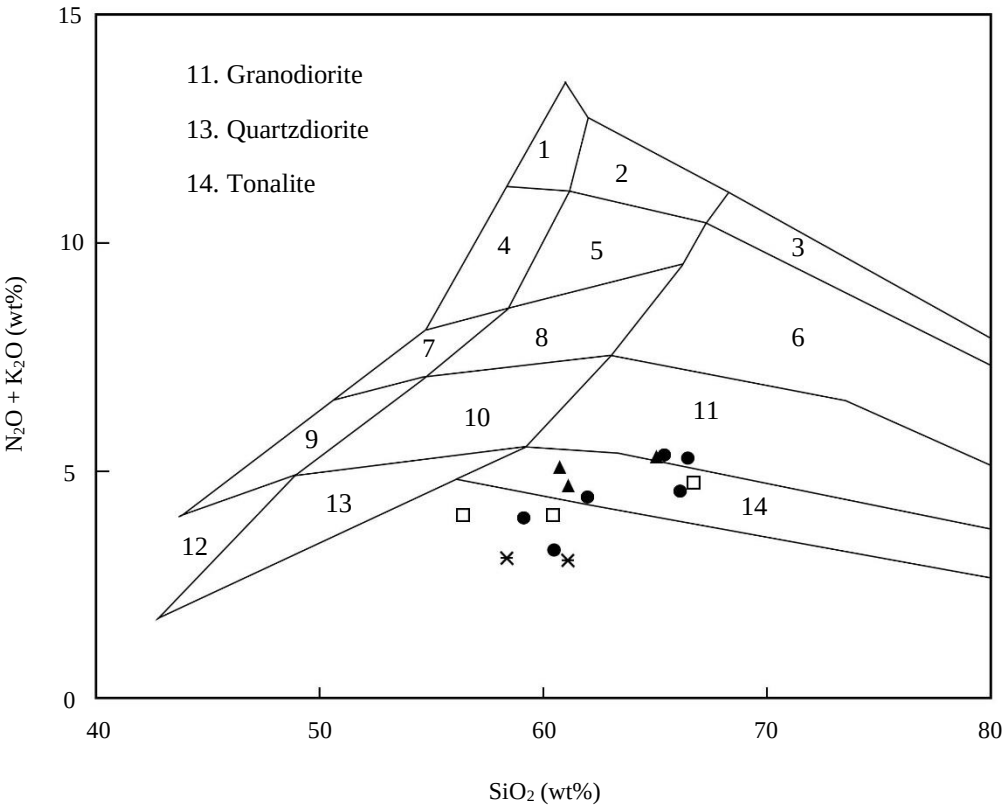

Figure 4. TAS classification for granitoids (Middlemost, 1985)

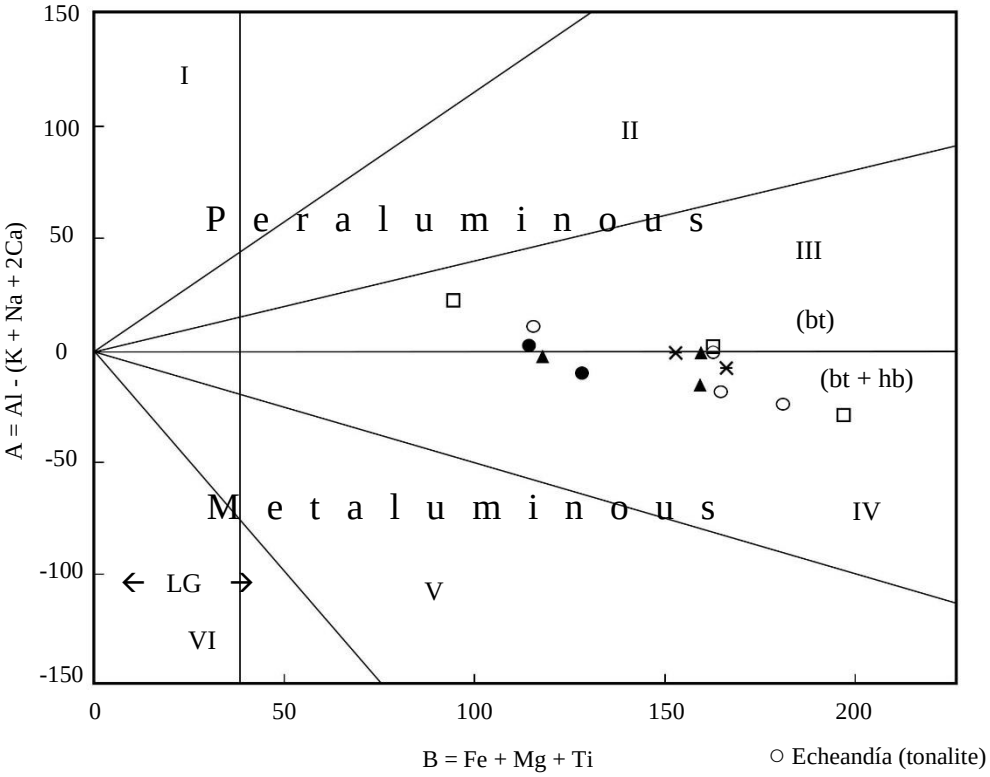

Figure 5. Aluminous character of granitoids based on cationic factors A-B (Debon & Le Fort, 1983)

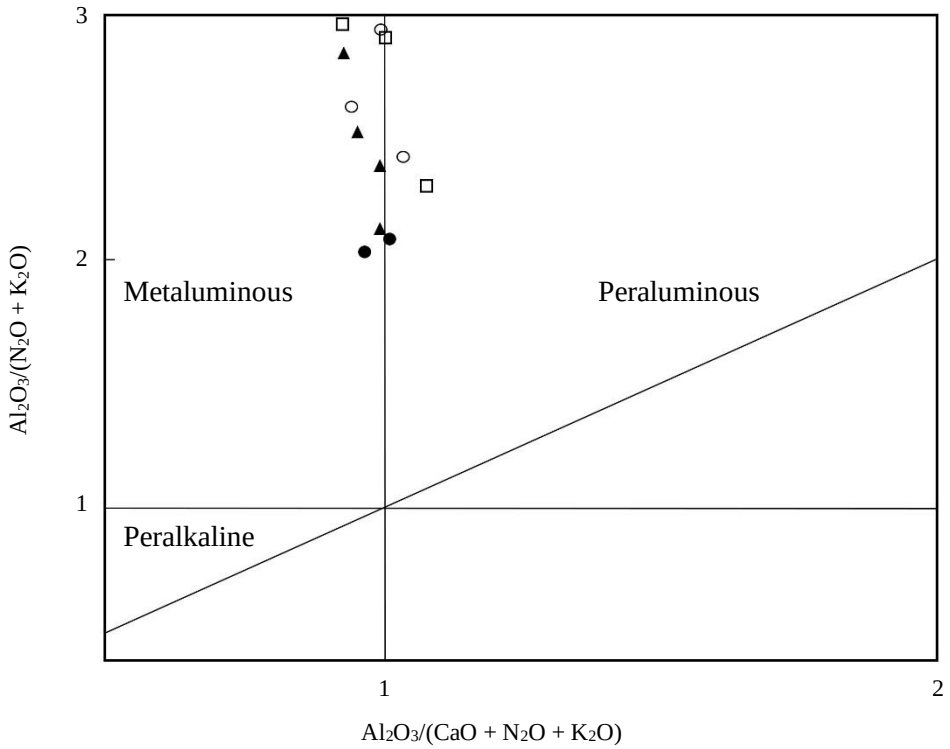

Figure 6. Aluminous character of granitoids based on weight percent of oxides (Maniar & Piccoli, 1989)

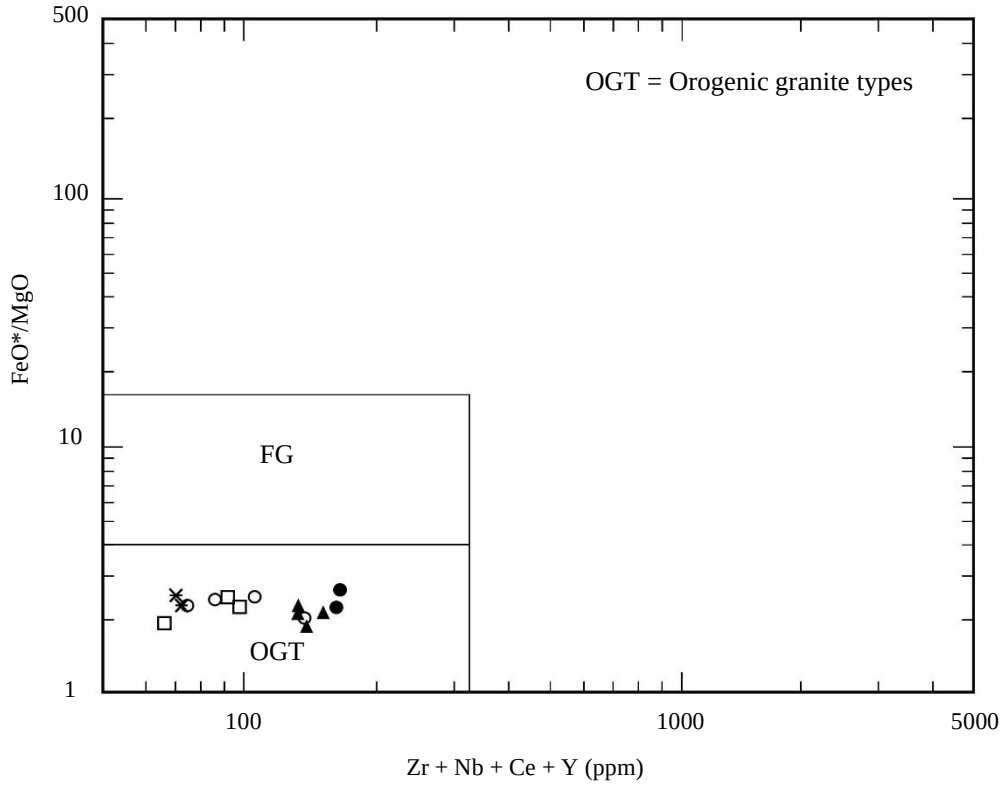

Figure 7. Tectonic character of granitoids (FeO/MgO - trace elements) (Whalen et al., 1987)

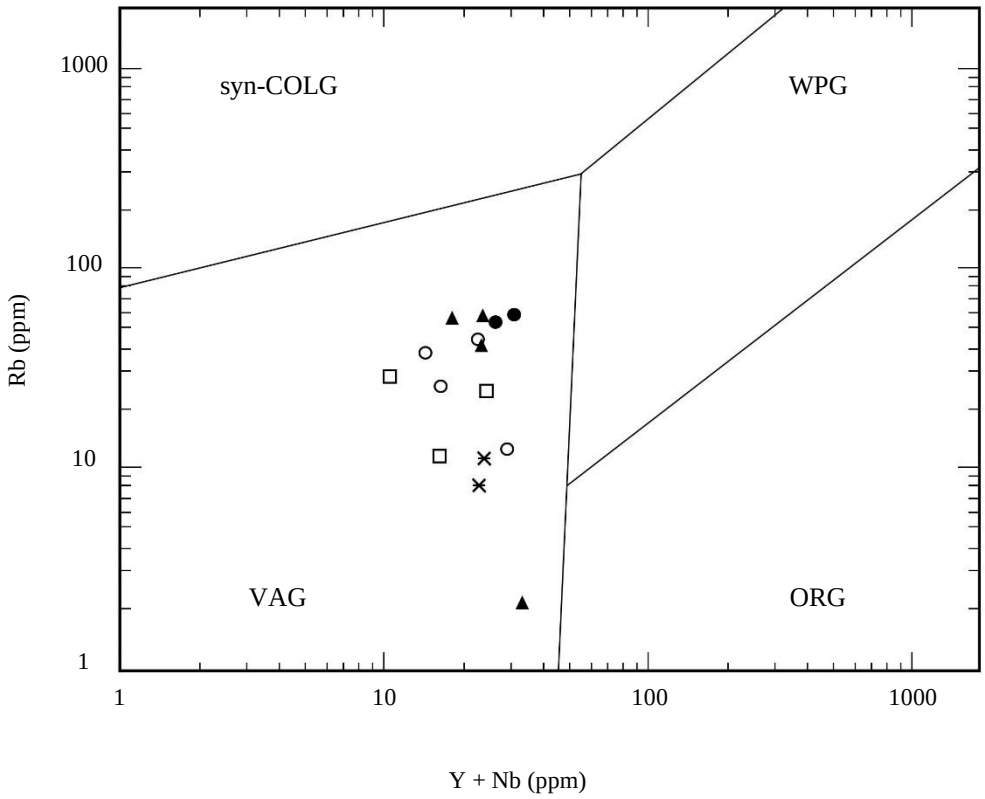

Figure 8. Tectonic discrimination (Rb vs. Y + Nb) of granitoids (Pearce et al., 1984)

Regarding tectonic emplacement, all the intrusions in the area are orogenic granite types (OGT) (Fig. 7); specifically, volcanic arc granites (VAG) (Fig. 8). The latter figure uses the concentrations of Rb, Y, and Nb, which are the most efficient discriminants for different tectonic settings of granites according to the studies by Pearce et al. (1984). However, post-orogenic granites cannot be distinguished from volcanic arc granites and syn-collisional granites in Pearce's diagrams. The diagram by Whalen et al. (1987) (Fig. 7) allows for this distinction, indicating that the granitoids in the area are all orogenic-type.

Figure 9 (Irvine and Baragar, 1971) indicates that all granitoids in the area are clearly subalkaline. Figure 10 classifies the studied granitoids within Type I (in the sense that they formed in a subduction zone), and Figure 11 (modified from Brown et al., 1984), valid for Mesozoic and Cenozoic arcs, shows that they are from either continental or immature island arcs based on Nb content for a fixed Rb/Zr ratio and the field in which they plot.

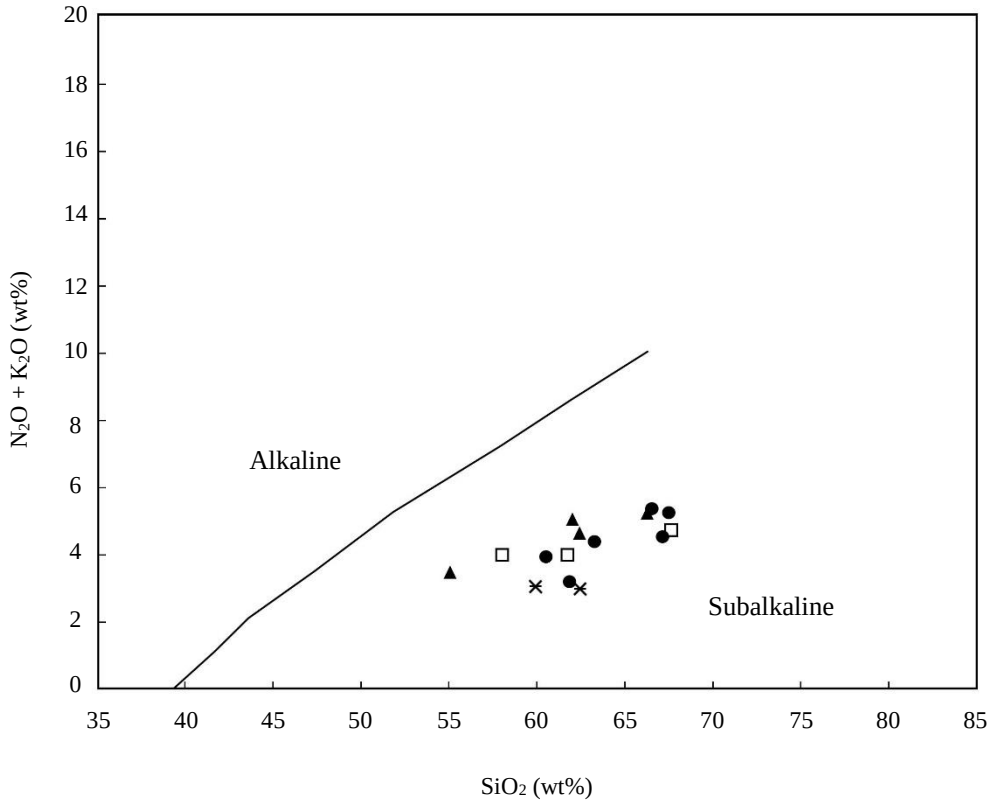

Figure 9. TAS distinction between alkaline and subalkaline granitoids (Irvine & Baragar, 1971)

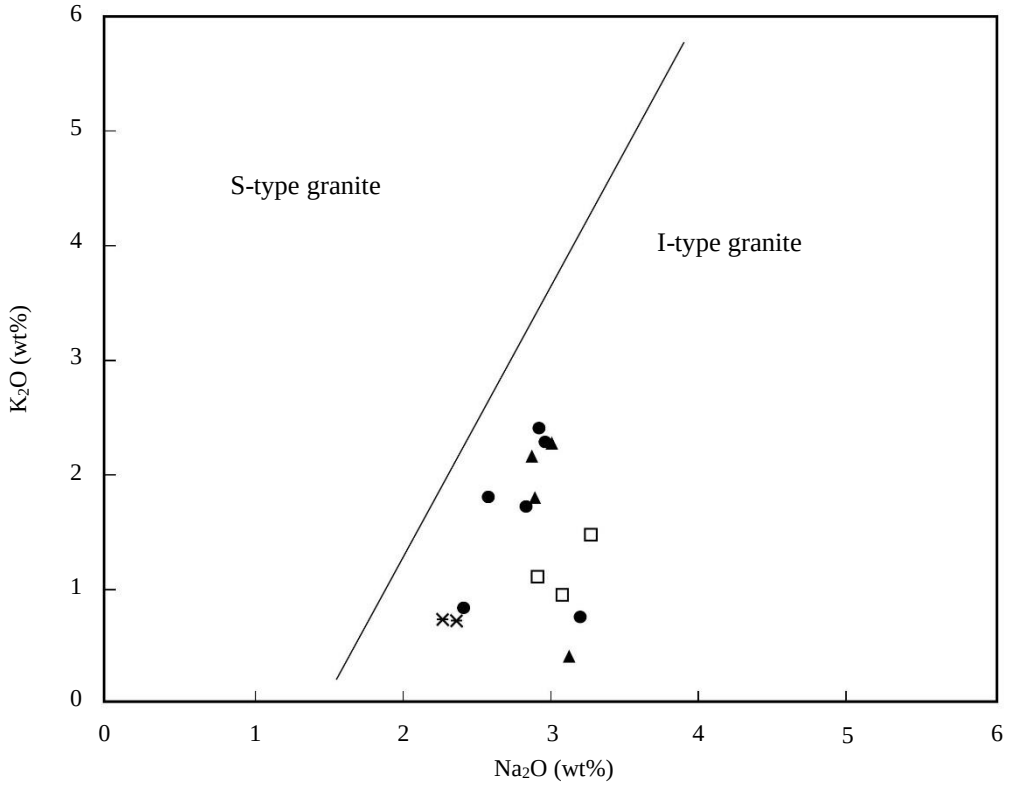

Figure 10. Discrimination (K_2O vs. Na_2O) between S-type and I-type granitoids

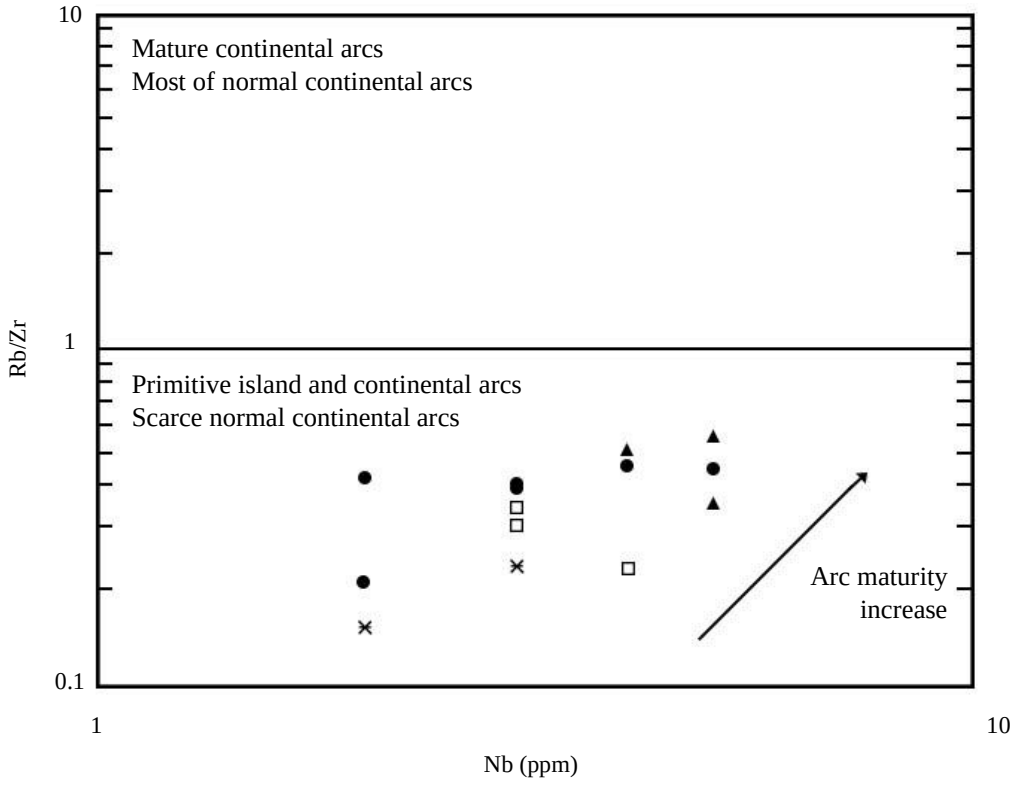

Figure 11. Maturity measurement for Mesozoic and Cenozoic arcs (Brown et al., 1984)

C. Diagrams of normalized trace element variation (spider diagrams)

Figures 12 and 13 present spider diagrams normalized to primitive mantle and MORB for the studied granitoids. These diagrams show a uniform pattern for samples from all units. When normalized to primitive mantle, a strong enrichment in the more mobile LIL elements is observed, in addition to Hf and Sm, along with moderate enrichment in all the others.

In the diagram normalized to MORB, enrichment is observed in the more mobile LIL elements, especially K, Rb, Th, and U; depletion in Nb, Nd, Ti, and Y; and concentrations close to one for the heavier LILs and the Rare Earth Elements.

The intermediate to high values of Rb, Th, U, and K can be interpreted as enrichment in a subduction zone. The diagrams are consistent with those of type I granitoids from primitive arcs, whether island or continental.

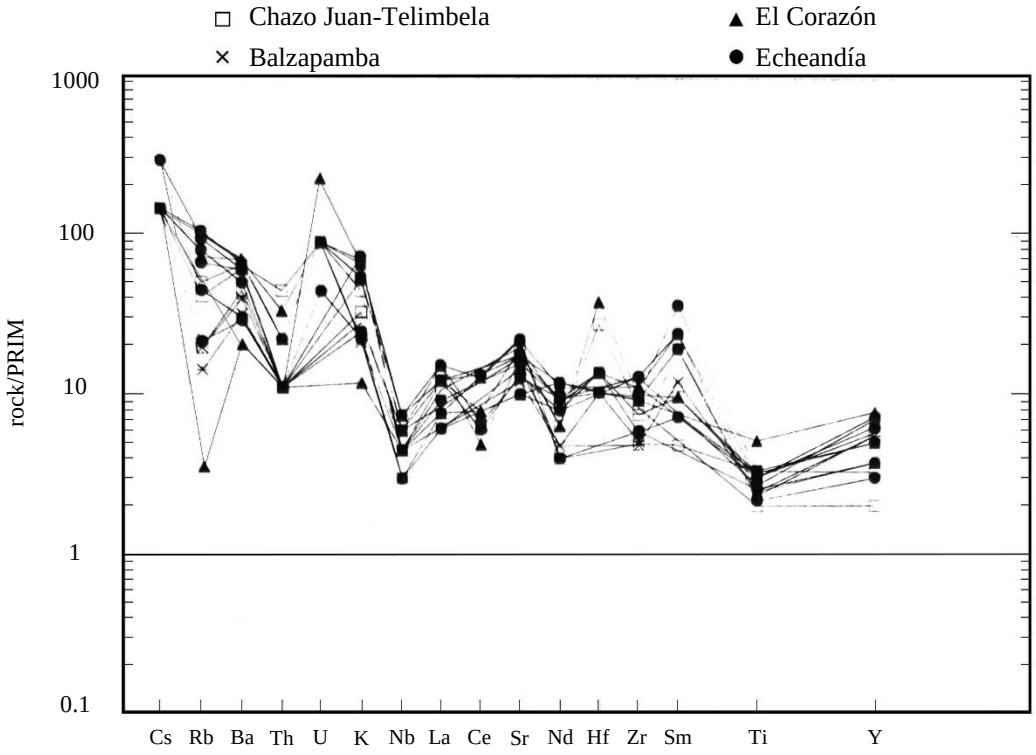

Figure 12. Spider diagram for granitoids (rock/PRIM)

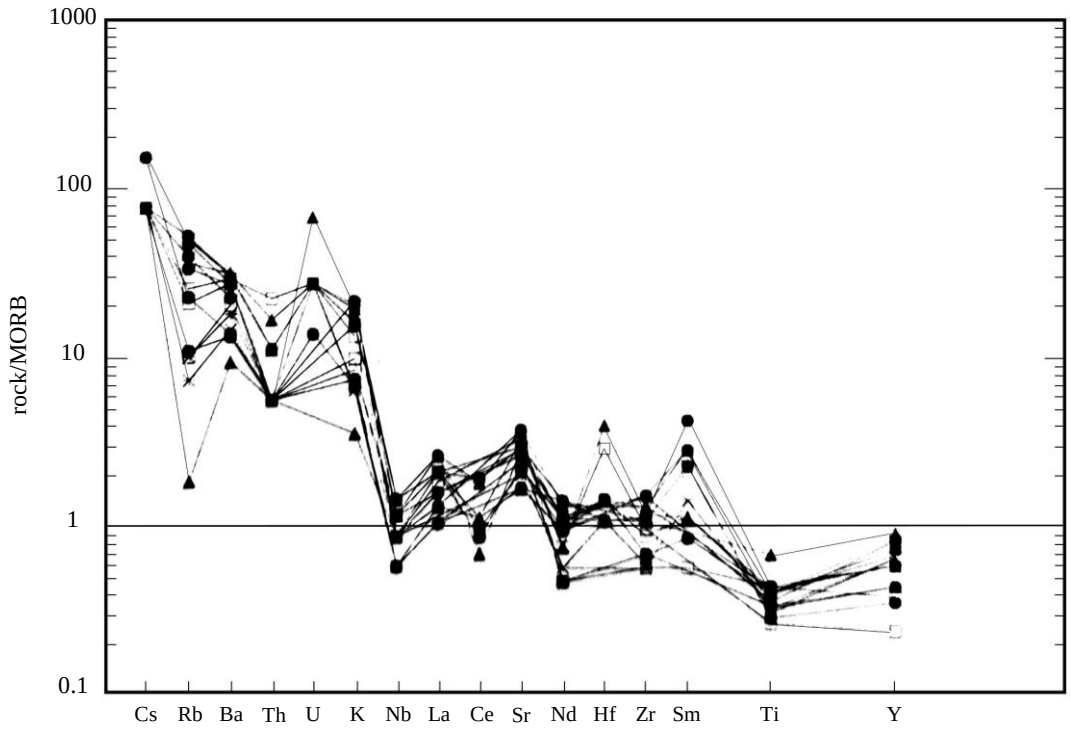

Figure 13. Spider diagram for granitoids (rock/MORB)

III. MAFIC ROCKS

The mafic rocks in the area belong to the Macuchi, Arrayanes, and Pallatanga Units. Additionally, there are gabbros, diorites, and microgabbros classified as undifferentiated gabbroids. These gabbroids have very similar chemical characteristics to those of Macuchi.

A. Classification

The chemical classifications of the mafic rocks, based on both major elements (Figs. 14, 15) and trace elements (Fig. 16), are equivalent. The rocks of Pallatanga have the composition of tholeiitic basalts, those from Macuchi vary from basalts to basaltic andesites, and those from Arrayanes range from basaltic andesites to andesites.

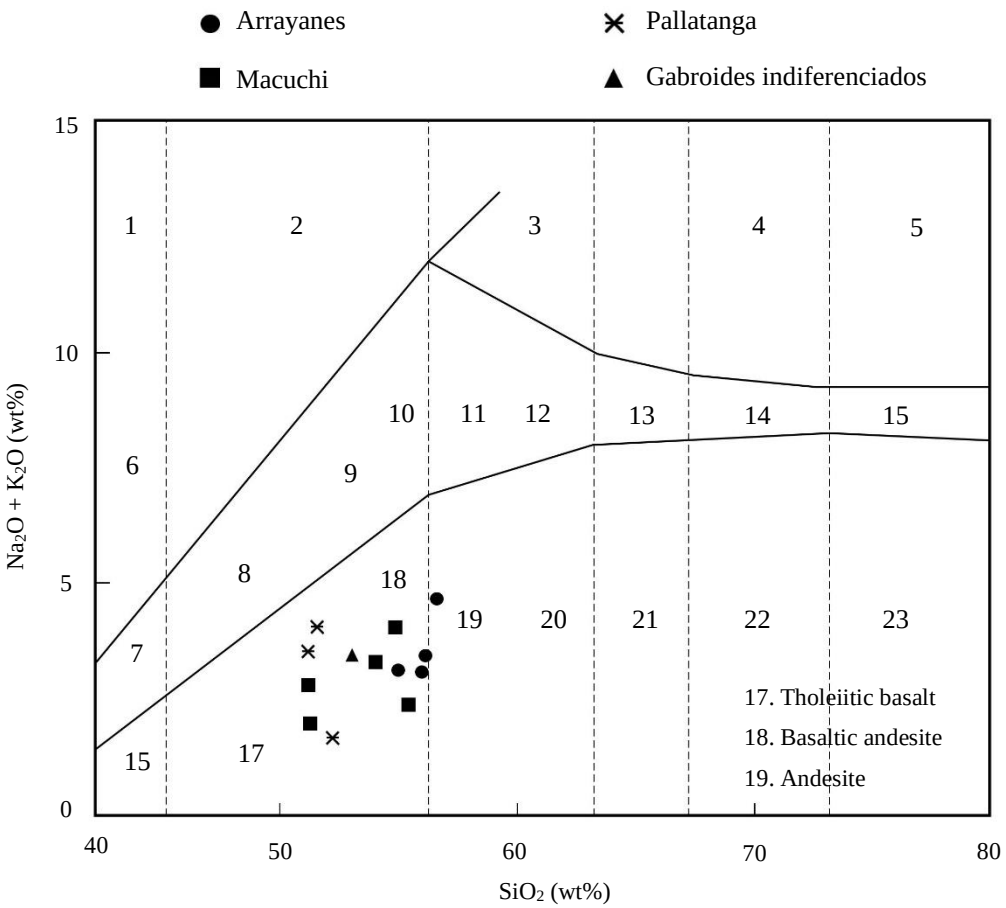

Figure 14. TAS classification for mafic rocks (Middlemost, 1985)

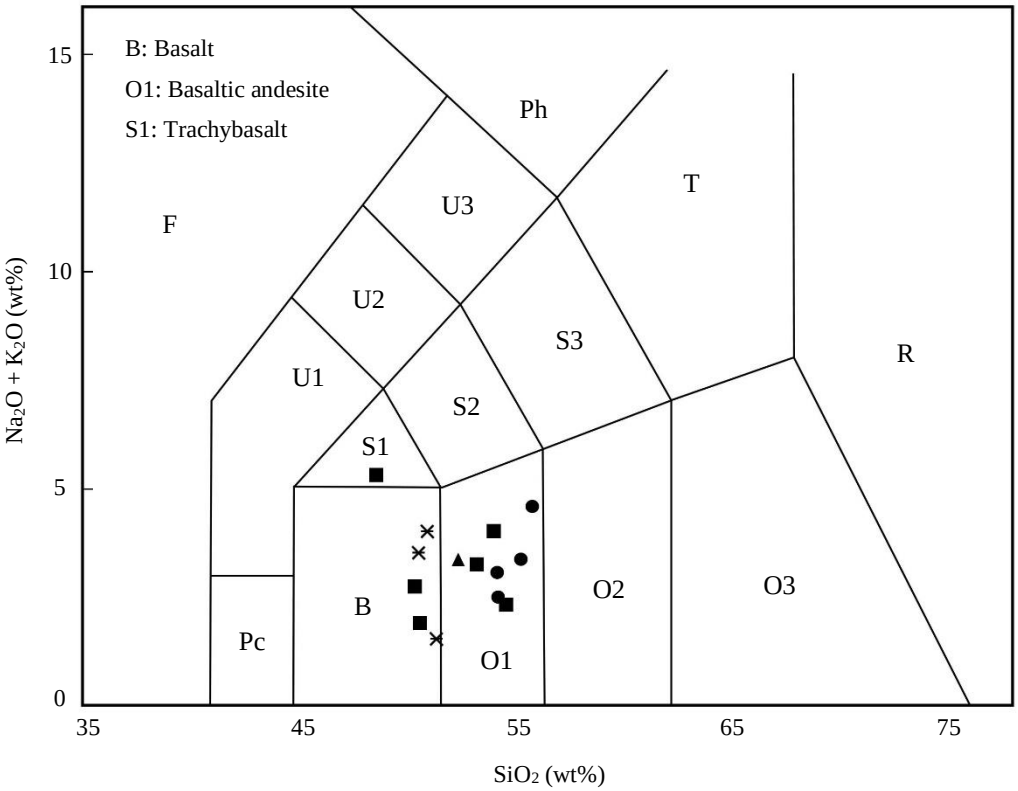

Figure 15. TAS classification for mafic rocks (Le Maitre, 1989)

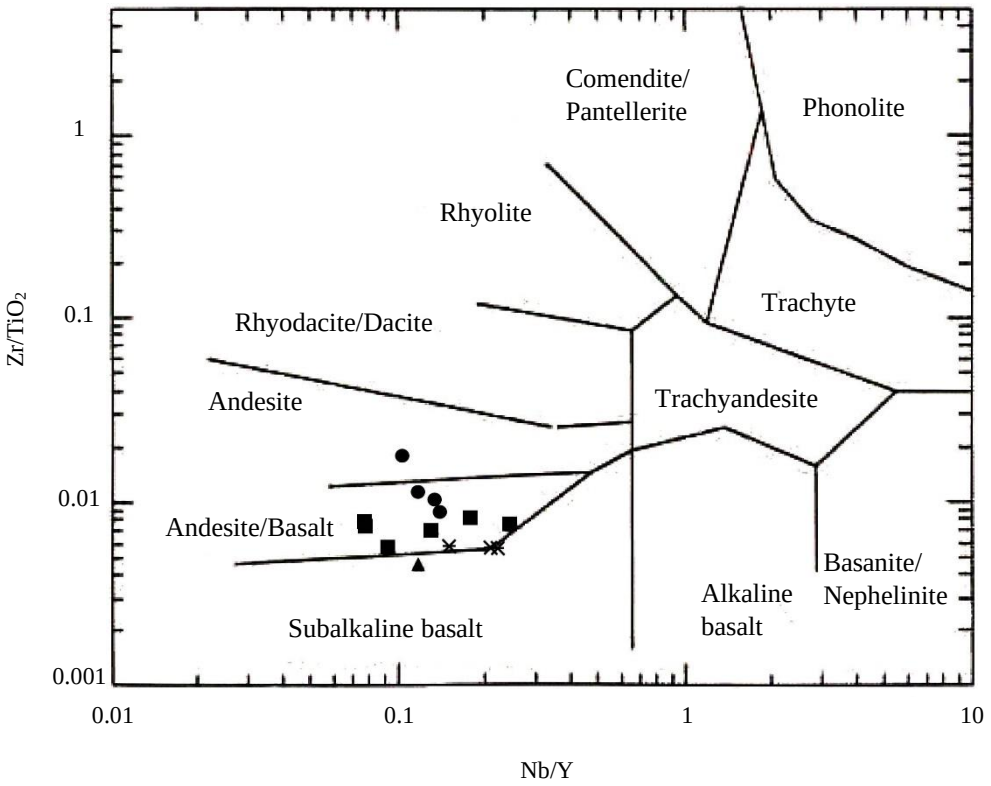

Figure 16. Zr/TiO_2 vs Nb/Y classification for mafic rocks (Winchester & Floyd, 1977)

B. Tectonomagmatic discrimination

The variation diagrams (Figs. 17, 18) indicate that the rocks of Pallatanga are tholeiitic, while those from Macuchi and Arrayanes have calc-alkaline components. In Fig. 18, it is primarily observed that the data from Pallatanga exhibit a typically tholeiitic slope, while the data from the other two groups form a more dispersed spectrum, which, although tholeiitic, suggests calc-alkaline contamination. Figure 19 confirms the tholeiitic nature of Pallatanga. The data for Macuchi and Arrayanes are inconclusive, although they could indicate an origin from an active margin. Collectively, these diagrams could imply a MORB-related origin for Pallatanga and an oceanic island arc origin for the other rocks. In an oceanic island arc, tholeiitic basalts predominate, but there are also calc-alkaline basalts (Miyashiro, 1982).

Figure 20, which compares trace elements, classifies the basalts of Pallatanga as ocean floor basalts and those from the other two groups as low-K tholeiites. Figure 21 suggests an oceanic island origin for Pallatanga, while the origin of Arrayanes and Macuchi would be orogenic with some affinity to a hotspot or oceanic floor, indicating an environment compatible with an oceanic island arc. Thompson et al. (1984) consider that the low-K tholeiites from oceanic island arcs are the hydrated equivalents of MORB related to subduction.

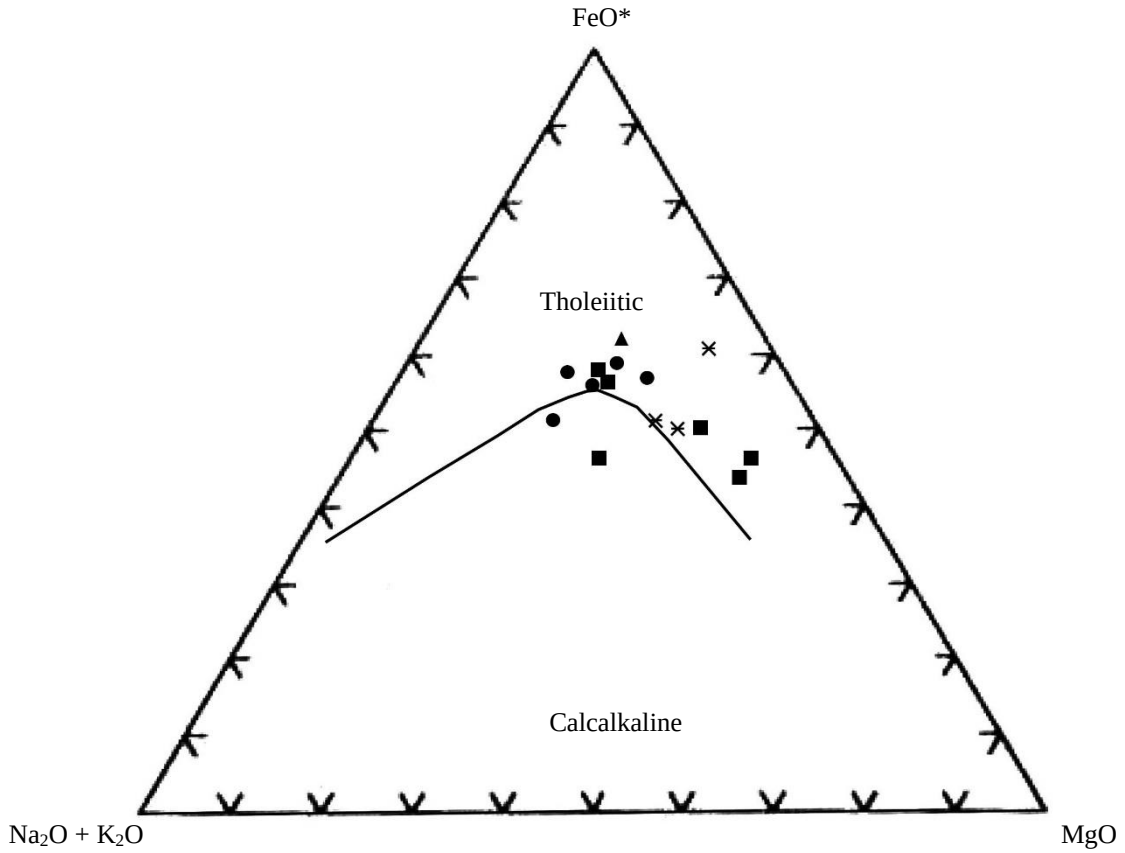

Figure 17. Variation diagram for mafic rocks (Irvine & Baragar, 1971)

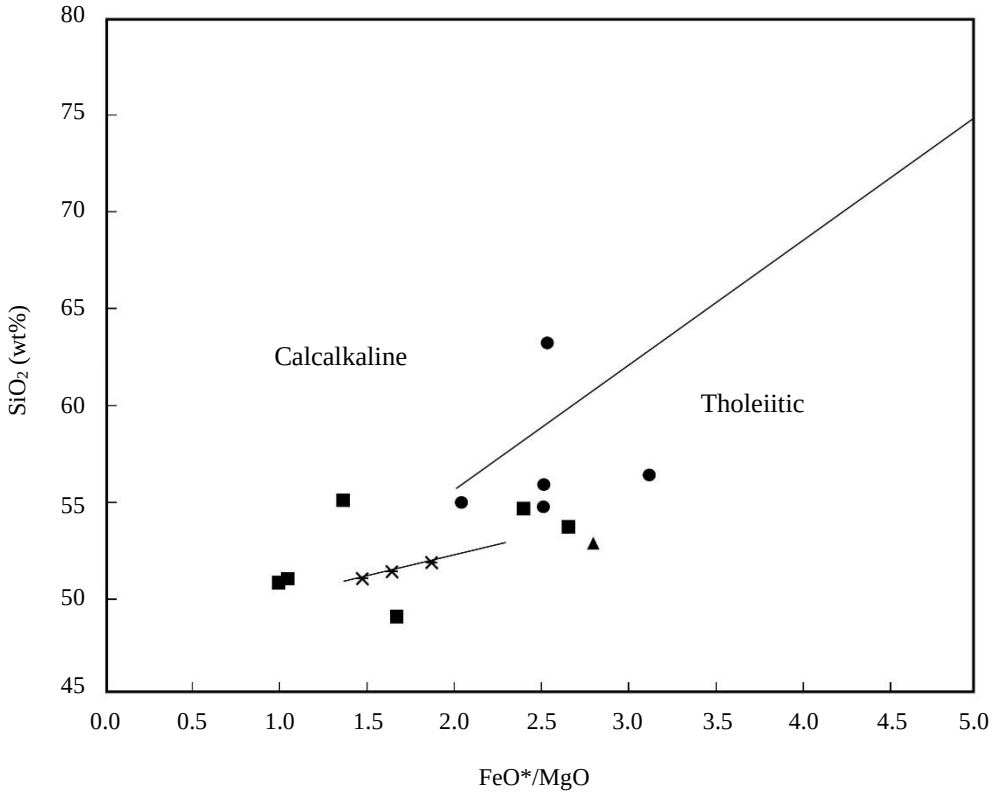

Figure 18. Variation diagram for mafic rocks (Miyashiro, 1974)

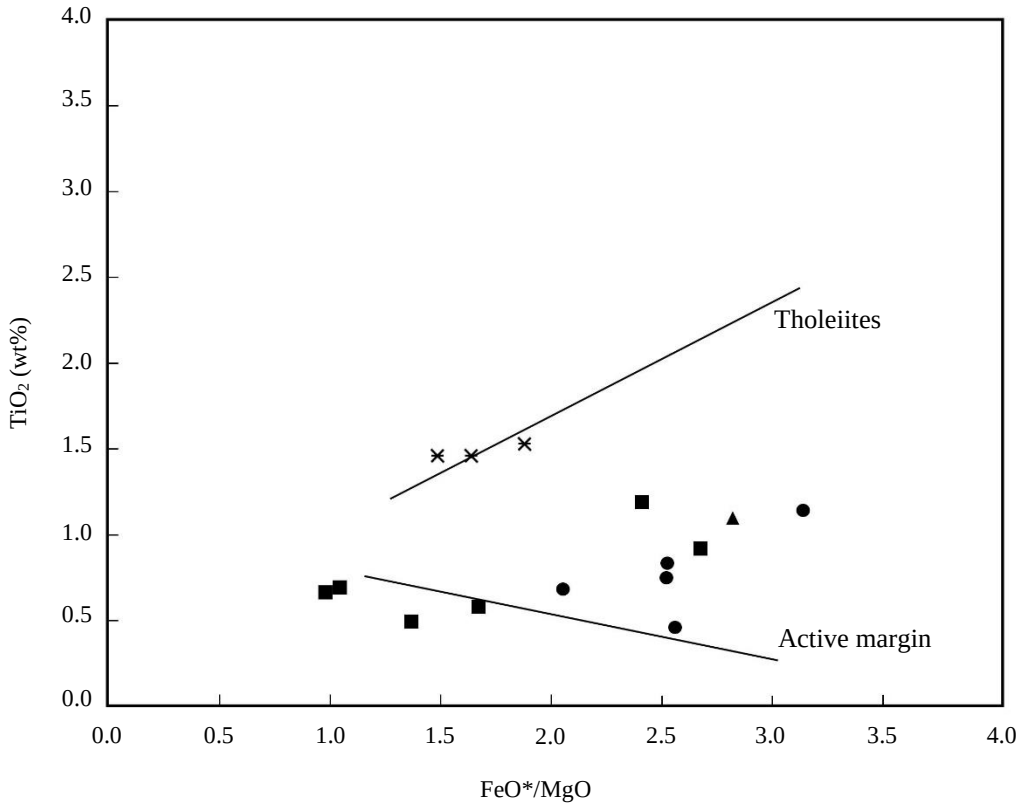

Figure 19. Comparison of tholeiites/mafic rocks from active margins (Miyashiro, 1974)

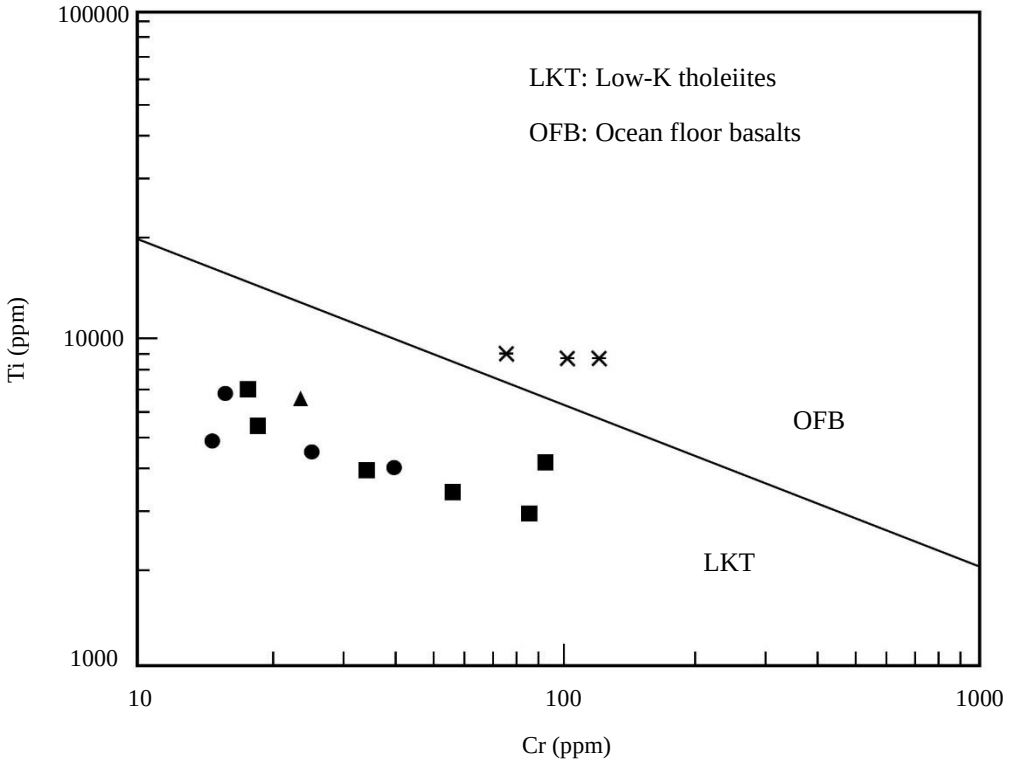

Figure 20. Discrimination between tholeiites (Pearce, 1975)

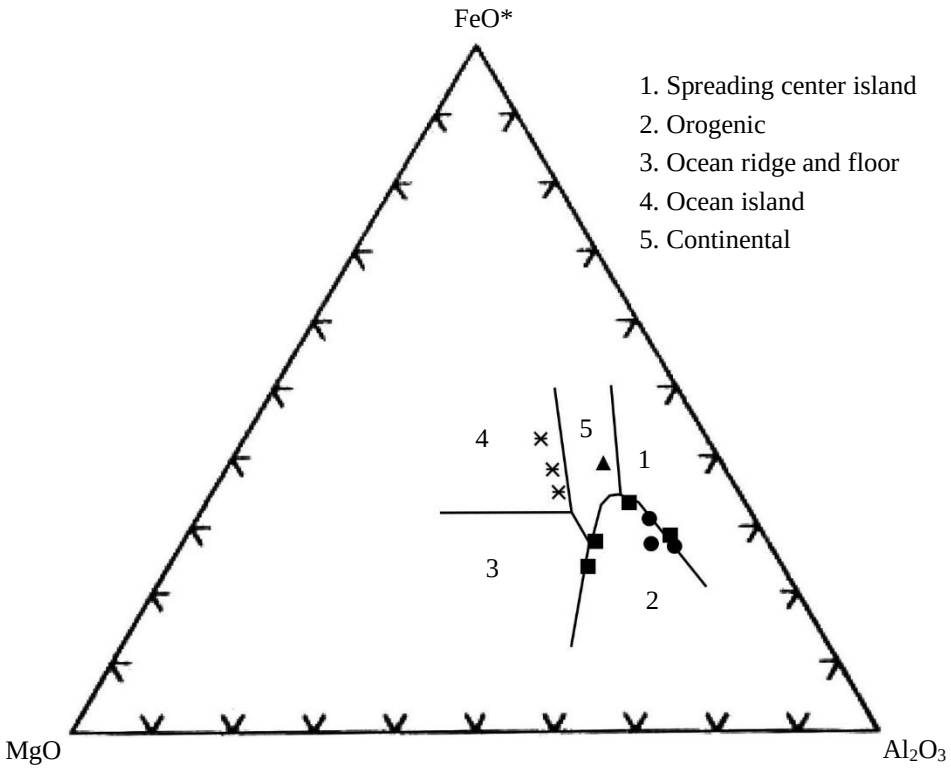

Figure 21. Discriminant diagram of tectonic environments (Pearce et al., 1977)

Figure 22 confirms the MORB affinity of Pallatanga and allows for a separation of the fields of Arrayanes and Macuchi. In Figure 23, it is seen that all the analyzed mafic rocks from the study area are from a destructive plate margin. Those from Pallatanga plot almost at the boundary between the P-MORB and active margin fields. It is interesting to note that most P-MORB analyses in this and other diagrams belong to the Galápagos Ridge.

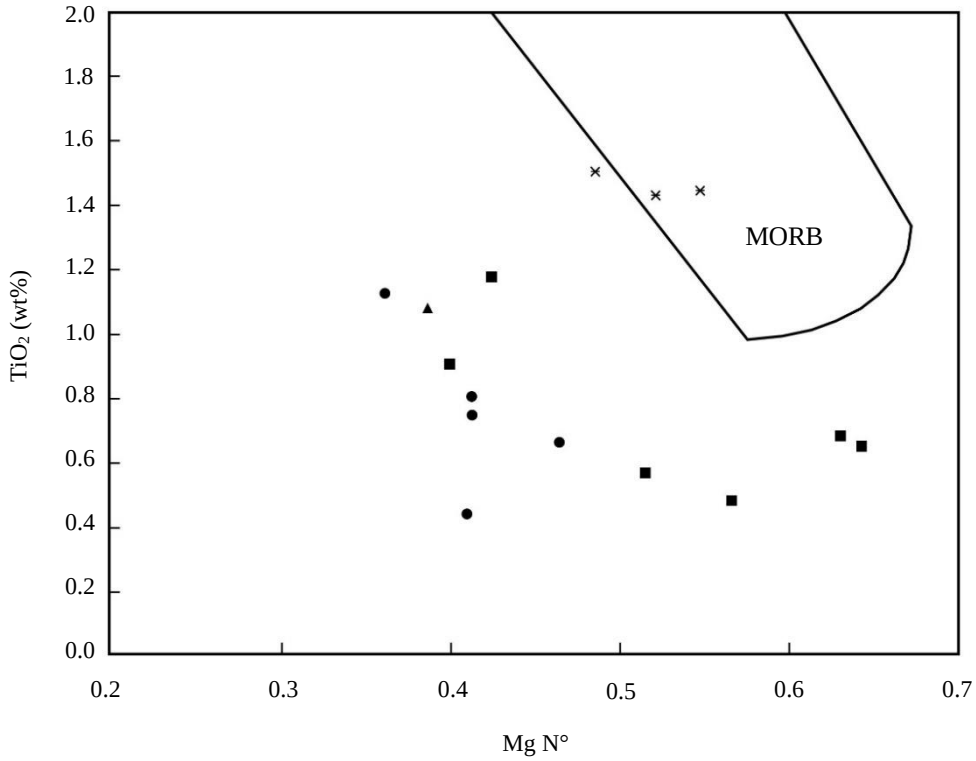

Figure 22. TiO_2 vs Mg number diagram indicating the MORB field

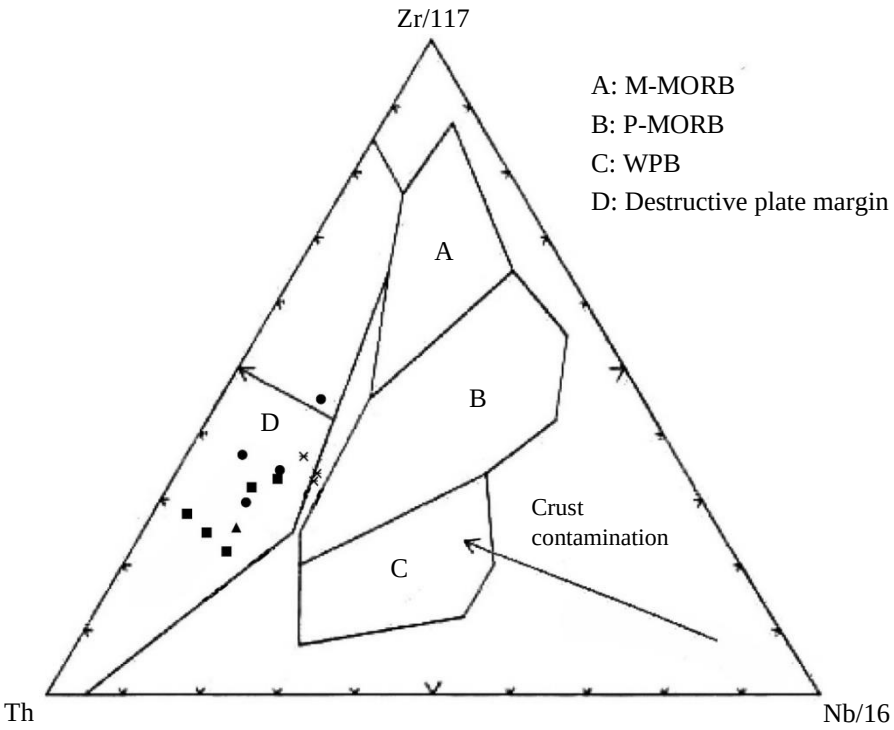

Figure 23. Discriminant diagram for mafic rocks (Wood, 1980)

Figure 24 confirms Macuchi as island arc tholeiite, while Pallatanga can be explained as contaminated MORB.

Figures 25 to 27 confirm that the analyses of Macuchi and Arrayanes tend to group individually. Figure 25 discriminates Pallatanga as ophiolitic basalt, and although it is not conclusive for the other two units, it marks a separation between them.

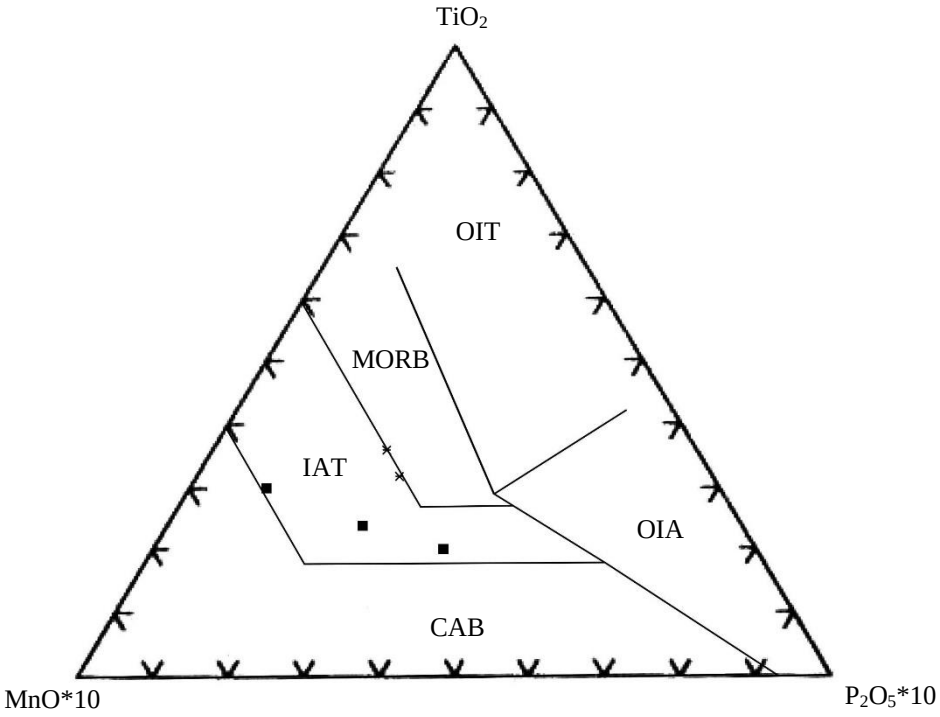

Figure 24. Discriminant diagram for mafic rocks (Mullen, 1983)

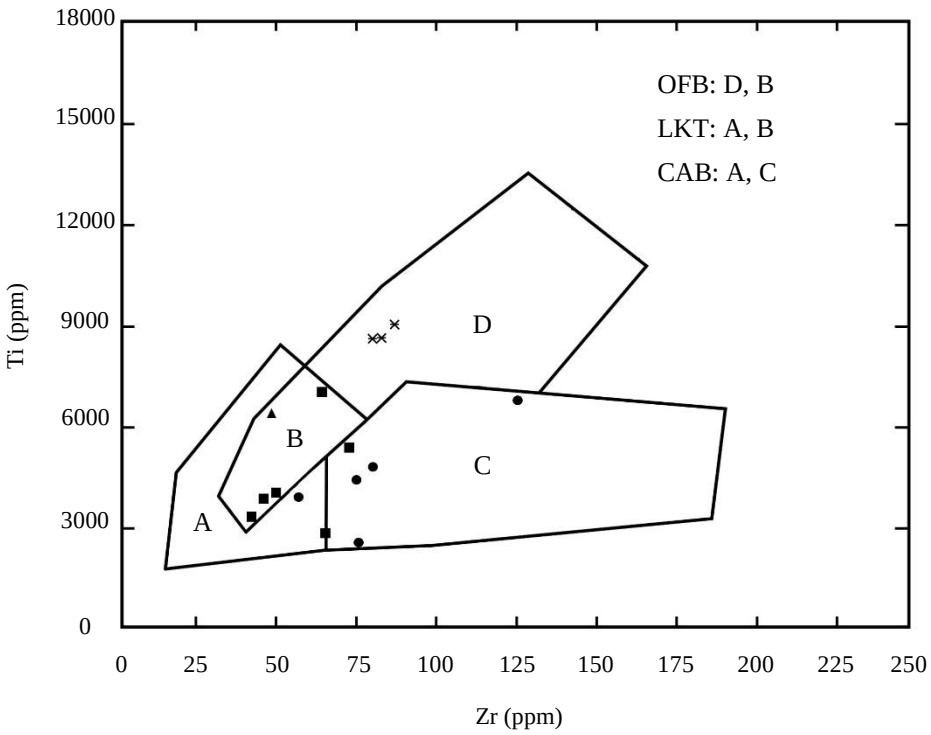

Figure 25. Discriminant diagram for mafic rocks (Pearce & Cann, 1973)

Figure 26, although it does not completely discriminate the tectonic environments of formation, shows that Macuchi and Arrayanes have some calc-alkaline affinity not present in Pallatanga.

Figure 27 suggests that Macuchi has more of an island arc character, while Arrayanes has a more calc-alkaline character, although tectonically it could be related to an island arc.

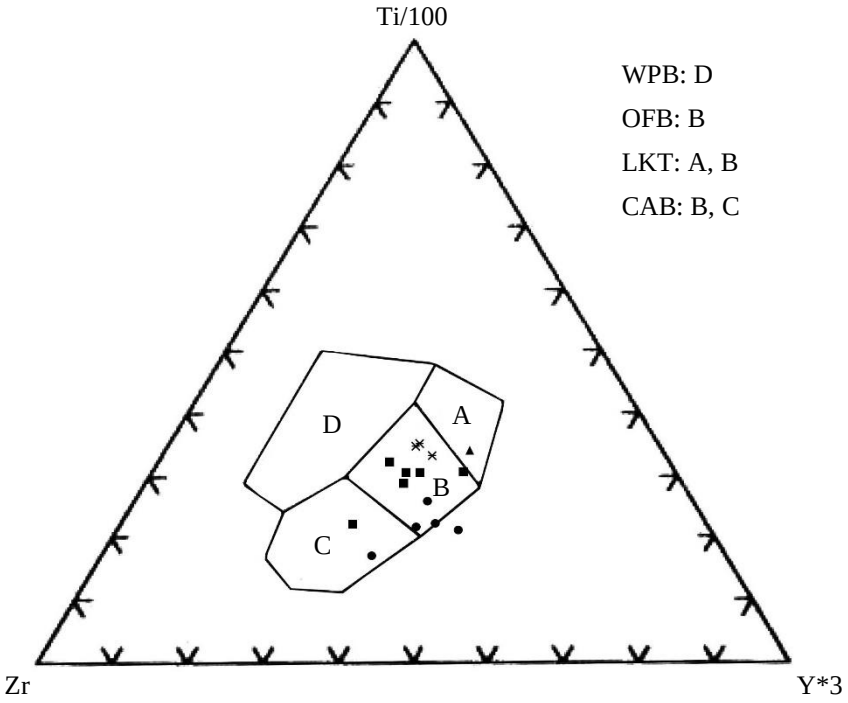

Figure 26. Discriminant diagram (Zr-Ti-Y) for mafic rocks (Pearce & Cann, 1973)

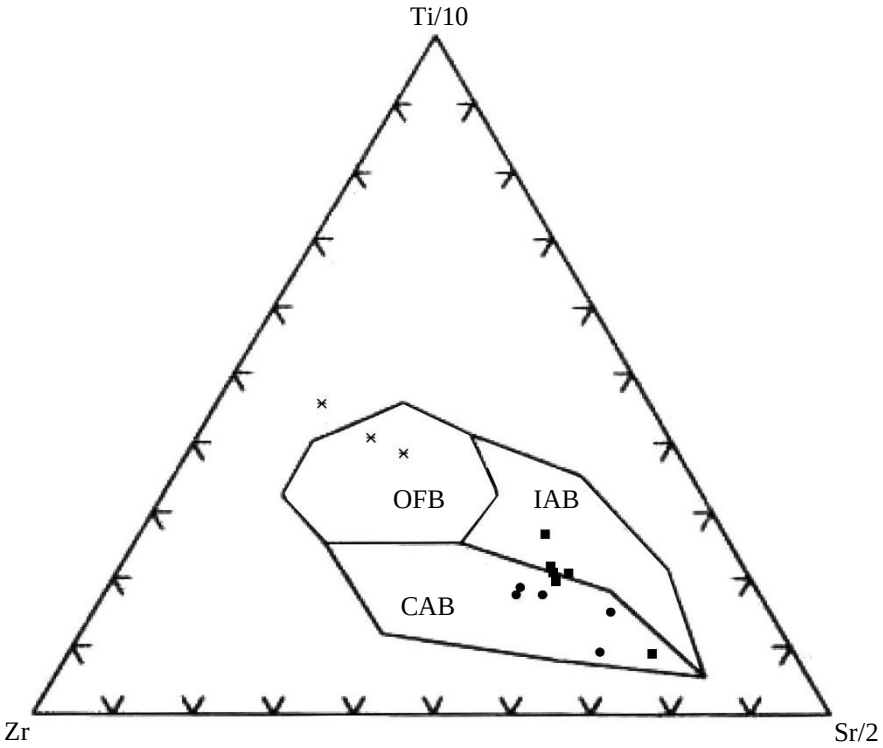

Figure 27. Discriminant diagram (Zr-Ti-Sr) for mafic rocks (Pearce & Cann, 1973)

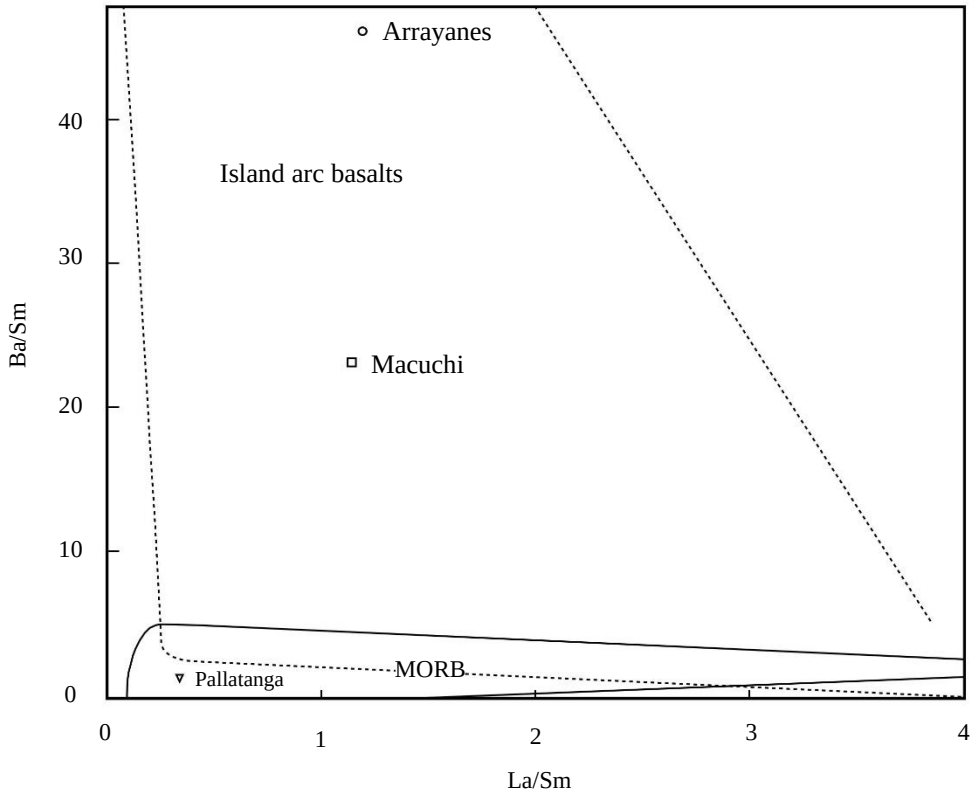

Figure 28. Discriminant diagram (island arc basalts/MORB) (Arculus & Power, 1986)

Figure 28 discriminates island arc basalts from MORB. The Pallatanga Unit plots within the MORB field; the Macuchi and Arrayanes Units fall within the island arc field, although outside the field of more common basalts, whose value on the abscissa is <10 (Wilson, 1989).

In general, these diagrams help us discriminate certain tectonic environments for the analyzed mafic rocks of the Western Cordillera, but they do not provide a unique, unambiguous answer. A geological interpretation with multiple approaches is necessary: petrological, mineralogical, geochemical, and tectonic. However, from the interpretation of these, it is clear that the tectonic setting of the rocks of Pallatanga is different from that of Macuchi and Arrayanes. Furthermore, although they do not discriminate a different tectonic environment for the latter two units, they allow for a distinction of their plotting fields, emphasizing their separation as units.

The most useful tectonomagmatic discrimination diagrams for ancient rocks are those that utilize trace element concentrations, which allow determining that the variations between different environments are greater than the variations between rocks and/or units belonging to the same tectonic setting.

The analyzed elements must be immobile or have low mobility to discern their origin. The diagrams that best fulfill these premises are the Normalized Trace Element Variation Diagrams, better known as Spider Diagrams.

For the present analysis, we have utilized the normalizations for MORB and chondrite employed in the NewPet program (Clarke, 1994) and those calculated by Sun (1980) for island arc basalts (tholeiitic-IAT, calc-alkaline-IACAB), ocean island basalts (OIB), and Rare Earth Elements.

C. Normalized trace element variation diagrams (spider diagrams)

Figures 29, 30, and 31 present spider diagrams for typical rocks from the Arrayanes, Macuchi, and Pallatanga Units, respectively. They compare the variations of trace elements concerning the MORB normal composition.

In the spider diagram of the Arrayanes Unit, a notable enrichment of the more mobile LIL (large ion lithophile) elements is observed: Cs, Rb, Ba, Th, K, Sr; a slight depletion in Ti and values close to one for Nb, Ce, Zr, Y.

The variation of the more mobile LIL elements can be interpreted, in part, as a behavior of the fluid phase and, on the other hand, as contamination from the crust. The limited variation of the less mobile (HFS) elements is controlled by the source chemistry. For Nb, Ce, Zr, Nd, and Y, it is possible to draw a parallel to the unity line, suggesting a primary origin related to MORB. The values nearly equal to 1 for the Rare Earth Elements (Nb, Ce, Y) reinforce this criterion. Positive values in the Nb-Y segment could correspond to contamination in a subduction zone, while negative values would signify a degree of partial melting concerning MORB.

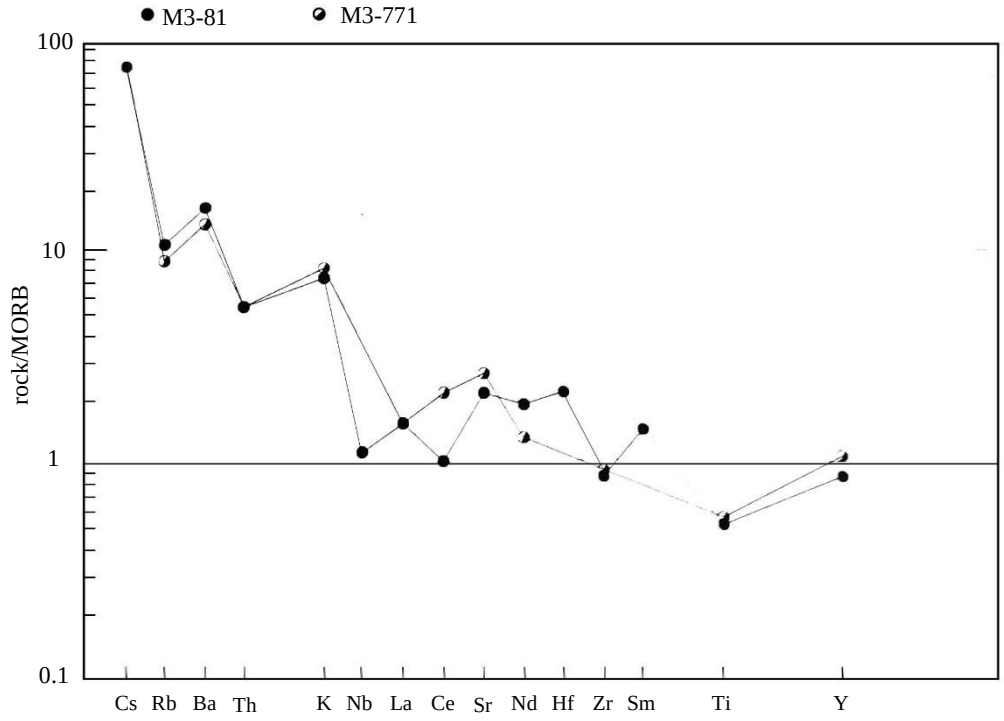

Figure 29. Spider diagram (rock/MORB) of rocks from the Arrayanes Unit

The spider diagram normalized to MORB for the Macuchi Unit is similar to that for the Arrayanes Unit. Enrichment is observed in Rb, Ba, Th, U, K, Sr, Hf, Sm; a very slight depletion in Zr, Ti, and perhaps Y; values practically equal to one for Nb, Nd, Y. If the values of La, Hf, and Sm are joined, a parallel to the unity line is obtained. In addition to the considerations mentioned for Arrayanes, it can be added that the enrichment in U points to contamination from upper continental crust, just as the values of Sm may indicate involvement of the crust in the generation of the magma.

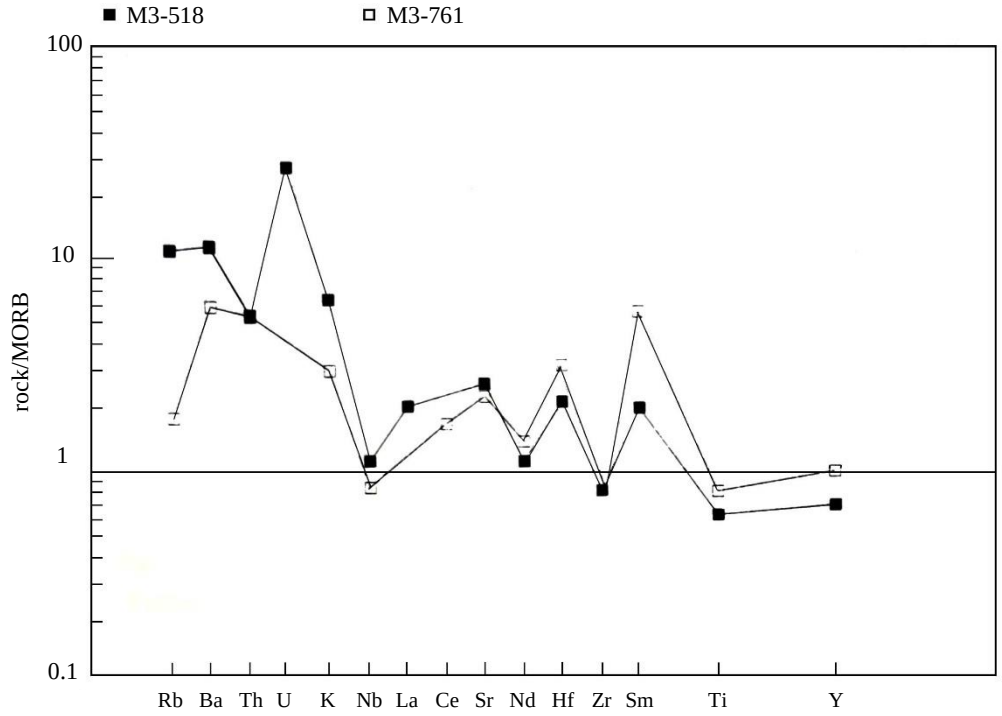

Figure 30. Spider diagram (rock/MORB) of rocks from the Macuchi Unit

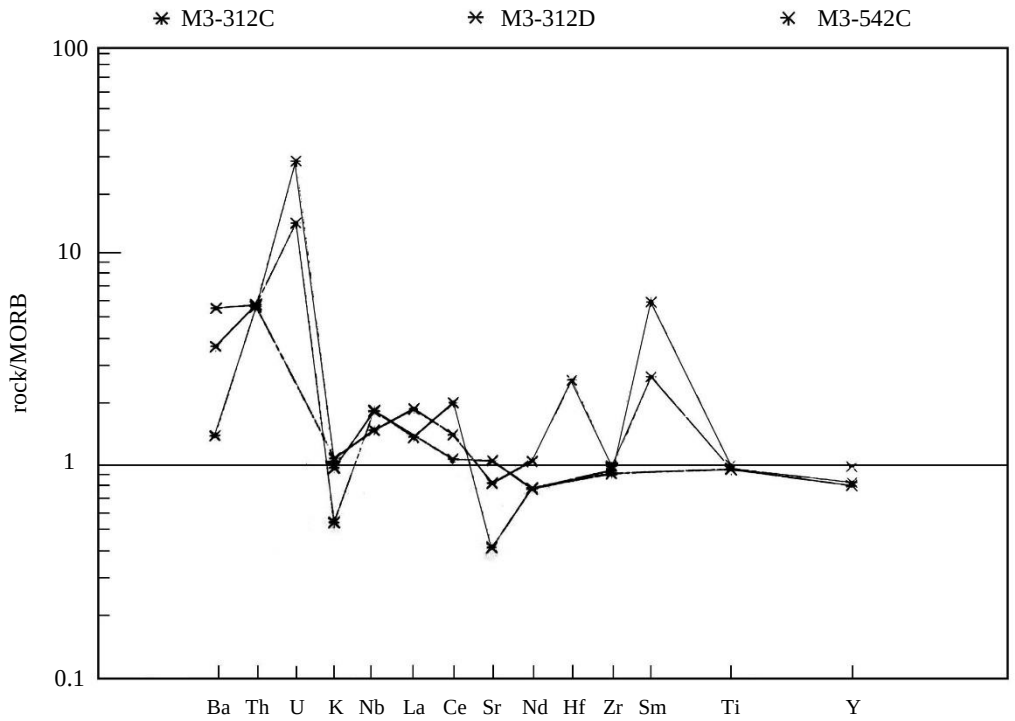

Figure 31. Spider diagram (rock/MORB) of rocks from the Pallatanga Unit

The spider diagram for the Pallatanga Unit shows, with respect to normal MORB, enrichment in U, lesser enrichment in Th, Hf, Sm, Nb, and La; slight depletion in K and Sr; and values equal to one for Nd, Zr, Ce, Ti, and Y. In general, the values of Ce to the right are similar to those of MORB; however, some fractionation is observed in the light Rare Earth Elements compared to the heavy Rare Earth Elements, which could be caused by the presence of olivine, orthopyroxene, and clinopyroxene. The high values for U, similar to those in the other two units, imply strong hydrothermal alteration (Albarede and Michard, 1986), confirming what was observed petrographically.

Figures 32 and 33 compare the incompatible trace elements of Macuchi, Arrayanes, and Pallatanga with the averages for ocean island basalts (OIB).

In Figure 32, it is observed that the values of incompatible elements for ocean island basalts are practically all higher than those for the Arrayanes and Macuchi Units. This indicates that the probability of OIB being the source for them is very low. The enrichment of incompatible elements in OIB compared to MORB could suggest that recycled continental lithosphere may be a component of the magmatism of ocean island basalts (McKenzie and O’Nions, 1983).

Figure 33 shows a depletion of Pallatanga compared to OIB in all incompatible elements, making it highly unlikely that OIB is the tectonic setting despite the FeO*-MgO-Al_2O_3 diagram in Figure 15.

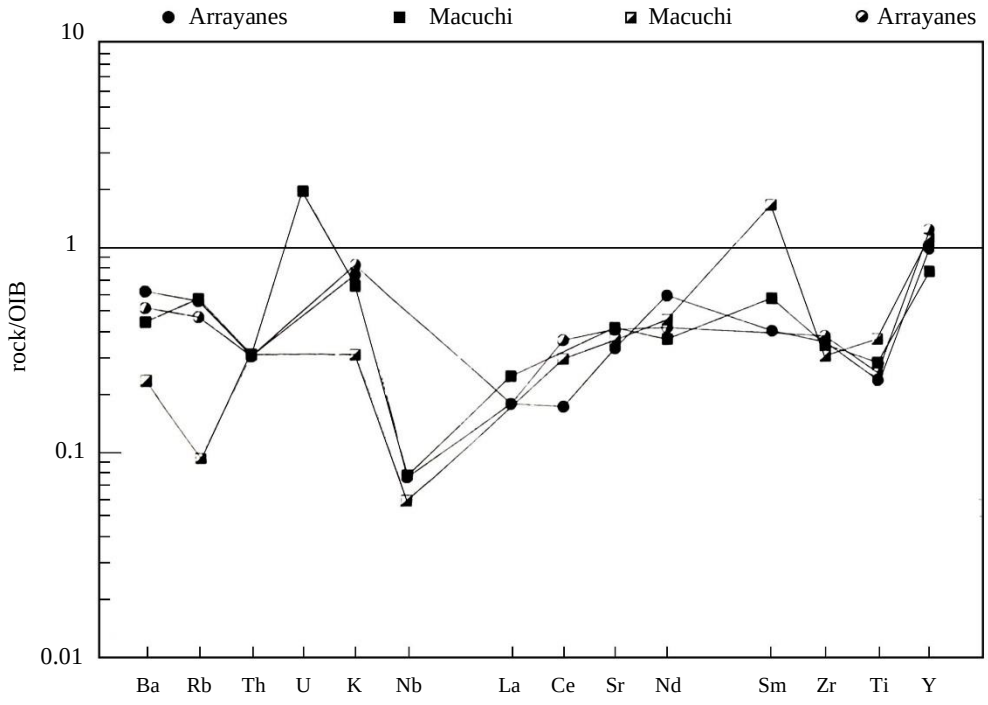

Figure 32. Spider diagram (rock/OIB) of rocks from the Arrayanes and Macuchi Units

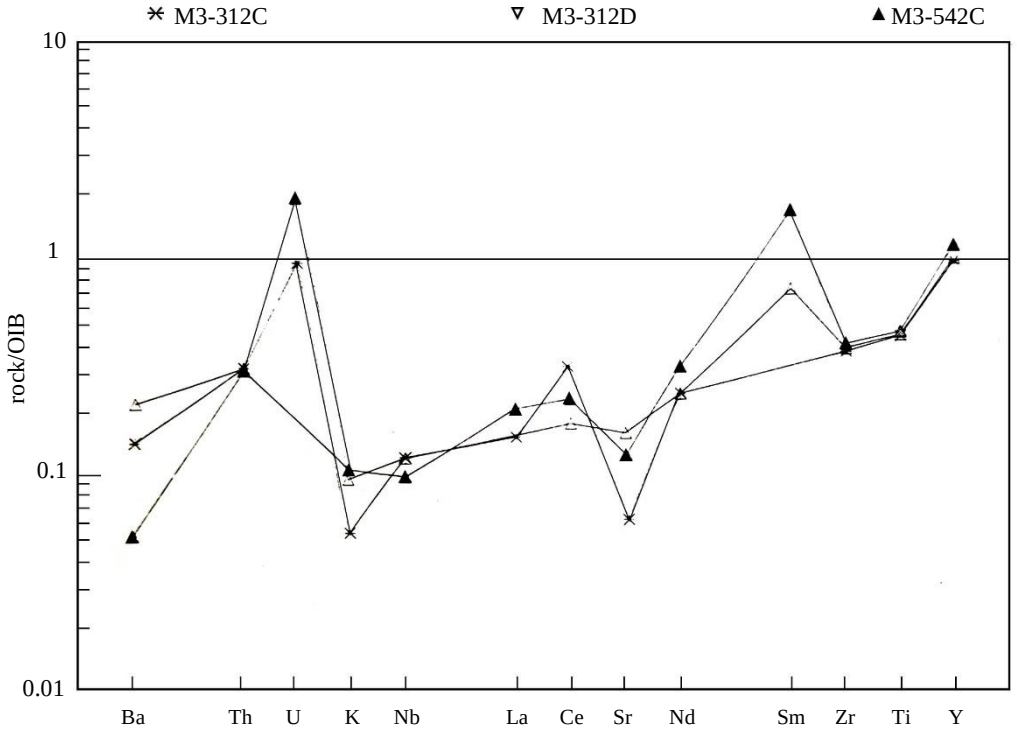

Figure 33. Spider diagram (rock/OIB) of rocks from the Pallatanga Unit

Comparing the distribution of incompatible elements in Macuchi and Arrayanes with average data for oceanic island arcs (Sun, 1980), it is observed that for Macuchi, the values of LIL elements (Ba, K, Sr), along with Y, are similar to those of IAT; while Nb, La, Ce, and Nd are slightly enriched (Fig. 34). Arrayanes (Fig. 35) shows greater enrichment in both mobile and immobile elements, especially Ce, Nd, and Y, resembling more an island arc basalt with calc-alkaline affinity (Fig. 36), where the mobile elements (Rb, Ba, K, Th, Ti) and Ce are nearly equal to 1, while there is slight enrichment in immobile elements (Nb, Nd, Zr) and Rare Earth Elements (Nb-Y). The corresponding diagram for Macuchi (Fig. 37) shows slight enrichment in immobile elements (Nb-Nd-Zr-Y) and depletion in mobile elements (Rb-Ba-K-Sr) and Ce.

Figure 38 is an extended diagram of Rare Earth Element (REE) incompatibility (modified from Anders and Grevesse, 1989). For Macuchi, a slight depletion in light Rare Earth Elements is observed, while for Arrayanes, there is a very slight enrichment in the same. Negative anomalies for Nb and Ti are also noted, which is characteristic of igneous rocks related to subduction (Wood et al., 1979; Briqueu et al., 1984). The model is compatible in abundance of elements and shape with a tholeiitic island arc for Macuchi and tholeiitic with some calc-alkaline affinity for Arrayanes (Wilson, 1989). The same conclusion is drawn from spider diagrams normalized to chondrites (Figs. 39-40).

The spider diagram for Pallatanga resembles MORB (Fig. 31) more than that of tholeiite of island arc (Fig. 41); indeed, the values for Ce, Sr, Nd, Zr, Ti, and Y practically coincide with those of MORB, while compared to IAT, the mobile elements are lower and the immobile elements and Rare Earth Elements are higher.

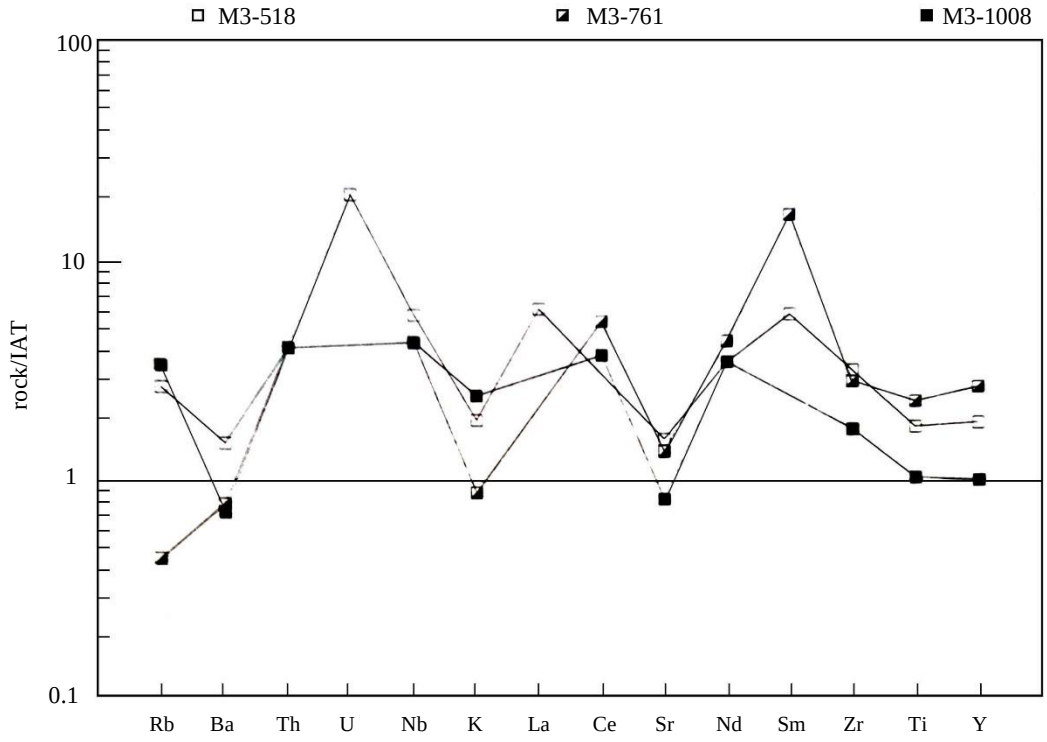

Figure 34. Spider diagram (rock/IAT) of rocks from the Macuchi Unit

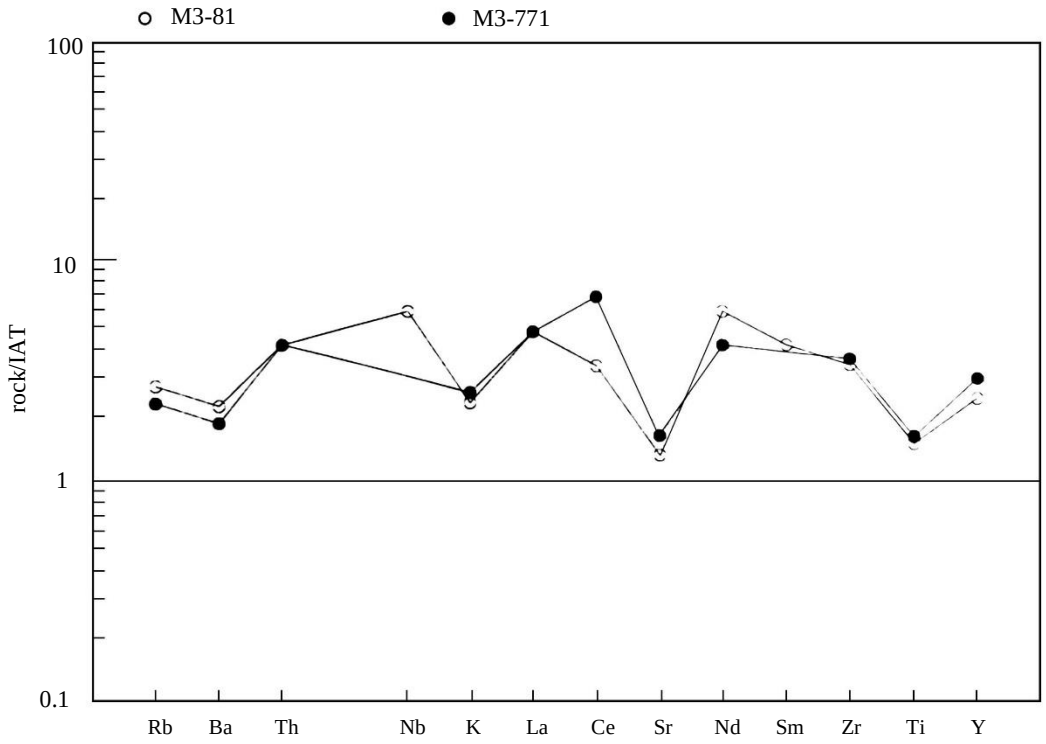

Figure 35. Spider diagram (rock/IAT) of rocks from the Arrayanes Unit

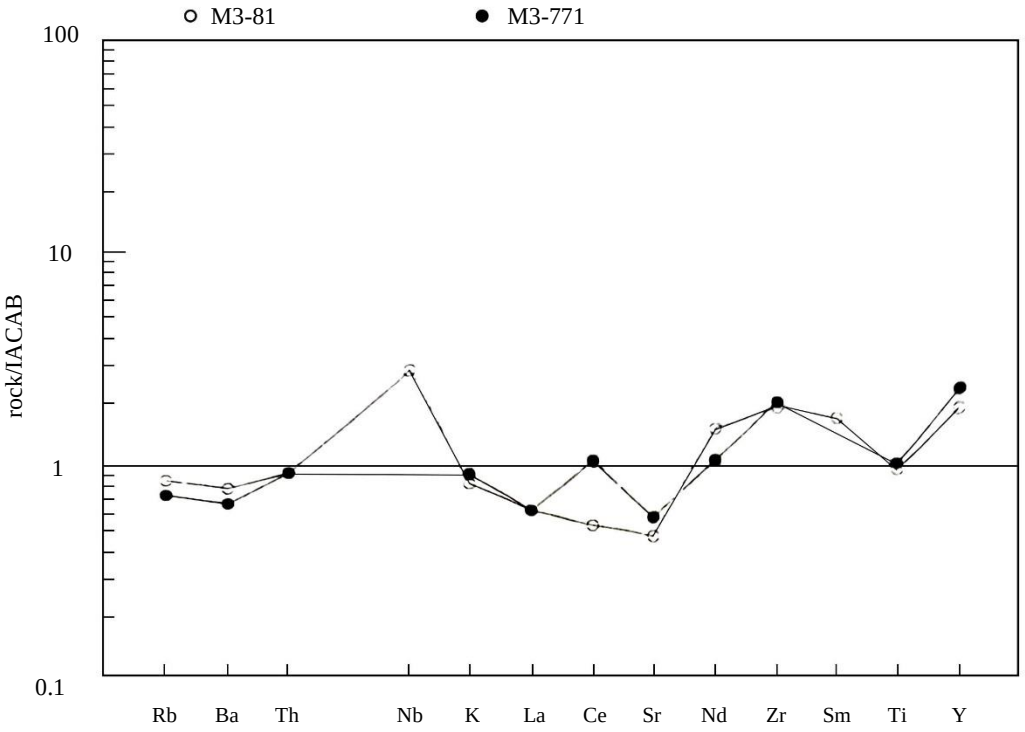

Figure 36. Spider diagram (rock/IACAB) of rocks from the Arrayanes Unit

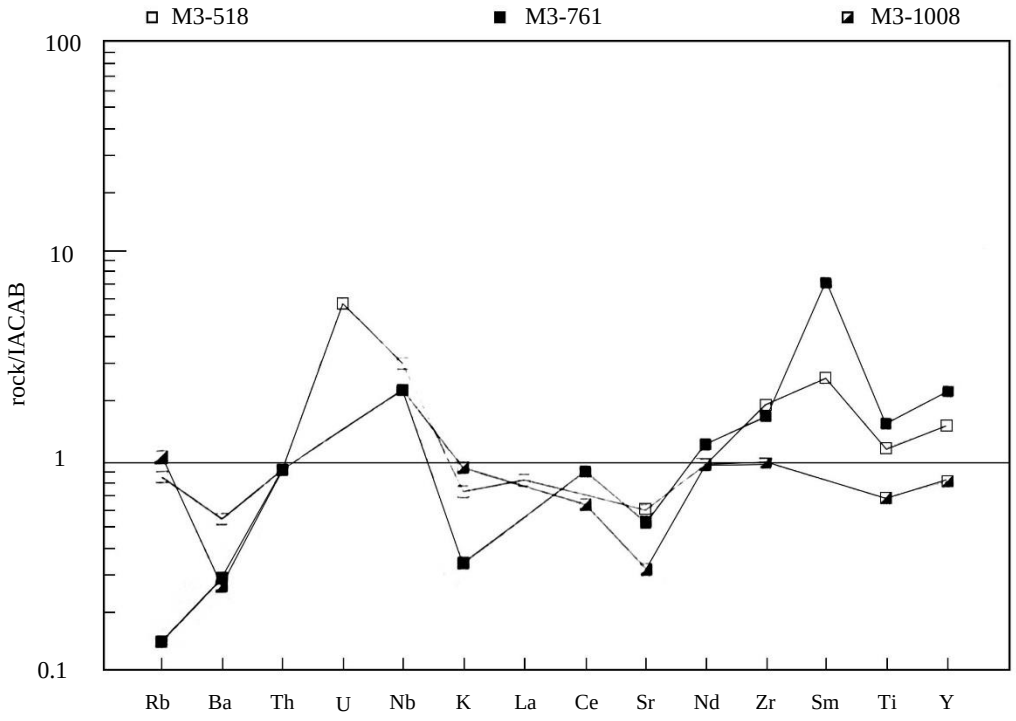

Figure 37. Spider diagram (rock/IACAB) of rocks from the Macuchi Unit

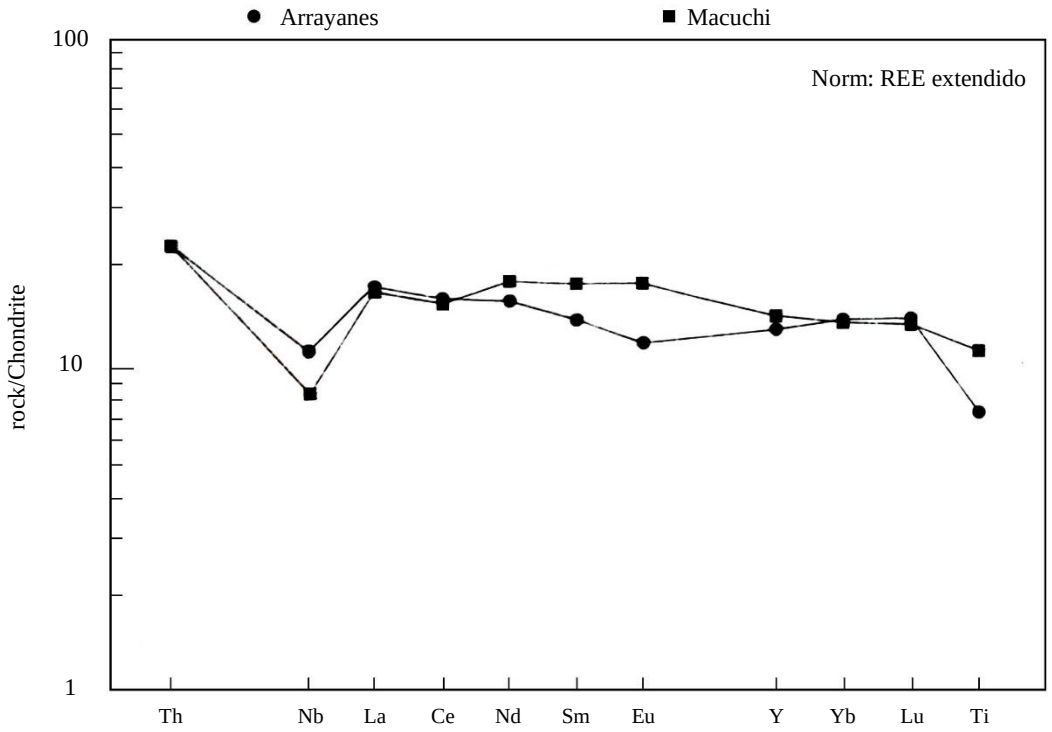

Figure 38. Extended diagram of Rare Earth Element incompatibility (REE) (rock/chondrite) for the Arrayanes and Macuchi Units

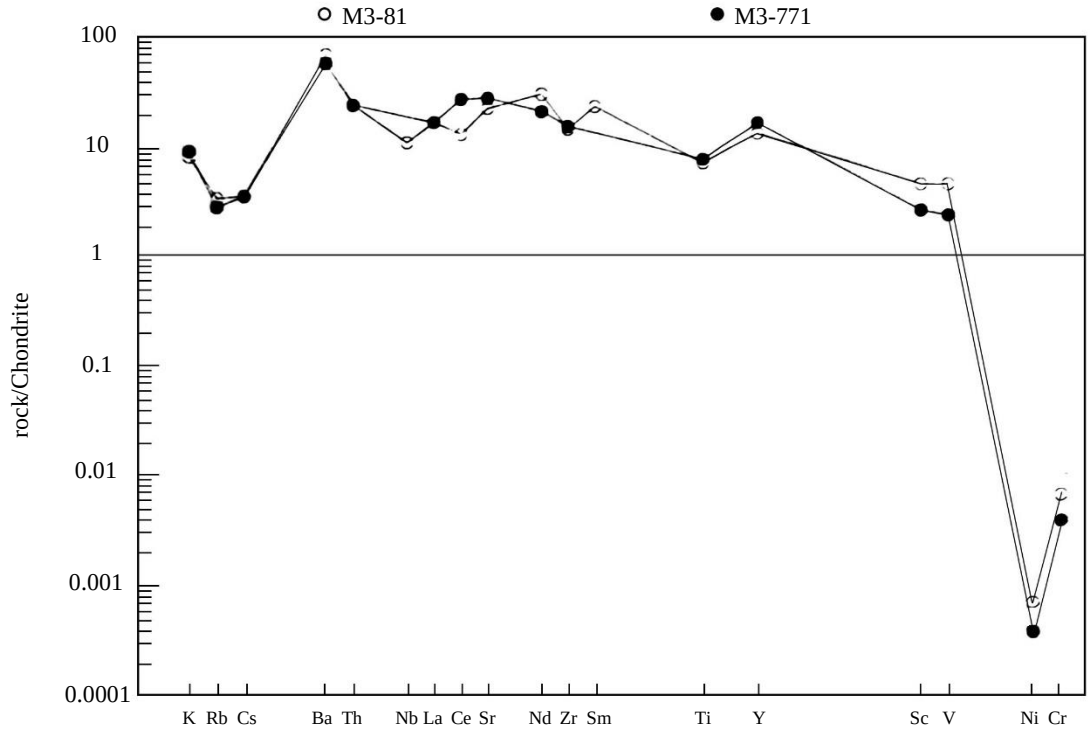

Figure 39. Spider diagram (rock/chondrite) of rocks from the Arrayanes Unit

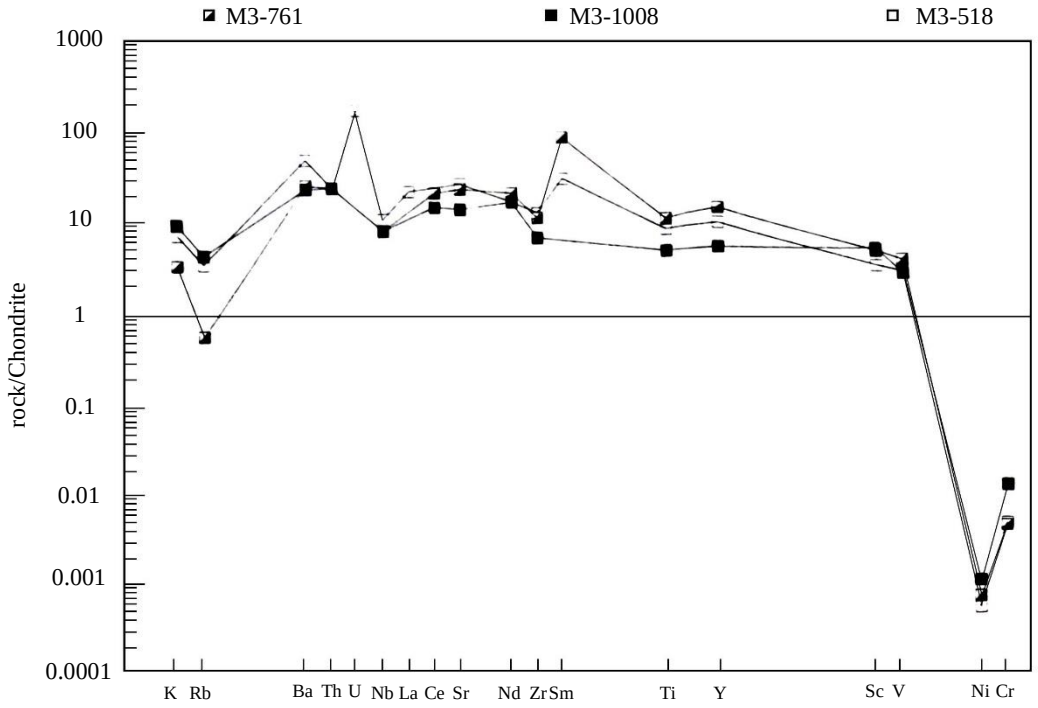

Figure 40. Spider diagram (rock/chondrite) of rocks from the Macuchi Unit

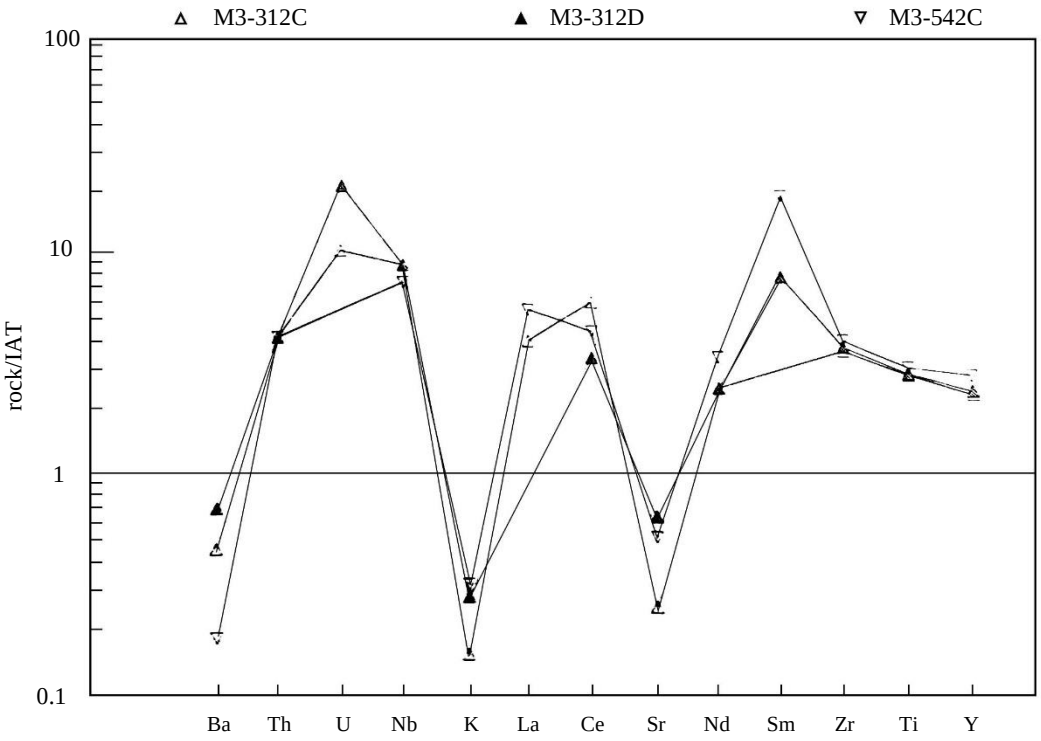

Figure 41. Spider diagram (rock/IAT) of rocks from the Pallatanga Unit

In Figure 42, it can be seen that the incompatibility pattern is relatively consistent with that of MORB. There is an enrichment across the range of trace elements except for Ni and Cr.

When the trace elements of Pallatanga are compared with those of P-MORB, a greater similarity is obtained. This may be due to P-MORB and oceanic floor are practically equally enriched MORB.

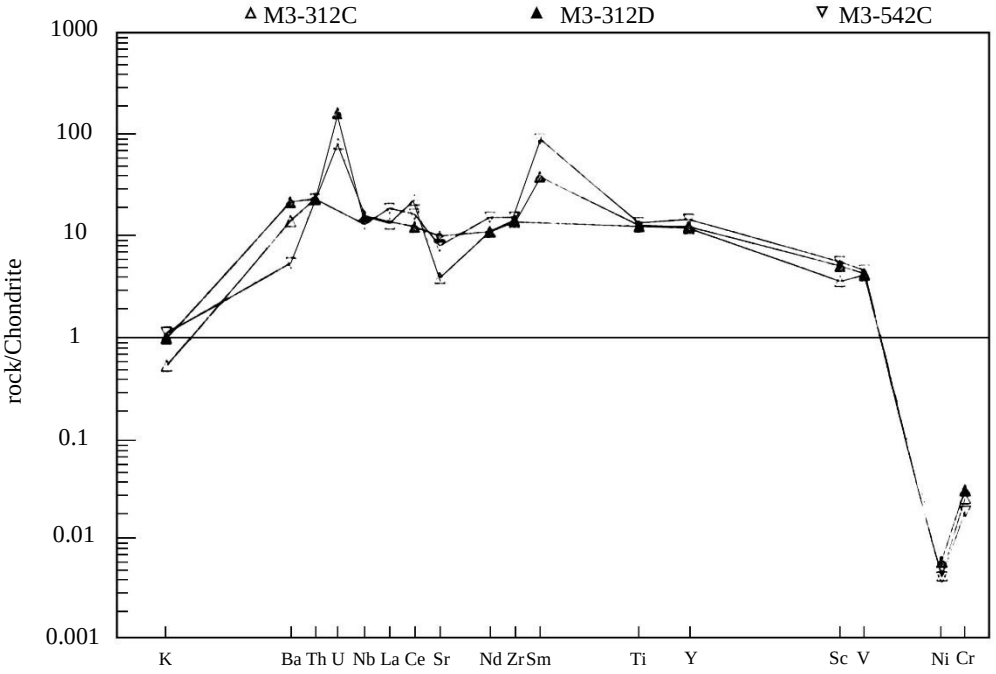

Figure 42. Spider diagram (rock/chondrite) of rocks from the Pallatanga Unit

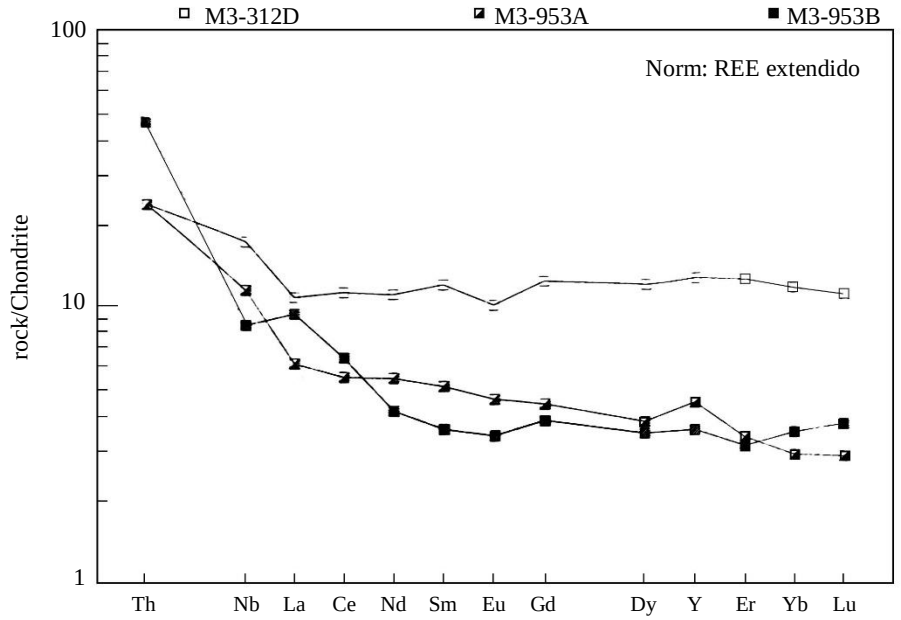

Figure 43. Extended diagram of Rare Earth Element incompatibility (rock/chondrite) for the Pallatanga Unit

The diagram in Figure 43 represents the Rare Earth Element (REE) incompatibility for the Pallatanga Unit. It is observed that the concentration of Rare Earth Elements is on the order of 10×chondrite or less, which is characteristic of primitive basalts (differentiated basalts can contain up to 10×chondrite; Wilson, 1989). One sample shows no fractionation of Rare Earth Elements, while two others are slightly enriched in light Rare Earth Elements. The basalts of Pallatanga are unfractionated, although there is a slight trend towards a small negative anomaly in Eu (plagioclase fractionation). The ratio $(La/Sm)_N$ is close to 1, which does not allow for a distinction between N-MORB or P-MORB. The diagram shows an enrichment in Nb and Ta, indicating that the rocks are not related to subduction and are compatible with MORB.

IV. CONCLUSIONS

Although chemical analyses are relatively scarce, some conclusions can be drawn from the geochemical study.

The granitoids outcropping in the studied region are very uniform geochemically. They all classify from granodiorites to tonalites and are grouped at the boundary between the two fields. They are predominantly meta-aluminous granitoids that have biotite and hornblende as essential phases and plot very close to the edge of the peraluminous field in the diagrams; in fact, a few fall into this field and have biotite as the essential mafic phase. All are orogenic granites, more specifically originating in a volcanic arc geotectonic environment.

The mafic rocks are grouped in the Arrayanes, Macuchi, and Pallatanga Units. Additionally, there are several outcrops of undifferentiated gabbroids that show strong affinities with Macuchi both in the field, petrographically and chemically.

The Arrayanes and Macuchi Units are geochemically similar, but in several diagrams, they are grouped into defined fields, even though these correspond to the same tectonic environment or nomenclature. The rocks of Macuchi are primarily basalts and basaltic andesites, while those of Arrayanes are basaltic andesites and andesites. Both are primitive basaltic rocks that suggest an oceanic island arc tectonomagmatic environment. Macuchi has a well-defined tholeiitic character of low-K basalt, although some calc-alkaline affinity is noted. In Arrayanes, this affinity is much more pronounced and could be due to it constituting a more mature phase of the same arc or a later arc that is more contaminated by continental crust. The same conclusions can be drawn from the analysis of spider diagrams. The trace element incompatibility with respect to N-MORB and OIT norms corresponds to a somewhat contaminated oceanic island arc environment for Macuchi and considerably more contaminated for Arrayanes. The extended diagrams of Rare Earth Element incompatibility with respect to chondrites also suggest a clear subduction component.

The Pallatanga Unit is classified as tholeiitic related to MORB, and its chemistry is different from that of Macuchi and Arrayanes. The spider diagrams show similarity with N-MORB and P-MORB, especially with N-MORB, although some contamination by crust and fluid phase is noticeable. The Rare Earth Element diagrams indicate that they are primitive basalts and do not present any subduction component.

In conclusion, the mafic rocks of Macuchi and Arrayanes are low-K tholeiites formed at a destructive plate margin. Arrayanes is enriched in Zr, but both have a certain calc-alkaline affinity, which is greater in Arrayanes. The distribution of major and trace elements is compatible with an oceanic island arc geotectonic environment. A similar conclusion can be drawn for the Macuchi Unit with the mineralogical analysis of the pyroxenes (Aguirre and Atherton, 1987).

The Pallatanga Unit has a different tectonic environment from the other units studied. The geochemical and petrographic evidence suggests a somewhat altered MORB, with affinities to transitional MORB and oceanic floor. The preferred interpretation is that they originate from oceanic floor, an interpretation reinforced by its close geochemical similarity with the Piñón Formation.

V. REFERENCES

ALBAREDE F. and MICHARD A., (1986) Transfer of continental Mg, S, O and U to the mantle through hydrothermal alteration of the oceanic crust, Chem. Geol. 57, 1-15.

ANDERS E. and GREVESSE N. (1989) Abundances of the elements: meteoric and solar, Geochim. Cosmochim. Acta 53, 197-214.

ARCULUS R. J., and POWELL R. (1986) Source component mixing in the regions of arc magma generation, Jour. Geophys. Res. 91, 5913-5926.

AGUIRRE L. and ATHERTON M. P. (1987) Low grade metamorphism and geotectonic setting of the Macuchi Formation, Western Cordillera of Ecuador. *Journal of Metamorphic Geology,* **5**, 473-494.

BAEDKE S. J. and THOMPSON T. A. (1993) Triplot 2.0, Indiana University, Bloomington, U.S.A.

BRIQUEU L., BOUGAULT H. and JORON J. L. (1984) Quantification of Nb, Ta, Ti and V anomalies in magmas associated with subduction zones: petrogenetic implications. *Earth and Planetary Science Letters,* **68**, 297-308.

BROWN G. C., THORPE R. S. and WEBB P. C. (1984) The geochemical characteristics of granitoids in contrasting arcs and comments on magma sources, *Journal Geological Society, London,* **141**, 413-426.

CLARKE D. (1994) NewPet for DOS Centre for Earth Resources Research, Department of Earth Sciences, Memorial University of Newfoundland.

DEBON F. and LE FORT P. (1983) A chemical-mineralogical classification of common plutonic rocks and associations, Transactions of the Royal Society of Edinburgh Earth Sciences, 73, 135-149.

IRVINE T. N. and BARAGAR W. R. A. (1971) A guide to the chemical classification of the common volcanic rocks. *American Journal of Earth Sciences,* **8**, 523-548.

LE MAITRE R. W (1989) A classification of Igneous Rocks and glossary of terms Blackwell Publications London, 193p.

LEBRAT M. (1985) Caractérisation géochimique du volcanisme anté-orogénique de l'Occident Equatorien : implications géodynamiques. Unpubl. Ph. D. Thesis. Centre Geologique et Geophysique de Montpellier. 119p.

MANIAR P. D. and PICCOLI P. M. (1989) Tectonic discrimination of granitoids, Geological Society of America Bulletin, 101, 635-643.

McKENZIE D. and O'NIONS R. K. (1983) Mantle reservoirs and ocean island basalts. Nature, 301, 229-231.

MIDDLEMOST E. A. K. (1985) Magmas and Magmatic Rocks. Longman Group Limited, Essex.

MIYASHIRO A. (1974) Volcanic rock series in island arcs and active continental margins, American Journal of Science, 271, 321-355.

MIYASHIRO A., AKI K. and CELAL SENGOR A. M. (1982) Orogeny, Wiley & Sons, Chichester, 242 p.

MULLEN E. D. (1983) $MnO/TiO_2/P_2O_5$: a minor element discriminant for basaltic rocks of oceanic environments and its implications for petrogenesis, Earth and Planetary Science Letters, 62, 53-62.

PEARCE J. A. (1975) Basalt geochemistry used to investigate past tectonic environments on Cyprus. *Tectonophysics*, **25**, 41-77.

PEARCE J. A. and CANN J. R. (1973) Tectonic setting of basic volcanic rocks determined using trace element analyses, Earth and Planetary Science Letters, 19, 290-300.

PEARCE J. A., GORMAN B. E. and BIRKETT T. C. (1977) The relationship between major element chemistry and tectonic environment of basic and intermediate volcanic rocks, Earth and Planetary Science Letters, 36, 121-132.

PEARCE J. A., HARRIS N. B. W. and TINDLE A. G. (1984) Trace element discrimination diagrams for the tectonic interpretation of granitic rocks. *Journal of Petrology*, **25**, 956-983.

SUN S. S. (1980) Lead isotopic study of young volcanic rocks from mid-ocean ridges, ocean islands and island arcs, Phil. Trans. R. Soc. A297, 409-445.

THOMPSON R. N., MORRISON M. A., HENDRY G. L. and PARRY S. J. (1984) An assessment of the relative roles of a curst and mantle in magma genesis: an elemental approach,

WHALEN J. B., CURRIE K. L. and CHAPPELL B. W. (1987) A-type granites: geochemical characteristics, discrimination and petrogenesis. *Contributions Mineralogy and Petrology*, **95**, 407-419.

WINCHESTER J. A. and FLOYD P. A. (1977) Geochemical discrimination of different magma series and their differentiation products using immobile elements, Chemical Geology, 20, 325-343.

WOOD D. A. (1980) The application of a Th-Hf-Ta diagram to problems of tectonomagmatic classification and to establishing the nature of crustal contamination of basaltic lavas of the British Tertiary volcanic province. *Earth and Planetary Scientific Letters*, **50**, 11-30.

WOOD D. A., JORON J. L., and TREUIL M. (1979) A Re-appraisal of the use of trace elements to classify and discriminate between magma series erupted in different tectonic settings. Earth Planet, Sci. Lett. 45, 326-336.

WILSON M. (1989) Igneous Petrogenesis, Chapman & Hall, London, 466p.

APPENDIX 3 OF REPORT:

GEOLOGY OF THE WESTERN CORDILLERA
OF ECUADOR
BETWEEN 1°00' AND 2°00' S

GEOCHRONOLOGY

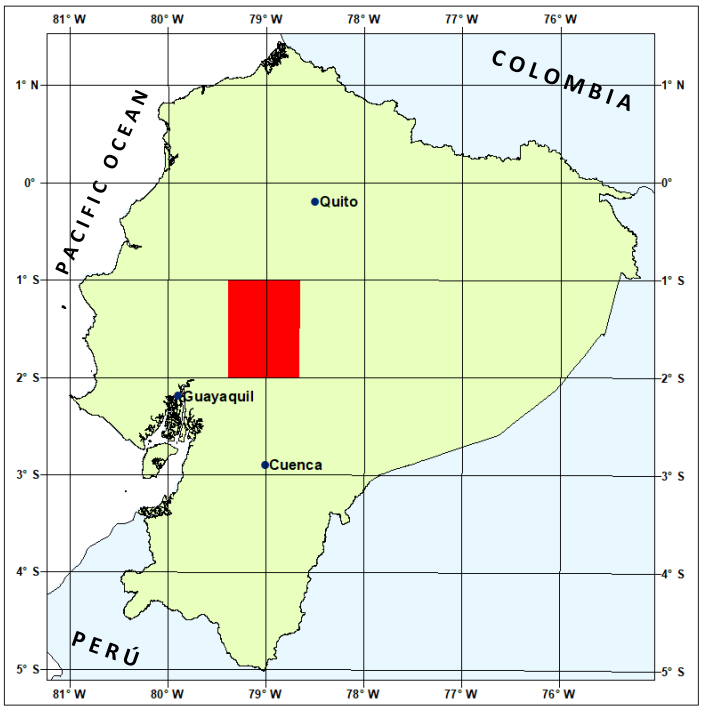

GEOLOGICAL INFORMATION MAPPING PROGRAMME
(LOCATION OF MAP 3 AREA)

W. MCCOURT
P. DUQUE
L. PILATASIG

QUITO, 1997

Table 1. Geochronology using the Potassium-Argon method

Sample #	Topographic sheet	UTMX	UTMY	Unit/Intrusive	Mineral	Age (Ma)
M3-308	Angamarca	7282	98855	Dyke	Hornblende	23.65 ± 0.35
M3-103	Guaranda oeste	7037	98159	Telimbela pluton	Biotite	21.37 ± 0.26 21.42 ± 0.26 (21.40 ± 0.19)
M3-103	Guaranda oeste	7037	98159	Telimbela pluton	Hornblende	19.80 ± 0.27 20.76 ± 0.58 (19.97 ± 0.36)
M3-137	El Corazón	7246	98739	El Corazón pluton	Biotite	15.82 ± 0.19 15.82 ± 0.19 (15.82 ± 0.19)
M3-137	El Corazón	7246	98739	El Corazón pluton	Hornblende	16.06 ± 0.23 16.08 ± 0.52 (16.06 ± 0.21)
M3-209	San Miguel de Bolívar	7073	97984	Las Guardias pluton	Biotite	33.57 ± 0.41 33.18 ± 0.40 (33.37 ± 0.29)
M3-209	San Miguel de Bolívar	7073	97984	Las Guardias pluton	Hornblende	34.69 ± 0.47 32.81 ± 0.88 (34.27 ± 0.78)
M3-272A	Villa La Unión	7362	98002	Juan de Velasco porphyry	Hornblende	10.06 ± 0.19 10.28 ± 0.69 (10.08 ± 0.18)
M3-480	El Corazón	7213	98676	El Corazón pluton	Biotite	10.82 ± 0.63
M3-482	Moraspungo	7208	98686	El Corazón pluton	Hornblende	13.97 ± 0.21 14.89 ± 0.46 (14.13 ± 0.35)
M3-620	Ventanas	6911	98358	Echeandía pluton	Biotite	23.14 ± 0.79
M3-639	San José de Camarón	7061	98458	Chazo Juan pluton	Biotite	21.16 ± 0.25 21.16 ± 0.25 (21.16 ± 0.25)
M3-639	San José de Camarón	7061	98458	Chazo Juan pluton	Hornblende	19.61 ± 0.28 18.94 ± 0.71 (19.52 ± 0.26)
M3-656	San José de Camarón	7137	98347	Chazo Juan pluton	Hornblende	22.98 ± 0.34 23.36 ± 0.57 (23.08 ± 0.29)
M3-685	Ventanas	6825	98371	Echeandía pluton	Biotite	26.49 ± 0.73
M3-763	Simiátug	7244	98672	El Corazón pluton	Hornblende	14.90 ± 0.31 13.04 ± 1.32 (14.80 ± 0.41)
M3-773	Ventanas	6893	98428	Echeandía pluton	Hornblende	25.53 ± 0.33 25.73 ± 0.55 (25.58 ± 0.28)
M3-788	Guaranda oeste	7069	98159	Telimbela pluton	Biotite	19.11 ± 0.79
M3-851	San Miguel de Bolívar	6987	98043	Balzapamba pluton	Hornblende	33.16 ± 0.43 32.74 ± 0.88 (33.08 ± 0.39)
M3-889	Chillanes	6986	97838	Undushig pluton	Biotite	25.46 ± 0.31 25.37 ± 0.31 (25.42 ± 0.22)
M3-889	Chillanes	6986	97838	Undushig pluton	Hornblende	23.93 ± 0.34 25.01 ± 0.83 (24.08 ± 0.38)
M3-973	Angamarca	7226	98732	El Corazón pluton	Hornblende	14.89 ± 0.20 14.59 ± 0.46 (14.84 ± 0.18)

Note: Ages calculated using 1976 IUGS constants (Steiger & Jager, 1977)

(14.84 ± 0.18) indicates weighted mean age

Table 2. Geochronology using the fission track method

Sample #	Topographic sheet	UTMX	UTMY	Unit/Intrusive	Mineral	Age (Ma)
M3-961	Guamote	7539	97910	Saraguro Group	Zircon	24.4 ± 1.1
M3-977	Angamarca	7497	98821	Saraguro Group	Zircon	16.8 ± 1.4

Note: Ages calculated using 1976 IUGS constants (Steiger & Jager, 1977)

APPENDIX 4 OF REPORT:

GEOLOGY OF THE WESTERN CORDILLERA
OF ECUADOR
BETWEEN 1°00' AND 2°00' S

PETROGRAPHIC DESCRIPTIONS

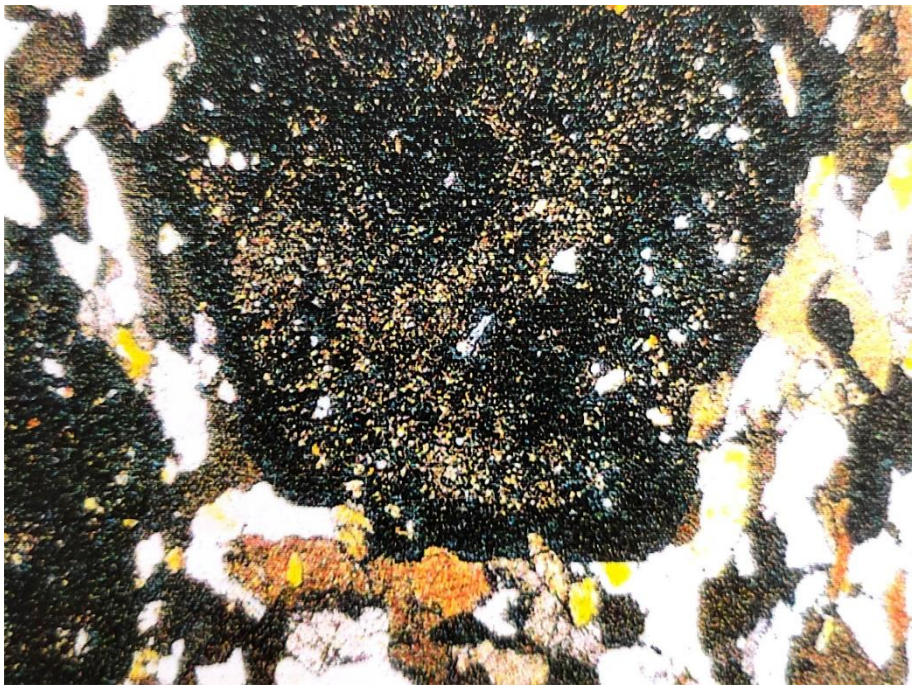

GEOLOGICAL INFORMATION MAPPING PROGRAMME
(LOCATION OF MAP 3 AREA)

W. MCCOURT
P. DUQUE
L. PILATASIG

QUITO, 1997

Sample	UTMX	UTMY	Unidad	Rock type	Description	Minerals
M3-LP-8646	0	0		Sandstone	Clastic rock; fine-grained	arc-qtz-plg-opq
M3-LP-7848A	0	0		Basalt	Massive, fine-grained, equidimensional rock	plg-glass-px-chl-epdt-opq
M3-BX-166	7394	98200	Apagua	Sandstone	Grey, fine-grained rock, good sorting, few mafics	qtz-bio-arc-opq-ms-plg-chl
M3-PD-163	7359	98224	Apagua	Sandstone	Grey, fine-grained rock, massive, good bedding, minor shale horizons	qtz-ms-chl-opq-bio-plg-cc
M3-PD-440	7311	97976	Apagua	Sandstone	Grey, clastic, fine-grained rock	clasts: qtz-plg-ms-epdt-opq; matrix: arc
M3-BX-97	7114	98245	Apagua	Micaceous sandstone	Grey, fine-grained, slightly clastic rock	cement: qtz; fine clasts: qtz-bio-opq
M3-PD-361A	7251	97921	Apagua	Siliceous siltstone	Black, fine-grained, fractured rock, tectonic cleavage development	arc-qtz-opq-epdt-ms
M3-PD-290	7370	98100	Apagua (?)	Sandstone	Grey, fine-grained, crudely bedded rock	qtz-arc-opq-ms-bio
M3-PD-438	7302	97968	Apagua (?)	Sandstone	Grey, clastic, medium-grained, impure, practically uncemented rock	lithics-qtz-px (aug di)-cc-plg-opq-bio-ms-fossils(?)
M3-LP-1053B	7278	98053	Apagua (?)	Shale	Grey, fractured, ferruginous, fine- to medium-grained rock	arc-opq-qtz-cc-epdt
M3-PD-726	7078	98264	Arrayanes	Andesite	Grey-green, porphyritic, medium-grained rock in a fine-grained matrix	phenocrysts: plg (An_{52})-amph (hb)-opq; matrix: plg
M3-PD-725	7060	98266	Arrayanes	Basaltic andesite	Grey porphyritic, medium-grained rock in a fine-grained matrix	phenocrysts: plg (An_{54})-amph (hb)-opq-epdt; matrix: plg
M3-PD-771	7029	98319	Arrayanes	Basaltic Andesite	Greenish-black, porphyritic rock, fine-grained matrix	phenocrysts: plg (An_{60})-cpx (aug di)-opq-serp; matrix: plg-chl-opq (devitrified glass)
M3-PD-98	7102	98153	Arrayanes	Basaltic Andesite	Green, porphyritic rock, medium-grained matrix, intersertal	phenocrysts: plg (An_{60}); matrix: plg-amph-cpx-chl-opq
M3-LP-1035	7156	98462	Arrayanes	Sandstone	Grey, fine-grained, clastic rock, angular quartz clasts in clayey matrix	clasts: qtz-opq-ms: matrix: arc
M3-PD-192	7113	97877	Arrayanes	Sandstone	Fine-grained rock, interbedded with non-calcareous shale	clasts: qtz-opq; cement: arc
M3-PD-198	7049	97870	Arrayanes	Sandstone	Green, clastic, fine-grained rock	clasts: epdt-qtz-chl-cpx: matrix: qtz-chl-epdt
M3-PD-456A	7053	97879	Arrayanes	Sandstone	Cream, massive, clastic, fine- to medium-grained rock	qtz-chl-ms-plg ($An_{32?}$)-opq-bio-cc
M3-PD-82	7051	98353	Arrayanes	Micaceous sandstone	Black, fine-grained, slightly porphyroclastic rock	crystals: qtz-ms-opq-bio (?); matrix: qtz-carbonaceous material
M3-PD-198B	7049	97870	Arrayanes	Volcanic sandstone	Fine-grained, clastic rock	clasts: qtz-epdt-plg-cc; matrix: arc
M3-PD-456	7053	97879	Arrayanes	Volcanic sandstone	Green, porphyroclastic, altered rock	clasts: epdt-plg-qtz-lithics-cc; matrix: chl
M3-PD-894	7011	97798	Arrayanes	Volcanic sandstone	Green, bedded, slightly silicified, clastic, fine-grained rock	clasts: qtz-epdt-chl-cc-opq; matrix: arc-plg
M3-PD-807	7098	97853	Arrayanes	Volcanic sandstone (?)	Green-grey, porphyroclastic rock, recrystallized clasts in green matrix	clasts: qtz-epdt-plg-opq; matrix: pyribol(?)-epdt(?)
M3-PD-816	7057	98108	Arrayanes	Volcanic sandstone (?)	Green, fine-grained, clastic, slightly recrystallized rock	clasts: qtz-plg-chl-opq; matrix: chl-plg (devitrified glass)
M3-BX-120	6993	97997	Arrayanes	Basalt	Black, porphyritic fine-grained matrix, altered rock	matrix: plg-devitrified glass; phenocrysts: plg saus-px (aug)-epdt(s)-serp(s)-opq
M3-BX-121	6976	98007	Arrayanes	Basalt	Black, porphyritic rock	phenocrysts: plg saus-cpx (aug di)-opx-alt. red-epdt-opq; matrix: plg-epdt-px
M3-BX-128	7157	94894	Arrayanes	Basalt	Grey, porphyritic rock, fine-grained matrix	phenocrysts: plg (An_{62})-epdt(s)-chl(s)-cc(s)-qtz-opq-sph; matrix: devitrified glass
M3-PD-81A	7044	98356	Arrayanes	Basalt	Black, slightly porphyritic rock, fine-grained matrix	plg-cpx (aug di)-amph (hb)-epdt (s)-opq
M3-PD-657	7135	98514	Arrayanes	Hornfels (volcanic sandstone?)	Grey rock, slightly porphyroblastic, some appearance of stained schist	porphyroblasts: plg-epdt-bio-px-opq; matrix: qtz-bio
M3-PD-658B	7130	98523	Arrayanes	Hornfels (volcanic sandstone?)	Blocks within sec. sdmt, equidimensional, medium-grained, non-oriented, sc. porphyroblastic	porphyroblasts: epdt; matrix: qtz-plg-cc-opq-zr
M3-PD-724A	7024	98256	Arrayanes	Hornfels (volcanic sandstone?)	Medium-grained, uniform, non-oriented rock	epdt-amph-cc (s)

Sample	UTMX	UTMY	Unidad	Rock type	Description	Minerals
M3-PD-827A	7085	98147	Arrayanes	Hornfels (volcanic sandstone?)	Partially molten rock, porphyritic appearance, aphanitic green matrix.	blasts: cc-plg-qtz; matrix: amph-chl-opq-plg
M3-PD-704	7047	98018	Arrayanes	Hornfels (sandstone)	Porphyritic texture, large quartz phenocrysts and smaller epidote phenocrysts in cryptocrystalline matrix	blasts: qtz-bio-epdt; matrix: qtz-chl (esc)
M3-PD-709	7030	98052	Arrayanes	Hornfels (sandstone)	Allotriomorphic, medium-grained, quartz crystals with intersertal epidote	qtz-epdt-opq
M3-PD-90A	7170	98355	Arrayanes	Hornfels (sandstone)	Green, fine-grained, massive, fine-grained rock	qtz-ms-opq-chl
M3-RV-105	7007	98186	Arrayanes	Hornfels (epidosite)	Medium-grained, massive	epdt (2Vx~80)-qtz; ga in hand sample
M3-PD-699	7051	97989	Arrayanes	Hornfels (tuffaceous rock)	Green rock, porphyroblastic, medium-grained blasts in a fine-grained matrix	blasts: plg-qtz-px-bio; matrix: plag-ms-opq
M3-PD-862	7125	97791	Arrayanes	Siltstone	Black rock, fine-grained, non-oriented, sparse clasts, semi-angular, some > gr. remaining	arc-qtz-plg-opq
M3-PD-69	7131	98523	Arrayanes	Shale	Very fine-grained, silicified, good sorting, oriented texture	clay-mat. micaceous-opq-chl
M3-PD-774	7014	98260	Arrayanes	Crystalline tuff	Rlack-green, porphyritic, fine-grained rock, chloritized amygdules	clasts: plg-cc (s), matrix: plg-opq-px; amygdales: chl
M3-PD-99	7093	98153	Arrayanes	Crystalline tuff	Silicified, clastic rock, fine-grained matrix	clasts: qtz-plg-opq-ms(s)-epdt(s); matrix: plg-qtz-glass (partially devitrified)
M3-BX-131	7064	98515	Arrayanes	Vitreous tuff	Green, fine-grained, porphyritic rock	clasts: plg (An_{44})-opq; clasts: volcanic lithics-mafics; matrix: plg
M3-PD-198A	7049	97870	Arrayanes	Vitreous tuff	Clastic, medium-grained rock, angular clasts in yellow-brown matrix	qtz-plg-epdt(s)-pump(s)
M3-BX-74	7070	98505	Arrayanes	Vitreous basaltic tuff	Green, porphyroclastic rock, fine-grained matrix	clasts: plg-px-epdt-chl-basaltic lithics; matrix: plg-glass
M3-PD-796	7077	98085	Arrayanes (?)	Hornfels (hornblendite)	Grey, granoblastic, fine-grained rock, somewhat larger amphibole crystals bordered by smaller serpentine	amph(eden)-serp-opq
M3-BX-993	6921	98881	Calope	Micro-quartzodiorite	Porphyritic rock, partially fractured phenocrysts in matrix of somewhat more acidic composition	amph(hb)-plg-qtz-opq-epdt(s)-chl(s)-cc(s)
M3-PD-977	7497	98821	Calpa	Andesite	Porphyritic, fine-grained, trachytic rock (plagioclase microlites oriented in subdomains)	phenocrysts: plg (An_{38})-amph-opq-epdt(s); matrix: plg-opq-glass
M3-PD-967	7437	98215	Calpa	Vitreous tuff	Grey, porphyroclastic rock, crystal fragments and lithics in glassy matrix	clasts: lithics-plg-px-ol-opq; matrix: glass-plg
M3-BX-114	7100	98256	Cuaternario	Basalt	Black, slightly porphyritic, slightly altered rock	phenocrysts: plg-amph-epdt(s)-pyrite(s); matrix: plg-opq-devitrified glass
M3-BX-94	7155	98245	Cuaternario	Basalt	Grey, porphyritic, altered rock, fine-grained matrix	phenocrysts: plg (An_{60})-px (aug di)-opq-chl(s)-epdt(s); matrix: plg-opq-chl
M3-PD-66A	7073	98713	Cuaternario	Trachy-andesite	Grey, porphyritic, altered rock	phenocrysts: plg (An_{38})-amph (hb)-san-qtz-opq; matrix: glass-preh
M3-PD-620	6911	98358	Echeandía	Granodiorite	Allotriomorphic textured rock, granular, medium to coarse-grained, quartz-feldspar crystals with intersertal biotite-amphibole	qtz-plg (An_{40})-kfs-bio-amph (hb)-zr-opq
M3-PD-620A	6911	98358	Echeandía	Granodiorite	Hypidiomorphic textured rock, granular, medium to coarse grained	plg (An_{44})-qtz-kfs-amph (hb)-bio-opq-sph
M3-PD-656	7137	98347	Echeandía	Granodiorite	Hypidiomorphic textured rock, granular, medium to coarse grained	plg (An_{44})-qtz-kfs-amph (hb)-bio-opq
M3-PD-667	6875	98291	Echeandía	Granodiorite	Hypidiomorphic textured rock, medium-grained	plg (An_{40})-qtz-kfs-amph (hb)-bio-opq-zr
M3-PD-773	6893	98428	Echeandía	Granodiorite	Allotriomorphic, granular, medium-grained, somewhat altered rock	plg (An_{44})-qtz-kfs-amph (hb)-bio-sph-opq-chl(s)-epdt(s)
M3-PD-87	7133	98346	Echeandía	Granodiorite	Hypidiomorphic rock, coarse-grained	plg (An_{54})-qtz-kfs(?)-bio-hb-chl(s)-opq
M3-PD-688	6837	98325	Echeandía	Micro-tonalite	Porphyritic rock, coarse- to medium-grained phenocrysts in fine- to medium-grained matrix	plg (An_{54})-qtz-kfs-amph (hb)-bio-opq-zr-chl(s)
M3-PD-91	7173	98353	Echeandía	Micro-granite	Porphyritic rock, medium-grained phenocrysts, fine-grained matrix	plg (An_{52})-qtz-hb-bio-opq-kfs(?)
M3-PD-695	6875	98226	Echeandía	Pegmatite	Coarse-grained rock, allotriomorphic, quartz crystals with tourmaline needles	qtz-tour(elbaite)-zr
M3-PD-619	6937	98407	Echeandía	Tonalite	Hypidiomorphic textured rock, granular, medium-grained, somewhat ophiolitic, altered	plg (An_{47})-amph (hb)-qtz-bio-opq
M3-PD-621	6858	98354	Echeandía	Tonalite	Rock with hypidiomorphic texture, granular, medium-grained, amphibole aprx. intersertal	plg-qtz-amph (hb)-bio-opq-chl(s)
M3-PD-624	6853	98375	Echeandía	Tonalite	Rock with hypidiomorphic texture, granular, medium-grained, intergrowths, spaces between plagioclase occupied by amphibole-biotite	plg (An_{45})-qtz-amph (hb)-bio-opq
M3-PD-639	7061	98458	Echeandía	Tonalite	Allotriomorphic textured rock, granular, medium-grained	plg (An_{45})-bio-cpx (aug di)-qtz-opq-epdt-zr
M3-PD-685	6825	98371	Echeandía	Tonalite	Hypidiomorphic textured rock, granular, medium-grained	plg (An_{50})-qtz-kfs-cpx (aeg, aug)-opx (hy)-bio-opq

Sample	UTMX	UTMY	Unidad	Rock type	Description	Minerals
M3-PD-765	6897	98297	Echeandía	Tonalite	Hypidiomorphic, granular, coarse- to medium-grained, somewhat altered rock.	plg (An_{38})-qtz-amph (hb)-kfs (mcl)-opq-chl(s)-bio(s)-ms(s)
M3-BX-487	7126	98737	El Corazón	Aplite	Kaolinized rock, fine-grained, massive, white, sugary texture	plg-qtz-kfs-bio-opq-cc(s)
M3-PD-478	7194	98722	El Corazón	Diorite	Grey, hypidiomorphic, granular, medium-grained rock	plg (An_{48})-amph (hb)-kfs-qtz-px-opq
M3-BX-462	7138	98821	El Corazón	Granodiorite	Hypidiomorphic, granular, medium-grained, massive rock	plg (An_{337})-qtz-kfs-amph-zr-opq-alt
M3-BX-480	7213	98676	El Corazón	Granodiorite	Hypidiomorphic rock, medium-grained, local sulphide concentration	plg (An_{46})-qtz-kfs-bio-amph (hb)-opq
M3-BX-482	7208	98686	El Corazón	Granodiorite	Hypidiomorphic, granular, medium-grained rock	plg (An_{45})-qtz-kfs-amph (hb)-bio-opq
M3-BX-538	7270	98720	El Corazón	Granodiorite	Allotriomorphic, granular, coarse- to medium-grained, somewhat altered rock	plg (An_{40})-qtz-kfs (?)-bio-amph (hb)-chl-opq
M3-PD-137	7246	98739	El Corazón	Granodiorite	Hypidiomorphic, medium-grained rock	plg-amph (hb)-bio-qtz-kfs-opq
M3-PD-516	7213	98778	El Corazón	Granodiorite	Hypidiomorphic, granular, medium-grained, massive rock	plg (An_{40})-qtz-kfs-bio-amph (hb)-opq
M3-PD-516A	7213	98778	El Corazón	Granodiorite	Hypidiomorphic, granular, medium-grained rock	plg (An_{54})-qtz-kfs-amph (hb)-bio-opq
M3-PD-745	7133	98872	El Corazón	Granodiorite	Hypidiomorphic, granular, medium-grained, altered rock	plg (An_{46})-qtz-kfs (mcl)-amph (hb)-opq-bio(s)
M3-PD-747A	7131	98870	El Corazón	Granodiorite	Hypidiomorphic, granular, medium-grained, altered rock	plg (An_{50})-amph (hb)-kfs-qtz-opq-chl(s)-cc(s)
M3-PD-763	7244	98672	El Corazón	Granodiorite	Hypidiomorphic, granular, coarse-grained, somewhat altered rock	plg (An_{40})-qtz-amph (hb)-kfs-bio-opq-sph
M3-PD-973	7226	98732	El Corazón	Granodiorite	Hypidiomorphic, granular, medium- to coarse-grained, slightly altered rock	plg (An_{50})-qtz-kfs (or)-amph (hb)-bio-zr-opq-ms(s)
M3-PD-992	7099	98883	El Corazón	Granodiorite	Hypidiomorphic, granular, medium to fine-grained, strongly altered rock	plg-qtz-kfs-amph (hb)-opq-chl(s)-epdt(s)
M3-PD-222	7241	98837	El Corazón	Micro-granodiorite	Subvolcanic looking rock, fine-grained, seriate, pilotaxitic texture	plg (An_{45})-qtz-bio-hb-sulfides-kfs(?)
M3-BX-463	7142	98817	El Corazón	Monzodiorite	Allotriomorphic, granular, fine-grained rock	plg (An_{60})-kfs-qtz-amph-bio-opq-epdt(s)
M3-PD-505	7140	98762	El Corazón	Tonalite	Allotriomorphic, granular, medium-grained, highly altered rock	plg-amph-qtz-ms
M3-BX-421	7311	97822	Gabroide indiferenciado	Quartz-gabbro	Green, hypidiomorphic, granular, medium-grained, slightly altered rock	px (aug di)-plg (An_{63})-amph-qtz-chl-opq-epdt(s)
M3-PD-873	6959	97830	Gabroide indiferenciado	Quartz-gabbro	Medium-grained, slightly porphyritic rock	plg (An_{70})-px (aug di)-qtz-opq-amph(s)-serp(s)
M3-PD-199A	7046	97870	Gabroide indiferenciado	Gabbro	Green, porphyritic, medium-grained, altered rock	plg (An_{65})- px (aug di)-opq-chl(s)-epdt(s)-serp(s)
M3-PD-201	7002	97847	Gabroide indiferenciado	Gabbro	Hypidiomorphic, coarse-grained rock	plg-cpx (aug di)-opq-qtz(tr)-epdt(s)-serp(tr)-chl(s); local concentration: px
M3-PD-242	7123	97418	Gabroide indiferenciado	Gabbro	Grey-black, medium-grained, altered rock, pseudo-porphyritic appearance	plg (An_{60})-cpx (aug di)-opq-zr-amph(s)-chl(s)-serp(s)
M3-PD-245	7128	97926	Gabroide indiferenciado	Gabbro	Grey, hypidiomorphic, massive, medium to coarse-grained rock	plg-px (aug di)-amph-opq
M3-PD-504	7145	98760	Gabroide indiferenciado	Gabbro	Hypidiomorphic, granular, slightly porphyritic, medium to coarse-grained rock	plg-cpx (aug di)-opx(incl)-chl(s)-opq
M3-PD-810	7094	97843	Gabroide indiferenciado	Gabbro	Hypidiomorphic, granular, medium-grained, altered rock	plg (An_{58})-amph(ferro hastingsite)-opq-cc(s)-epdt(s)
M3-PD-866	7091	97782	Gabroide indiferenciado	Gabbro	Hypidiomorphic, granular, coarse-grained, somewhat altered rock	plg (An_{60})-px (aug)-opq-sph-amph(ural)
M3-PD-872A	6960	97826	Gabroide indiferenciado	Gabbro	Hypidiomorphic, granular, fine-grained rock	plg-px-opq
M3-PD-902	6996	97845	Gabroide indiferenciado	Gabbro	Green, hypodiomorphic, granular, medium-grained, fairly altered rock	plg-px (aug)-serp-opq-amph(ural?)-qtz(s)
M3-RV-234	7015	97895	Gabroide indiferenciado	Gabbro	Hypidiomorphic, medium-grained, altered rock	px (aug di)-plg-opq-chl
M3-PD-499	7067	97718	Gabroide indiferenciado	Micro-gabbro	Green, medium-grained, somewhat porphyritic, altered rock	plg-px (aug di)-opq-chl(s)-epdt(s)
M3-PD-508	7133	98774	Gabroide indiferenciado	Micro-gabbro	Massive, fractured, altered, fine-grained, slightly clastic appearance rock, sulphide-bearing horizons	plg-amph (hb)-chl-opq-cc(s)
M3-PD-850	6938	97890	Gabroide indiferenciado	Micro-gabbro	Porphyritic, fairly altered rock	phenocrysts: plg-px-opq; matrix: plg-pyribol-sauss
M3-PD-890	6975	97854	Gabroide indiferenciado	Micro-gabbro	Banded, porphyritic rock, fine-grained matrix	phenocrysts: plg-px (aug)-chl-qtz-opq; matrix: plg-chl
M3-PD-891	6974	97856	Gabroide indiferenciado	Micro-gabbro	Porphyritic, highly altered rock, quartz veinlets	phenocrysts: plg-px (aug)-opq-chl(s); matrix: plg-opq-chl-qtz
M3-PD-238	7041	97929	Gabroide indiferenciado	Micro-gabbro with quartz	Slightly porphyritic, medium-grained matrix, altered rock	plg (An_{54})-px (aug di)-qtz-opq-chl(s)-amph(s)-epdt(s)
M3-BX-102	7077	98158	Illiuví	Tonalite	Hypidiomorphic, coarse-grained rock. In outcrop there is a concentration of mafics	plg (An_{64})-qtz-bio-hb-zr-opq-epdt(s)
M3-PD-103	7037	98159	Illiuví	Tonalite	Hypidiomorphic, coarse-grained rock. In outcrop there is a concentration of mafics	plg-bio-amph-qtz-kfs (or)-opq
M3-PD-778	7072	98270	Illiuví	Tonalite	Allotriomorphic, granular, medium-grained, altered rock.	plg-qtz-amph (hb)-bio-opq
M3-PD-787	7052	98154	Illiuví	Tonalite	Hypidiomorphic, granular, coarse- to medium-grained, altered rock	plg (An_{44})-qtz-kfs (mcl)-bio-amph (hb)-zr-opq
M3-PD-788	7069	98159	Illiuví	Tonalite	Hypidiomorphic, coarse- to medium-grained, granular rock	plg (An_{44})-qtz-kfs (mcl)-bio-amph (hb)-zr-opq
M3-PD-558A	7327	98797	Intrusivo en Apagua	Micro-diorite	Porphyritic rock, non-oriented matrix	phenocrysts: plg (An_{40})-amph (hb)-qtz-opq-cc-chl-epdt; matrix: plg

Sample	UTMX	UTMY	Unidad	Rock type	Description	Minerals
M3-PD-68A	7136	98515	Intrusivo en Arrayanes	Granodiorite	Hypidiomorphic, medium-grained, altered rock	zoned plg (An_{48})-qtz-kfs-px uralitized (aug di)-chl(s)-opq
M3-PD-897	6953	98079	Intrusivo en Arrayanes	Micro-gabbro	Porphyritic, medium-grained, fine-grained matrix, fairly altered rock	phenocrysts: plg-amph (hb)-serp-opq; matrix: plg-serp
M3-BX-123	7023	98114	Intrusivo en Arrayanes	Micro-tonalite	Green, fine-grained rock, ophitic texture	plg (An_{40})-cpx (aug di)-qtz-chl(s)-epdt(s)
M3-PD-601	7003	98597	Intrusivo en Macuchi	Micro-granodiorite	Grey, porphyritic, medium-grained rock	phenocrysts: plg (An_{32})-amph (hb)-opq-chl(s)-epdt(s); matrix: qtz
M3-PD-586	7109	98626	Intrusivo en Macuchi	Plagio-granite	Hypidiomorphic, granular, medium-grained rock, sparse mafic, somewhat altered	plg (An_{32})-qtz-kfs-bio-amph-sph-opq-chl(s)-epdt(s)
M3-PD-281	7297	98079	Intrusivo en Pallatanga	Micro-granite	Porphyritic, medium-grained, massive rock, very fine-grained matrix	phenocrysts: plg-qtz-bio-ms-kfs-apt; matrix: qtz-plg
M3-PD-272	7362	98002	Intrusivo en Yunguilla	Micro-granodiorite	Somewhat porphyritic, coarse-grained rock	phenocrysts: qtz-plg-amph (hb?)-kfs-opq; matrix: plg-qtz
M3-PD-272A	7362	98002	Intrusivo en Yunguilla	Micro-granodiorite	Porphyritic rock, fine-grained matrix, not oriented	phenocrysts: plg-amph (hb)-kfs-opq-apt; matrix: plg-qtz
M3-PD-384	7377	97958	Intrusivo en Yunguilla	Micro-granodiorite	White, fractured, porphyritic rock, fine-grained matrix, altered	phenocrysts: plg-amph-opq-kfs; matrix: qtz-plg
M3-PD-38	7282	98855	Intrusivo en Zumbagua	Micro-tonalite	Porphyritic, altered rock, quartzo-feldspathic matrix	plg ($An_{63?}$)-qtz-amph (hb)-opq-bio(s)-chl(s)-epdt(s)-cc(s)-ms(s)
M3-PD-40	7282	98855	Intrusivo en Zumbagua	Tonalite	Medium-grained, altered rock	plg-amph (hb)-qtz-opq-chl(s)-ms(s)
M3-PD-40A	7282	98855	Intrusivo en Zumbagua	Tonalite	Allotriomorphic, medium-grained, altered rock	plg (An_{55})-amph (hb)-opq-chl(s)-cc(s)-ser(s)
M3-PD-855	6975	98036	Las Guardias	Granodiorite	Hypidiomorphic, granular, coarse- to medium-grained, somewhat altered rock	plg (An_{46})-qtz-kfs-amph (hb)-px (aug di)-opq-epdt(s)-ms(s)-chl(s)
M3-BX-209	7073	97984	Las Guardias	Tonalite	Hypidiomorphic, medium-grained rock, mafics accumulation	plg (An_{45})-qtz-kfs-bio-hb-opq
M3-PD-851	6987	98043	Las Guardias	Tonalite	Hypidiomorphic, granular, coarse-grained, fairly altered rock	plg (An_{43})-qtz-kfs (or)-amph (hb)-bio-ms-opq
M3-PD-537A	7272	98604	Macuchi	Altered andesite	Porphyritic rock, strongly altered	phenocrysts: plg-Fe ox-cc-chl-ser-opq-qtz; matrix: plg-arc-opq
M3-BX190	7123	97854	Macuchi	Basaltic andesite	Porphyritic rock, sulphide-filled veinlets, medium-grained matrix	phenocrysts: plg (An_{51})-amph (hb)-epdt(s); matrix: plg-amph-opq-alt
M3-PD-140A	7140	98743	Macuchi	Basaltic andesite	Black rock, porphyritic, fine-grained matrix, intergranular texture	phenocrysts: plg (An_{54})-amph (hb)-opq; matrix intergranular: plg-bio-opq
M3-PD-190A	7123	97854	Macuchi	Basaltic andesite	Grey, porphyritic rock, fine-grained matrix	phenocrysts: plg (An_{55})-amph (hb)-epdt(s); matrix: plg-amph-opq-alt
M3-PD-761	7044	98729	Macuchi	Basaltic andesite	Green, highly altered, porphyritic rock	phenocrysts: plg-chl-opq; matrix: arc-chl(s); vesicles: qtz-chl
M3-BX-525	7174	98597	Macuchi	Volcanic sandstone	Green, fine-grained, uniform-grain rock	clasts: qtz-plg-opq; matrix: devitrified glass-plg
M3-PD-160	7317	98219	Macuchi	Volcanic sandstone	Clastic rock, medium-grained, subrounded, fine cement	qtz-plg (An_{36})-bio-chl-epdt-ms-opq; cement: qtz-bio
M3-PD-162	7342	98228	Macuchi	Volcanic sandstone	Clastic rock, medium-grained, uniform, subrounded, fine cement	qtz-plg (An_{36})-bio-chl-ms-cc-opq; cement: mat mic-devitrified glass
M3-PD-181	7210	98057	Macuchi	Volcanic sandstone	Brown, fine-grained rock, in stratified outcrop	clasts: lithics-cc-opq-plg-ol-px-epdt; matrix: cc-arc
M3-PD-203	7049	97943	Macuchi	Volcanic sandstone	Volcanoclastic, medium-grained, dirty rock	clasts: plg-lithics; matrix: epdt-plg
M3-PD-364	7240	97873	Macuchi	Volcanic sandstone	Green, medium-grained, uniform rock	plg-cpx (aug di)-opq-lithics-chl-cc
M3-PD-394A	7307	98085	Macuchi	Volcanic sandstone	Green, medium-grained, clastic rock, fine-grained matrix	qtz-plg-chl-epdt-bio-amph
M3-PD-394B	7307	98085	Macuchi	Volcanic sandstone	Green, tectonised, clastic, fine-grained matrix rock	clasts: qtz-ms-epdt-bio-chl-plg-opq-Fe ox-amph; cement: qtz-arc
M3-PD-884	7205	97958	Macuchi	Volcanic sandstone	Clastic, medium-grained, silicified rock, fine-grained matrix	clasts: qtz-plg-chl-pump-epdt-opq; matrix: qtz-plg-chl
M3-BX-523	7155	98594	Macuchi	Volcanic sandstone (?)	Green rock, int fract, weathered, fine-grained, somewhat clastic	phenocrysts: plg; matrix: plg-opq-arc-epdt-qtz
M3-PD-803	7185	97817	Macuchi	Volcanic sandstone (?)	Green, very fine-grained, crudely stratified rock	phenocrysts: chl-plg-qtz-mat mic-epdt
M3-BX-62	7056	98726	Macuchi	Basalt	Black, slightly porphyritic, pilotaxitic rock	phenocrysts: plg-px (aug di)-opq- Fe ox
M3-PD-132	7035	98553	Macuchi	Basalt	Fine-grained, porphyritic rock, pilotaxitic matrix	phenocrysts: plg (An_{65}); matrix: plg-opx-opq-chl
M3-PD-149	7291	98223	Macuchi	Basalt	Black rock, porphyritic, fine-grained matrix	phenocrysts: plg (An_{66})-px-ilm-cc(s)-epdt(s)-chlorophaeite(alt); matrix: plg-opq-chl-glass
M3-PD-159	7263	98218	Macuchi	Basalt	Greenish, fine-grained, porphyritic rock	phenocrysts: plg (An_{58-63})-chl-opq; matrix: devitrified glass

Sample	UTMX	UTMY	Unidad	Rock type	Description	Minerals
M3-PD-235A	7013	97925	Macuchi	Basalt	Green, porphyritic, fine-grained matrix, highly altered rock	phenocrysts: px (aug di)-plg-chl-opq; matrix: glass-plg
M3-PD-335C	7237	98026	Macuchi	Basalt	Grey, porphyritic rock, fine-grained matrix	phenocrysts: cpx (aug di)-plg-ol-opq; matrix: plg-amph
M3-PD-497	7152	98635	Macuchi	Basalt	Greenish rock, porphyritic, medium to fine-grained, fine-grained matrix	phenocrysts: plg-amph (hb)-cpx (aug di)-opq; matrix: amph-plg-opq
M3-PD-575A	6966	98846	Macuchi	Basalt	Green rock, intruded in 574, finer-grained, porphyritic	phenocrysts: plg (An_{62})-cpx (aug di)-opq-epdt; matrix: plg
M3-PD-917	7154	97707	Macuchi	Basalt	Porphyritic rock, fine-grained matrix, pillo lava (?)	phenocrysts: plg-ol-px (aug di)-opq; matrix: plg-serp(s)-epdt(s)
M3-PD-189	7188	97844	Macuchi	Altered basalt	Green rock, slightly porphyritic	phenocrysts: plg; matrix: plg-chl-cc-opq
M3-PD-400	7229	97962	Macuchi	Altered basalt	Porphyritic rock, small phenocrysts in cryptocrystalline matrix, hyalophitic texture	phenocrysts: plg ($An_{40?}$)-chl-cpx (aug di)-qtz-epdt-opq
M3-PD-365	7237	97873	Macuchi	Basalt with amygdales	Green rock, massive, slightly porphyritic, aphanitic matrix, non-oriented, vesicles	phenocrysts: plg-px (aug di)-epdt-cc-pump-qtz; matrix: plg-devitrified glass; amygdales
M3-BX-493	7132	98702	Macuchi	Tuffaceous basalt	Green rock, porphyritic, chloritic matrix, filled amygdales, slight pillo lava appearance	phenocrysts: plg-chl-px (aug di)-opq-epdt(s); matrix: plg-chl-opq (devitrified glass)
M3-PD-613B	6974	98540	Macuchi	Tuffaceous basalt	Green rock, porphyritic, fine-grained, few very altered phenocrysts	phenocrysts: chl-cc-opq-qtz (reempl)-opq; matrix: plg-devitrified glass; amygdales: qtz
M3-PD-674	6962	98155	Macuchi	Tuffaceous basalt	Porphyritic rock, coarse phenocrysts in medium-grained matrix, uniform composition	phenocrysts: plg-px (aug)-chl (devitrified glass)-epdt-opq; matrix: plg-chl-opq-epdt
M3-PD-582	7119	98609	Macuchi	Lithic breccia	Green rock, medium-grained, clastic	clasts: lithics-plg (An_{60})-px (aug?)-amph-opq; matrix: plg; amygdales: qtz
M3-BX-520	7053	98689	Macuchi	Volcanic breccia	Green rock, medium-grained, clastic	clasts: black lithics-plg-cpx-chl-opq
M3-BX-592	7134	98615	Macuchi	Volcanic breccia	Green, clastic, coarse- to medium-grained rock, similar amount of clasts and matrix	clasts: plg-amph-epdt-px (aug di)-lithics-opq-cc(s)-chl (glass)
M3-PD-323	7233	97927	Macuchi	Volcanic breccia	Green rock, clastic	clasts: lithics-chl-px-plg-epdt; matrix: devitrified glass
M3-PD-331	7229	100013	Macuchi	Volcanic breccia	Green, medium-grained, clastic, crude, green, bedding, no matrix	clasts: lithics-plg-chl-px-ol-opq
M3-PD-334	7241	98024	Macuchi	Volcanic breccia	Green rock, medium-grained, clastic	clasts: plg-cc-chl-lithics; matrix: chl-opq
M3-PD-366	7235	97868	Macuchi	Volcanic breccia	Green, massive, clastic rock, very sparse matrix	clasts: lithics-plg-px-epdt-cc; matrix: plg-devitrified glass
M3-PD-571	6957	98838	Macuchi	Volcanic breccia	Green, clastic, highly altered rock	clasts: px-plg-qtz-green lithics-preh(s); matrix: epdt-chl-devitrified glass-plg
M3-PD-736	6901	98853	Macuchi	Volcanic breccia	Porphyroclastic rock, lithic fragments and crystals, sparse matrix	clasts: lithics-plg-px-epdt-qtz-cc; matrix: plg-devitrified glass
M3-PD-518	7056	98713	Macuchi	Volcanic breccia (and. volc.)	Green rock, clastic, fine-grained matrix	clasts: black lithics-plg; matrix: plg-devitrified glass
M3-PD-919	7209	98138	Macuchi	Limestone	White, recrystallized, finely bedded, fine-grained rock	cc-qtz-arc
M3-PD-584	7115	98617	Macuchi	Quartz-basalt	Grey rock, fine-grained, slightly porphyritic, trachytic texture	phenocrysts: plg-amph (hb?)-qtz-opq-chl(s)-epdt(s); matrix: plg-amph
M3-PD-249	7226	97896	Macuchi	Chert	Green, massive, fine-grained, fractured, silicified rock	mega qtz-calced-micro qtz-chl-plg-epdt- Fe ox-opq
M3-PD-249A	7226	97896	Macuchi	Chert	Clast-like rock, fine-grained, whole and broken crystals in very fine matrix	clasts: qtz-plg-epdt-chl; matrix: micro qtz-calced-arc
M3-BX-142	7123	98723	Macuchi	Hyaloclastite	Black, porphyroclastic rock, fine-grained matrix	clasts: plg-px (aug di)-chl radial-chloritized lithics-cc ; matrix: chl
M3-PD-139	7140	98673	Macuchi	Hyaloclastite	Green rock, amygdaloidal, fine-grained matrix, altered	matrix: devitrified glass-plg; filled amygdales (chl-qtz-cc-epdt-mat mic)
M3-PD-140	7140	98743	Macuchi	Hyaloclastite	Fine-grained, amygdaloidal, altered rock	phenocrysts: plg alt; filled amygdales (chl-cc-qtz-epdt-preh); subangular clasts
M3-PD-368	7226	97858	Macuchi	Hyaloclastite	Clastic rock, chloritic matrix	clasts: lithics-plg-chl-epdt-opq; matrix: devitrified glass
M3-PD-710	7043	97862	Macuchi	Hyaloclastite	Dark green, clastic, medium-grained, roughly equigranular rock	px (aug di)-plg-chl (devitrified glass)-opq-qtz
M3-PD-737	7162	98911	Macuchi	Hyaloclastite	Green, faulted, highly altered rock	cc-chl-plg-qtz-serp-opq
M3-PD-179	7198	98084	Macuchi	Hyaloclastite (?)	Green rock, clastic	clasts: plg-volcanic lithics-cc-glass-px; matrix: devitrified glass-cc
M3-BX-215	6980	98042	Macuchi	Hornfels	Black, fine-grained, granofelsic rock	acicular crystals, non-oriented; crdt-bio-tc-ant-opq-plg(?)
M3-PD-214E	7005	98049	Macuchi	Hornfels	Calcareous, granofelsic rock	cc-wo-opq

Sample	UTMX	UTMY	Unidad	Rock type	Description	Minerals
M3-PD-215A	6980	98042	Macuchi	Hornfels	Green, fine-grained, somewhat fibrous, granoblastic, unoriented rock	bio-antoph-cord-ms-plg-opq
M3-PD-768	6834	98261	Macuchi	Hornfels	Black rock, fine-grained, non-oriented texture, slightly porphyritic, altered	cc-plg-preh-amph-opq
M3-PD-846	7011	98048	Macuchi	Hornfels (calcareous sandstone)	White, granofelsic, fine-grained rock	qtz-bio-cc-ga-ms-chl-plg-epdt
M3-BX-522	7151	98613	Macuchi	Hornfels (volcanic sandstone)	Black rock, fine-grained, massive, strongly silicified, shards	clasts: lithics-plg-px-cc-epdt; matrix: devitrified glass
M3-PD-645	6974	98387	Macuchi	Hornfels (volcanic sandstone)	Grey, fine-grained, granofelsic rock, signs of bedding	qtz-alt gris-opq-epdt-cpx(?)-mat micaceous
M3-PD-801C	7170	97829	Macuchi	Hornfels (volcanic sandstone)	Green, clastic, silicified rock, large clasts in fine matrix	blasts: qtz-plg-pump-bio; matrix: qtz-plg-epdt
M3-PD-206	7154	97924	Macuchi	Hornfels (sandstone)	Black, fine-grained, quartzose, recrystallised rock	qtz-cizo (2Vz~80)-sulfides-sph
M3-PD-305	7063	98026	Macuchi	Hornfels (sandstone)	White, quartzose, silicified, porphyroblastic rock, clasts slightly larger than matrix	qtz-plg-opq-chl-alt
M3-PD-306	7158	98093	Macuchi	Hornfels (sandstone)	Porphyroblastic, quartzose rock, abundant pyrite	qtz-ser-opq
M3-PD-672	6927	98237	Macuchi	Hornfels (sandstone)	Greenish white rock, fine- to medium-grained, porphyroblastic, fine-grained matrix	blasts: qtz-opq; matrix: qtz-ms
M3-PD-587	7106	98622	Macuchi	Hornfels (sandstone?)	Grey-green, fine-grained, equigranular, non-oriented rock, microcrystalline quartz-feldspar-opaque growth	qtz-bio-opq-amph (hb)-epdt
M3-PD-690A	6844	98283	Macuchi	Hornfels (fine-grained basalt?)	Black, fine-grained, slightly porphyritic rock	plg (An_{60})-amph (hb)-bio-opq-epdt(s)
M3-PD-679	7006	98184	Macuchi	Hornfels (basalt)	Green rock, fine-grained, crude banding	plg-epdt-opq-cc(s)
M3-PD-846A	7011	98048	Macuchi	Hornfels (calcarenite)	White, granofelsic, fine-grained rock	qtz-bio-wo-ms-opq
M3-PD-847	6913	98046	Macuchi	Hornfels (calcarenite)	Green, recrystallized, fine-grained rock	qtz-cc-plg-epdt-amph-opq
M3-PD-898	7022	98071	Macuchi	Hornfels (calcarenite)	Granofelsic rock, non-oriented, banded, two grain sizes in alternating bands (medium and fine)	qtz-amph (edenite)-ga-plg-cc-epdt(s)-sph
M3-PD-83A	7058	98336	Macuchi	Hornfels (meta-sandstone)	Granofelsic rock with very fine-grained xenoliths	plg-qtz-amph-chl-opq
M3-PD-214A	7005	98049	Macuchi	Hornfels (calcareous rock)	White rock, coarse-grained, granoblastic texture	cc-wo-opq-qtz
M3-PD-214	7005	98049	Macuchi	Hornfels (calcareous rock)	Calcareous, silicified, granoblastic rock, recrystallized quartz	plg-aug-chl-qtz-ser-opq
M3-PD-306A	7158	98093	Macuchi	Hornfels (volcanoclastic rock)	Equigranular, fine-grained, non-oriented rock	plg-qtz-chl-opq-devitrified glass
M3-PD-734	6976	98489	Macuchi	Hornfels (crystalline tuff)	Fine-grained, green clastic rock, relicts of clasts and amygdales	blasts: plg-amph (hb)-lithics-qtz-epdt-opq; matrix: qtz-plg-opq
M3-BX-146A	7152	98603	Macuchi	Quartzose siltstone	Green, fine-grained rock	qtz-arc-opq-chl
M3-PD-181A	7210	98057	Macuchi	Quartzose siltstone	Fine-grained rock, small subangular clasts, very fine-grained matrix	qtz-plg-opq-cc-chl-epdt-ms; matrix: arc
M3-PD-485	7128	98730	Macuchi	Quartzose siltstone	Green, clastic, fine-grained, silicified, bedded rock	arc-qtz-chl-opq-plg
M3-PD-844	7092	98089	Macuchi	Marble	Finely banded, altered, medium-grained, non-oriented rock	cc-epdt-qtz-alt
M3-PD-845	7086	98082	Macuchi	Marble	White, fine-grained, fine-grained, bedded, unoriented, altered rock	cc-wo-alt
M3-PD-848	6976	98042	Macuchi	Marble	Black, massive, fine-grained, unoriented rock	cc-opq-qtz-alt
M3-PD-199	7046	97870	Macuchi	Micro-diorite	Slightly porphyritic, medium- to coarse-grained, altered rock	plg (An_{44})-epdt(s)-chl(s)-opq
M3-PD-246	7137	97927	Macuchi	Micro-diorite	Grey, massive, medium to fine-grained, hypidiomorphic, altered rock	plg (An_{45})-amph- (hb?)-epdt-opq
M3-PD-756	7079	98779	Macuchi	Micro-diorite	Very altered rock, porphyritic appearance	phenocrysts: plg-epdt-amph (hb); matrix: opq-preh(s)
M3-BX-590	7130	98618	Macuchi	Micro-gabbro	Green, porphyritic rock, medium-grained matrix	phenocrysts: plg (An_{63})-amph-px (aug di)-opq-chl(s)-epdt(s); matrix: plg
M3-PD-331A	7234	100012	Macuchi	Micro-gabbro	Dark, medium-grained, pilotaxitic, domain oriented, subophitic rock	plg (An_{54})-px (aug di)-opq-amph(sc)-devitrified glass
M3-PD-397	7211	98139	Macuchi	Micro-gabbro	Green, massive, porphyritic rock, fine-grained matrix, intersertal	plg-cpx (aug di)-amph (hb)-chl-epdt-opq-qtz-cc
M3-PD-526	7201	98579	Macuchi	Micro-gabbro	Green-grey, massive, porphyritic, medium-grained phenocrysts in a fine-grained matrix	plg (An_{54})-px-amph (ural)-chl-cc-opq
M3-PD-861	7128	97796	Macuchi	Micro-gabbro	Porphyritic rock, fine-grained, matrix slightly smaller than phenocrysts, altered	phenocrysts: plg-amph-opq-epdt(s)-chl(s)-cc(s); matrix: plg-amph-epdt
M3-PD-711B	6932	98073	Macuchi	Skarn	White rock, cryptocrystalline, approximately uniform grain size	tr-wo-di-epdt-cc-opq
M3-PD-929	7218	97759	Macuchi	Tectonite (volcanic sandstone)	Green rock, medium-grained, tectonised, fault mirrors, tectonic cleavage	chl-amph-plg-qtz-opq
M3-BX-108	7020	98257	Macuchi	Crystalline tuff	Black rock, porphyritic appearance, fine-grained matrix	clasts: cpx (aug di)-ol-plg-cc-alt; amygdales: qtz-epdt-preh
M3-PD-191	7122	97865	Macuchi	Crystalline tuff	Green rock, sparse vitreous matrix, subangular clasts, altered crystals, sparse shards	clasts: volcanic lithics, volcanoclastic sediments (?); altered crystals: plg-opq

Sample	UTMX	UTMY	Unidad	Rock type	Description	Minerals
M3-PD-648	6997	98332	Macuchi	Crystalline tuff	Grey-green rock, somewhat recrystallized (cryptocrystalline quartz), filled amygdales	clasts: qtz-plg-lithics-opq-Fe ox-epdt(s)-chl(s); matrix: plg-qtz
M3-PD-694	6871	98283	Macuchi	Crystalline tuff	Altered rock, fine-grained, filled amygdales	plg-Fe ox-opq; amygdales: chl
M3-PD-718	7001	98278	Macuchi	Crystalline tuff	Green rock, tuffaceous, slightly porphyritic, fine-grained matrix, shards	clasts: plg-opq-devitrified glass-Fe ox; amygdales: chl-epdt; matrix: devitrified glass
M3-PD-718B	7001	98278	Macuchi	Crystalline tuff	Green, fine- to medium-grained, porphyroclastic rock, filled vesicles, altered	clasts: plg; matrix: devitrified glass-opq-plg; amygdales: zeol-cc-chl-qtz
M3-PD-719	6999	98277	Macuchi	Crystalline tuff	Green, porphyroclastic rock, partially devitrified glassy matrix	clasts: plg-ol-glass; amygdales: qtz; matrix: plg-devitrified glass
M3-PD-752	7071	98869	Macuchi	Crystalline tuff	Porphyroclastic rock, medium-grained clasts in fine-grained matrix	clasts: plg (An_{45})-cpx (aug di)-opq-cc(s); matrix: plag-chl(s)
M3-PD-756A	7079	98779	Macuchi	Crystalline tuff	Porphyroclastic rock, altered	clasts: plg (An_{45})-amph (hb)-lithics-opq-epdt(s)-cc(s)-preh(s); matrix: plg
M3-PD-926	7223	97746	Macuchi	Crystalline tuff	Green, medium-grained, tectonised, porphyritic rock, fine-grained matrix	phenocrysts: plg-opq-epdt(s)-cc(s)-chl(s); matrix: chl (devitrified glass)
M3-PD-369	7223	97856	Macuchi	Crystalline tuff (?)	Porphyroclastic rock, epidotized clasts in fine-grained matrix	clasts: epdt-plg-opq-cc; matrix: epdt-serp(?)
M3-PD-578	6969	98878	Macuchi	Dacitic tuff	Green, fine-grained, clastic, amygdaloidal rock	clasts: plg-qtz-amph (hb)-opq; matrix: plg-epdt; amygdales: epdt
M3-BX-138	7129	98726	Macuchi	Lithic tuff	Medium-grained, clastic rock, sparse fine-grained matrix, small angular clasts, shards	clasts: plg-lithics-epdt-cc-reddish mineral(?)-adularia-opq
M3-BX-141	7125	98730	Macuchi	Lithic tuff	Green, porphyroclastic rock, fine-grained matrix	clasts: plg-qtz-lithics-glass-cc-epdt; amygdales: qtz-chl; matrix: chl
M3-BX-146	7152	98730	Macuchi	Lithic tuff	Green rock, porphyroclastic, sparse fine-grained matrix	clasts: plg-qtz-lithics-px (aug di)-cc; amygdales: qtz-chl; matrix: chl-cc-plg-epdt-devitrified glass
M3-BX-996	6939	98879	Macuchi	Lithic tuff	Porphyroclastic rock, highly altered	clasts: lithics-plg-amph-opq-epdt(s); matrix: chl-plg (devitrified glass)
M3-PD-184	7210	98034	Macuchi	Lithic tuff	Green rock, clastic, chloritized shards, sparse matrix, rare amygdales	clasts: volcanoclastic lithics; crystals: plg (An_{54})-aug; matrix: chl-cc
M3-PD-485A	7128	98730	Macuchi	Vitreous tuff	Green, clastic, medium-grained rock, fine-grained matrix	clasts: plg-chl-reddish lithics-qtz-opq-rut-px; matrix: chl
M3-BX-143	7128	98718	Macuchi	Vitreous tuff	Green rock, clastic, partially filled vesicles, lithic fragments, fine-grained matrix	clasts: px (aug di)-plg-cc-qtz-chl-opq-epdt (s); matrix: chl (devitrified glass)
M3-PD-573	7998	98779	Macuchi	Vitreous tuff	Green rock, silicified, porphyritic, abundant amygdales	clasts: plg (An_{64})-epdt-qtz-px; amygdales: zeol-qtz-px; matrix: chl
M3-PD-579A	6928	98837	Macuchi	Vitreous tuff	Green, medium-grained, banded, clastic rock	clasts: plg-cpx (aug di)-qtz-lithics-opq-cc(s); matrix: devitrified glass-epdt
M3-PD-646	6991	98374	Macuchi	Vitreous tuff	Green rock, volcanoclastic, fractured, with fault mirrors, crystalline and vitreous fragments	plg-chl (devitrified glass)-arc-opq-qtz(s)-cc(s)
M3-PD-718A	7001	98278	Macuchi	Vitreous tuff	Green rock, fine-grained matrix, tuffaceous	clasts: plg-chl-opq; amygdales: pump-preh-alt; matrix: devitrified glass-opq-plg
M3-PD-718C	7001	98278	Macuchi	Vitreous tuff	Green, fine- to medium-grained rock, filled amygdales	plg-opq-epdt; amygdales: epdt-cc-chl-preh
M3-PD-720A	6996	98276	Macuchi	Vitreous tuff	Green rock, clastic, fine-grained	clasts: chl-plg-px (aug di)-qtz; amygdales: qtz-arc-chl; matrix: glass
M3-PD-976	7419	98621	Macuchi	Vitreous tuff	Green rock, fine-grained, porphyritic, filled amygdales	clasts: cpx-plg-chl-opq; amygdales: qtz-chl; matrix: devitrified glass
M3-PD-239	7044	97933	Macuchi	Altered vitreous tuff	Green rock, vesicular	qtz-chl-epdt-pump-amph-plg-opq; partially filled amygdales
M3-PD-214C	7005	98049	Macuchi	Ultramylonite	Fully crushed rock, black, tectonic cleavage, cc veinlets	qtz-opq-arc-cc
M3-BX-998A	6935	98863	Macuchi (?)	Andesite	Porphyritic rock, fine-grained matrix	phenocrysts: plg (An_{44})-amph (hb)-opq-epdt(s); matrix: chl-plg-opq-bio
M3-LP-1057	7114	97890	Macuchi (?)	Sandstone	Clastic rock, granular, medium to coarse grained, subrounded, covered by reddish patina	qtz-alt-opq
M3-PD-627	6789	98444	Macuchi (?)	Basalt	Green, recrystallised, porphyritic, altered rock, fine- to medium-grained matrix	phenocrysts: plg (An_{63})-px (aug di)-opq-epdt(s)-chl(s)-cc(s); matrix: plg-cpx

Sample	UTMX	UTMY	Unidad	Rock type	Description	Minerals
M3-LP-2011	0	0	Macuchi (?)	Limestone	Fine-grained, massive, non-oriented rock, fossils (?)	cc (ca. 99%)-opq
M3-BX-467	7131	98789	Macuchi (?)	Hornfels	Porphyroblastic rock, silicified, medium-grained matrix	blasts: px (aug di)-ser-plg-opq-chl(s)-amph(s)-epdt(s); matrix: chl
M3-PD-469A	7178	98739	Macuchi (?)	Hornfels	Green, medium to fine-grained, recrystallized, granofelsic rock	qtz-chl-ms-bio-opq
M3-PD-224	7233	98829	Macuchi (?)	Hornfels (sandstone)	Black, fine-grained, granofelsic rock	qtz-plg (An_{44})-ms-bio-opq
M3-PD-517	7194	98759	Macuchi (?)	Hornfels (fine-grained basalt?)	Green, fine-grained, slightly porphyroblastic, altered, fractured rock	plg-amph-opq-epdt
M3-PD-909	7124	97827	Macuchi (?)	Hornfels (crystalline tuff)	Black rock, slightly porphyritic, amygdaloid	blasts: plg-amph-qtz-opq; amygdales: qtz; matrix: plg-chl-amph(hb)-qtz
M3-LP-042	0	0	Macuchi (?)	Crystalline tuff	Rock with porphyritic aspect, chloritized amygdales	clasts: plg; amygdales: chl; matrix: plg-px-epdt
M3-PD-338	7240	98030	Pallatanga	Tuffaceous andesite	Green rock, porphyritic, fine-grained matrix, amygdales	phenocrysts: cpx (pig?)-plg (An_{35}); amygdales: preh-zeol; matrix: devitrified glass
M3-PD-316	7316	97854	Pallatanga	Volcanic sandstone	Medium-grained clastic rock, recrystallized, sparse matrix	clasts: plg-serp-ol-px-cc-opq-qtz(s)-lithics; matrix: devitrified glass
M3-BX-545	7414	98601	Pallatanga	Basalt	Porphyritic, medium-grained, highly weathered rock	phenocrysts: plg (An_{58})-cpx (aug)-opx-ol-opq; matrix: plg-devitrified glass
M3-PD-547	7418	98583	Pallatanga	Basalt	Grey black rock, porphyritic, medium-grained, fine-grained matrix	phenocrysts: plg (An_{65})-opx (aug di?)-ol-opq-cc; matrix: devitrified glass
M3-PD-248	7223	97898	Pallatanga	Picritic basalt (?)	Black-green, massive, medium-grained, slightly porphyritic rock, fine-grained matrix	phenocrysts: cpx-ol-plg-chl-qtz(s)-epdt(s); matrix: plg-Fe ox-px-epdt-ol(?)
M3-PD-248A	7223	97898	Pallatanga	Picritic basalt (?)	Mafic rock, porphyritic, vesicular, altered, abundant epidote	phenocrysts: px (aug di)-serp-ser(s); amygdales: qtz-preh; matrix: px-ol-plg
M3-PD-338B	7240	98030	Pallatanga	Vesicular basalt	Green, massive, porphyritic, altered rock	phenocrysts: cpx (aug di)-plg-epdt; amygdales: plg; matrix: devitrified glass
M3-PD-396B	7283	98095	Pallatanga	Calcarenite (altered ultramafic rock)	Red rock, fine-grained, massive, unoriented	qtz-Fe ox-verm(?)
M3-PD-301	7322	97847	Pallatanga	Quartz-gabbro	Dark, medium-grained, hypidiomorphic rock	plg-px-qtz-chl-cc
M3-BX-1019	7284	98086	Pallatanga	Gabbro	Coarse- to medium-grained, granular, hypidiomorphic, altered rock	clasts: lithics-glass-ol-px (aug)-cc(s)-serp(s)-chlorophaeite
M3-PD-152	7343	98224	Pallatanga	Gabbro	Fine- to medium-grained, granular, altered, massive rock	cpx (aug)-epdt-plg-opq-ol
M3-PD-162C	7342	98228	Pallatanga	Gabbro	Holocrystalline, medium-grained, altered rock	cpx (di)-amph (hb)-ol-plg-chl(s); veinlets: preg-Tc-serp
M3-PD-162D	7342	98228	Pallatanga	Gabbro	Holocrystalline, medium-grained, altered rock	cpx(di)-plg(?)-ol-amph(s)-chl(s); veinlets: cc
M3-PD-267	7328	97886	Pallatanga	Gabbro	Dark, medium-grained, hypidiomorphic rock	plg-px (aug)-serp-chl-epdt-opq
M3-PD-267B	7328	97886	Pallatanga	Gabbro	Dark, medium-grained, hypidiomorphic rock	cpx-plg-epdt-opq-sph(s)-chl(s)
M3-PD-301A	7322	97847	Pallatanga	Gabbro	Dark, medium-grained, hypidiomorphic rock	plg-px (aug di)-amph-serp
M3-PD-312	7337	97932	Pallatanga	Gabbro	Massive, tectonised, medium-grained rock, cc veinlets	px (aug)-plg-ol-serp-chl-cc-sph-opq
M3-PD-312C	7337	97933	Pallatanga	Gabbro	Fine- to medium-grained, partially serpentinized, ophitic-textured, massive rock	plg-px (aug di)-serp-cc-opq
M3-PD-312D	7337	97933	Pallatanga	Gabbro	Fine- to medium-grained, ophitic, massive rock, cut by cc veinlets	plg-px (aug di)-serp-cc-opq
M3-PD-542C	7385	98546	Pallatanga	Gabbro	Hypidiomorphic, granular, medium-grained, partially altered rock	plg-px-chl-opq
M3-PD-953A	7323	97847	Pallatanga	Gabbro	Slightly porphyritic, medium-grained, partially serpentinized rock	plg-serp-px (aug)-opq-chl
M3-PD-953B	7323	97847	Pallatanga	Gabbro	Slightly porphyritic, medium-grained, partially serpentinized rock	plg-serp-px (aug)-opq
M3-PD-312E	7337	97933	Pallatanga	Altered gabbro	Slightly porphyritic, fine-grained, partially serpentinised rock, highly altered	px (aug di)-plg-serp-cc-epdt-opq
M3-BX-1018	7294	98093	Pallatanga	Hyaloclastite	Clastic rock, subangular lithics, crystal fragments, slightly devitrified glass forming shards	clasts: lithics-glass-ol-px-cc(s)-serp(s)-chlorophaeite; matrix: opq-cc-alt
M3-PD-335	7237	98023	Pallatanga	Micro-gabbro	Green rock, hypidiomorphic, medium-grained, very altered	aug-pig-plg (An_{50})-amph(s)-opq
M3-PD-338D	7240	98030	Pallatanga	Micro-gabbro	Porphyritic rock, medium-grained matrix	phenocrysts: plg (An_{44})-px (aug di)-serp; matrix: plg-px-opq-tc(s)-epdt(s)
I-85-MC	0	0	Pallatanga	Orthopyroxenite with amphibole	Hypidiomorphic rock, granular, coarse to medium-grained, altered edges to tc	opx-amph-saph-tc-opq
I-85-MG	0	0	Pallatanga	Orthopyroxenite with amphibole	Hypidiomorphic rock, granular, coarse to medium grained, edges altered to tc	opx-amph(orto?)-tc-opq-saph

Sample	UTMX	UTMY	Unidad	Rock type	Description	Minerals
M3-BX-542	7385	98546	Pallatanga	Pillow lava (?)	Black-green, fine-grained, porphyritic, highly altered rock, spheroidal structures	phenocrysts: plg-px-opq-chlorophaeite-ol(?)-qtz(vet)-cc(vet); matrix: devitrified glass
M3-PD-162E	7342	98228	Pallatanga	Pyroxenite with olivine	Hypidiomorphic, granular, medium-grained, altered rock	cpx (di)-ol-serp(s)
M3-PD-162F	7342	98228	Pallatanga	Pyroxenite with olivine/Melilitolite (?)	Hypidiomorphic, granular, medium-grained, altered rock	cpx (aug di)-ol-opq-serp?(s)(melilite?)
M3-PD-953	7323	97847	Pallatanga	Plagio-peridotite	Hypidiomorphic, granular, medium-grained, partially serpentinized, altered rock	px (aug)-plg-serp-opq-alt(ol?)
M3-PD-162B	7342	98228	Pallatanga	Serpentinized green rock	Very fine-grained rock, vein-cut, altered	serpentinized in hand sample; thin section: altered, brown; chl-epdt-serp
I-8544	0	0	Pallatanga	Serpentinite	Oriented, micro-folded, highly deformed rock	serp-chl-opq
M3-PD-266	7328	97905	Pallatanga	Serpentinite	Dark, medium-grained, hypidiomorphic rock	serp-tc
M3-PD-312A	7337	97933	Pallatanga	Serpentinite	Massive rock, medium-grained, good serpentine development, cc veinlets	serp-px (aug di)-cc-opq-qtz(s)
M3-PD-314	7328	97911	Pallatanga	Serpentinite	Porphyritic looking rock, medium-grained	serp-tc-opq
M3-PD-316C	7316	97854	Pallatanga	Serpentinite	Tectonised, fine-grained rock	serp-opq
M3-PD-326A	7234	97948	Pallatanga	Serpentinite	Green, foliated, medium-grained, porphyroblastic rock	serp-opq-chl-tc
M3-PD-326B	7234	97948	Pallatanga	Serpentinite	Tectonised rock, massive, non-oriented, plagioclase-epidote veinlets	serp-sph-epdt(vet)-plg(vet)
M3-PD-396	7283	98095	Pallatanga	Serpentinite	Fragmental, intensely tectonised rock	serp-ol-px-tc-opq-cc
M3-PD-542D	7385	98546	Pallatanga	Serpentinite	Fine-grained rock, non-oriented, phyllosilicates in radial aggregates	serp-px (aug di)-opq-cc
M3-PD-358	7233	97942	Pallatanga	Serpentinite (Mylonite)	Aphanitic rock, oriented, pseudomorphs of eye-shaped blasts in stress direction, replacement	serp-opq
M3-PD-358A	7233	97942	Pallatanga	Serpentinite (Mylonite)	Aphanitic rock, oriented, pseudomorphs of eye-shaped blasts in stress direction, replacement	serp-opq
M3-PD-953C	7323	97847	Pallatanga	Serpentinite (pillow lava)	Porphyritic rock, with amygdales, fine-grained matrix	phenocrysts: serp; amygdales: chl-qtz; matrix: serp
M3-PD-338A	7240	98030	Pallatanga	Crystalline tuff	Green rock, medium-grained, clastic, chloritized matrix	clasts: plg-chl-px (aug di)-ms-lithics; matrix: chl-cc-plg
M3-PD-338C	7240	98030	Pallatanga	Crystalline tuff	Tectonised, porphyroclastic rock	clasts: lithics-plg-px-serp-opq; amygdales: calced-zeol; matrix: devitrified glass
M3-PD-152A	7343	98224	Pallatanga	Vitreous tuff	Medium-grained, sheared, vesicular rock	clasts: plg-epdt-cpx; amygdales: plg-epdt; matrix: devitrified glass-serp
M3-PD-162A	7342	98228	Pallatanga	Websterite	Hypidiomorphic, granular, medium-grained, altered rock	cpx (aug di)-hy-sp-serp-chl-clzo-opq
M3-PD-326	7234	97948	Pallatanga	Websterite	Green, massive, medium-grained, rock, fault-mirror	serp-cpx (di)-opx(hy)-opq
M3-PD-326C	7234	97948	Pallatanga	Websterite	Green, massive, medium-grained, tectonised, massive rock	serp-cpx (aug di?)-opx-opq
AI-8545	0	0	Pallatanga	Websterite with spinel	Hypidiomorphic, granular, coarse-grained rock	opx-cpx-sp-serp
MI-8545	0	0	Pallatanga	Websterite with spinel	Hypidiomorphic, granular, coarse-grained rock	cpx-sp-serp
M3-PD-152B	7343	98224	Pallatanga	Websterite with spinel	Hypidiomorphic, granular, medium grained, altered rock	cpx (aug di)-opx-sp-opq
M3-PD-341	7238	98051	Pallatanga (?)	Andesite	Porphyritic rock, small phenocrysts, trachytic matrix	phenocrysts: plg-px (aug di)-opq-qtz; amygdales: qtz; matrix: devitrified glass-plg
M3-PD-399A	7242	98019	Pallatanga (?)	Tectonised calcareous sandstone	Fine-grained rock, intensely tectonised, cc veinlets	arc-qtz-cc-opq-plg
M3-PD-42	7270	98847	Pilaló	Andesite	Black, slightly porphyritic, medium-grained rock	phenocrysts: plg-px (aug di)-opq; matrix: plg-px-devitrified glass-opq
M3-PD-42A	7270	98847	Pilaló	Micro-diorite	Porphyritic rock, large phenocrysts, medium-grained matrix	phenocrysts: plg (sauss An_{38})-chl; matrix: plg-epdt-px-chl-ms-opq
M3-PD-219A	7259	98847	Pilaló (?)	Lithic breccia	Green, medium-grained, clastic rock	clasts: qtz-lithics; matrix: epdt-chl-plg (devitrified glass)
M3-PD-219	7259	98847	Pilaló (?)	Tuffaceous breccia	Green rock, fragmental, fine-grained matrix	clasts: volcanic and volcanoclastic lithics; altered crystals: plg-px; matrix: devitrified glass
M3-BX-218	7262	98848	Pilaló (?)	Hornfels	Green, recrystallized, porphyritic rock	phenocrysts: plg; amygdales: chl-cc; matrix: plg-epdt-ms-opq-cc
M3-RH-315	0	0	Pujilí	Amphibolite	Foliated, medium-grained, blastic, very fresh rock	plg (An_{62})-amph (hb)-epdt

Sample	UTMX	UTMY	Unidad	Rock type	Description	Minerals
M3-LP-1059	7225	98221	Santa Fe (?)	Tonalite	Hypidiomorphic, granular, medium- to fine-grained, altered rock	plg (An_{44})-qtz-kfs-amph (hb)-opq
M3-PD-950	7315	97815	Sibambe	Andesite	Gray, porphyroclastic rock, partially fractured clasts in fine-grained matrix	phenocrysts: plg (An_{51})-px (aug?)-oxyhb-opq-qtz-epdt(s); matrix: glass
M3-PD-961	7538	97910	Sibambe	Basaltic andesite	Porphyritic rock, medium-grained matrix, brown, nearly isotropic	phenocrysts: plg-serp-opq-cc(s); matrix: slightly devitrified glass
M3-PD-970	7293	98226	Sibambe	Basaltic andesite	Porphyritic rock, fine-grained matrix	phenocrysts: plg (An_{50})-cpx (aug)-opq-chl(s)-epdt(s)-cc(s); matrix: glass-plg
M4-PD-4	7152	99021	Unacota	Limestone	Grey, fine-grained rock	cc recrystallized; cc (99%), qtz intergranular
M3-PD-889	6986	97838	Undushig	Monzodiorite	Hypidiomorphic, granular, medium to coarse-grained, slightly altered rock	plg (An_{50})-qtz-kfs-amph (hb)-bio-sph-opq
M3-PD-264A	7324	97885	Yunguilla	Sandstone	Coarse-grained, clastic rock, fine-grained matrix	clasts: lithics-cc-plg-qtz-amph-px-epdt-chl; matrix: arc
M3-PD-321	7360	97922	Yunguilla	Sandstone	Fine-grained, clastic, slightly oriented rock	clasts: qtz-plg-opq; matrix: arc
M3-PD-424	7315	97826	Yunguilla	Basalt	Porphyritic, fine- to medium-grained rock, matrix not oriented	phenocrysts: plg (An_{52}); matrix: plg (An_{41})-px-opq
M3-PD-174	7376	98275	Yunguilla	Limestone	Calcareous rock, dirty appearance, massive, whitish	cc-qtz-lithics-opq
M3-PD-320A	7346	97923	Yunguilla	Limestone	Fine-grained, stratified, folded, calcareous rock	cc-qtz-plg-opq
M3-PD-446	7444	98228	Yunguilla	Limestone	Clastic rock, medium-grained, recrystallized	cc-qtz-fossils (trz)
M3-PD-172	7415	98195	Yunguilla	Impure limestone	Calcareous rock, dirty aspect, intensely tectonised, medium grained, uniform	cc-qtz interstitial-arc-opq
M3-PD-178	7347	98233	Yunguilla	Limestone (?)	Green rock, no protolith recognisable, strongly tectonised	cc-alt-opq
M3-PD-316D	7316	97854	Yunguilla	Hornfels (Meta-sandstone)	Fine-grained, altered rock	qtz-plg-epdt-pump-chl-cc
M3-RV-264C	7324	97885	Yunguilla	Hornfels (altered ultramafic rock?)	Medium- to fine-grained rock, non-oriented micaceous flakes with intersertal quartz	verm-qtz-opq
M3-LP-1043	7145	98506	Zumbagua	Andesite	Porphyritic rock, fine-grained matrix	phenocrysts: plg (An_{43})-amph(hb)-opq; matrix: plg-amph-opq
M3-PD-974	7323	98551	Zumbagua	Basalt	Grey, porphyritic rock, fine-grained matrix	phenocrysts: opx-cpx (aug)-plg (An_{66})-opq; matrix: plg-opq
M3-PD-975	7362	98547	Zumbagua	Basalt	Porphyritic rock, columnar appearance, fine-grained matrix	phenocrysts: plg (An_{64})-px (aug di)-opq-cc(s); matrix: plg-devitrified glass
M3-PD-764	7224	98484	Zumbagua	Basaltic ignimbrite	Brownish-grey rock, fragmental, partially broken crystals in unoriented glassy matrix	fragments: plg (An_{63})-cpx (aug)-opx-opq-alt; matrix: glass-plg
M3-PD-552	7343	98827	Zumbagua	Vitreous tuff	Black rock, massive, clastic	clasts: plg-lithics-chl-cc-cpx-opq-epdt; matrix: devitrified glass-plg
M3-PD-552B	7343	98827	Zumbagua (?)	Andesite with hornblende	Porphyritic rock, medium-grained felsic matrix	phenocrysts: plg (An_{47})-amph (hb)-cpx-opq; matrix: plg